Isolation, characterisation and properties of 8,8-methylmethine flavan-3-ol-malvidin-3-glucoside pigments found in red wines

by

David F. Lee

8/8/2008

Thesis submitted for the degree of
Doctor of Philosophy

University of Adelaide
School of Agriculture, Food and Wine

Abstract

This study concerns the isolation, characterisation and physio-chemical properties of 8,8-methylmethine-(epi)catechin-malvidin-3-glucoside compounds found in red wines. 8,8-Methylmethine-(epi)catechin-malvidin-3-glucoside compounds were isolated via chromatographic methods developed in this study. The compounds were characterised via nuclear magnetic resonance spectrometry which, with the aid of molecular modelling, afforded their possible 3-dimensional structures. Their physio-chemical properties including ionisation and hydration constants, colour parameters and chemical stabilities were determined. The formation of 8,8-methylmethine-flavan-3-ol-malvidin-3-glucoside compounds and other pigments in wines was also studied.

8,8-Methylmethine-(epi)catechin-malvidin-3-glucoside compounds were also synthesised by condensing malvidin-3-glucoside with (epi)catechin in the presence of acetaldehyde. Diastereomers of 8,8-methylmethine-(epi)catechin-malvidin-3-glucoside pigments were isolated from the reaction using size-exclusion liquid chromatography followed by cation-exchange liquid chromatography.

The structures of the four 8,8-methylmethine-catechin (and epicatechin)-malvidin-3-glucoside diastereomers were determined using mass spectrometry and one and two-dimensional nuclear magnetic resonance spectroscopy. It was found that for all four compounds, the methylmethine bridge occurs at the 8-positions of malvidin-3-glucoside and (epi)catechin and that the 3-dimensional structural differences between the diastereomers is the positioning of the (epi)catechin moiety with respect to the glucoside group. One diastereomer has the (epi)catechin on the same side, with respect to the malvidin entity whilst it is on the opposite side for the other diastereomer. The proposed structures also afforded the malvidin entity protection from nucleophilic attack via steric hindrance by the (epi)catechin moiety.

8,8-Methylmethine-(epi)catechin-malvidin-3-glucoside pigments have greater colour stability with regards to changes in pH and SO_2 bleaching compared to malvidin-3-glucoside providing evidence that little or no hydration in aqueous solutions is occurring for these compounds. Further evidence for little or no hydration occurring is the presence

of isosbestic points in the UV-vis spectra observed for the 8,8-methylmethine-(epi)catechin-malvidin-3-glucoside in the pH range 2 to 7. Although the 8,8-methylmethine-(epi)catechin-malvidin-3-glucoside pigments have greater colour stability to pH, SO_2 and oxidation, compared to malvidin-3-glucoside, they have lower temporal stabilities and under both aerobic and anaerobic conditions they have significantly higher degradation rate constants than malvidin-3-glucoside.

The ionisation constants of the 8,8-methylmethine-(epi)catechin-malvidin-3-glucoside compounds were determined using high voltage paper electrophoresis (HVPE) and UV-visible spectroscopy. The first ionisation constants (pKa_1) of the 8,8-methylmethine-(epi)catechin-malvidin-3-glucoside compounds were found to be higher than that of malvidin-3-glucoside whereas the second and third ionisation constants (pKa_2 and pKa_3) were found to be lower. The correlation of the ionisation constants between HVPE and UV-visible spectroscopy supports the proposal that there is little or no occurrence of hydration for the 8,8-methylmethine-(epi)catechin-malvidin-3-glucoside compounds in the pH range investigated.

8,8-Methylmethine-flavan-3-ol-malvidin-3-glucoside compounds were the major pigments formed during fermentations of chemically defined grape juice media containing malvidin-3-glucoside and various flavan-3-ols. The yeast strain used for fermentation had a major influence on the levels and rates of formation of these pigments during fermentation. The yeast strain used also has an important influence on wine pigment composition, concentration and evolution during maturation thereby affecting the colour density and hue of the resultant wines. The initial formation of 8,8-methylmethine-flavan-3-ol-malvidin-3-glucoside compounds and their subsequent gradual degradation during maturation, allowed a pool of malvidin-3-glucoside to be available for the formation of other colour stable and more temporally stable pigments.

Acknowledgements

Thanks to my principle supervisor Associate Professor Graham P. Jones and my co-supervisor Dr Ewald Swinny for their helpful advice and guidance.

Dr Robert Asenstorfer is gratefully acknowledged for his technical input, especially regarding the determination of pK values by HVPE and spectroscopic methods.

The people of the AWRI are acknowledged for their help, especially Yoki Hayasaka and Gayle Baldock for performing the mass spectrometry.

Thanks to Dr Michelle Walker and Colin McBryde for their guidance with the model wine making.

Thanks to Philip Clements for performing the NMR spectroscopy.

The staff of Kathleen Lumley College are thanked for providing accommodation conducive to studying.

This project was funded by the Cooperative Research Centre for Viticulture.

Declaration

This thesis describes my research carried out in the School of Agriculture, Food and Wine, the University of Adelaide and contains no material which has been accepted for the award of any other degree or diploma in any University. To the best of my knowledge this thesis contains no material previously published or written by any other person except where due reference is made in the text.

I give my consent for a copy of this thesis, when deposited in the Library of the University of Adelaide, to be available for the loan and photocopying.

David Lee

Contents

List of Tables

List of Figures

List of Abbreviations

AM1	Austin Model 1
CDGJM	Chemically Defined Grape Juice Media
CY3G	Cyanidin-3-glucoside
DEPT	Distortionless Enhancement by Polarization Transfer
DP3G	Delphinidin-3-glucoside
DQCOSY	Double Quantum Correlated Spectroscopy
HCl	Hydrochloric Acid
HMBC	Heteronuclear Multiple Bond Correlation
HMQC	Heteronuclear Multiple Quantum Coherence
HSQC	Heteronuclear Single Quantum Coherence
HVPE	High Voltage Paper Electrophoresis
MC1	8,8-methylmethine-catechin-malvidin-3-glucoside diasteromer
MC2	8,8-methylmethine-catechin-malvidin-3-glucoside diasteromer
ME1	8,8-methylmethine-epicatechin-malvidin-3-glucoside diasteromer
ME2	8,8-methylmethine-epicatechin-malvidin-3-glucoside diasteromer
MOPAC	Molecular Orbital Package
MV3G	Malvidin-3-glucoside
MV3GACET	malvidin-3-(acetyl)glucoside
MV3GCOU	malvidin-3-(coumaryl)glucoside
NaCl	Sodium Chloride
NMR	Nuclear Magnetic Resonance
PE3G	Peonidin-3-glucoside
PT3G	Petunidin-3-glucoside
ROESY	Rotational Nuclear Overhauser Effect Spectroscopy
TFA	Trifluoroacetic Acid
TLC	Thin Layer Chromatography

List of publications arising from this thesis

Refereed journals

Lee, D. F.; Swinny, E. E.; Jones, G. P. NMR identification of ethyl-linked anthocyanin-flavanol pigments formed in model wine ferments. *Tetrahedron Lett.* **2004**, *45*, 1671-1674.

Lee, D. F.; Swinny, E. E.; Asenstorfer, R. E.; Jones, G. P. Factors affecting the formation of red wine pigments. In *Red Wine Color: Revealing the Mysteries*; A. L. Waterhouse and J. A. Kennedy, Eds.; American Chemical society: Washington, **2004** pp 125-142.

Asenstorfer, R.E., Lee, D.F. and Jones, G.P. Influence of structure on the ionization constants of anthocyanins and anthocyanin-like wine pigments. *Anal. Chim. Acta* **2006** *563*, 10-14.

Chapter 1 - Literature Review

1.1 Introduction

The colour of red wine evolves, during ageing, from a bright red colour due to anthocyanin-based pigments extracted from grape skins (Ribereau-Gayon, 1974) to brick red (Sudraud, 1958). It has been postulated that this is due to grape-derived anthocyanins undergoing condensation reactions to form colour stable pigmented polymers (Somers, 1971) whose contribution towards wine colour increases during wine aging (Somers, 1971).

Condensation reactions between grape-derived anthocyanins and flavan-3-ols (catechins, proanthocyanidins, condensed tannins etc.) can occur in the absence (Jurd, 1967; Somers, 1971) or the presence (Timberlake and Bridle, 1976; Vivar-Quintana et al., 1999) of carbonyl compounds, secreted by yeast during fermentation or produced by the oxidation of alcohols (Weeks, 1969; Litchev, 1989). The linkages formed by the carbonyl compounds between anthocyanins and flavan-3-ols can either be alkyl (Timberlake and Bridle, 1976) or vinyl (Francia-Aricha et al., 1997). Carbonyl compounds can also react with anthocyanins to create vitisins and related compounds (Bakker and Timberlake, 1997; Benabdeljalil et al., 2000).

1.2 Anthocyanins

Grape anthocyanins are the glucosides of anthocyanidins and are found in the skins of grapes. They include malvidin-3-glucoside ($R_1 = R_2 = OCH_3$, $R_3 = OH$, Figure1.1), cyanidin-3-glucoside ($R_1 = R_3 = OH$, $R_2 = H$, Figure1.1), peonidin-3-glucoside ($R_1 = H$, $R_2 = OCH_3$, $R_3 = OH$, Figure1.1), petunidin-3-glucoside ($R_1 = OCH_3$, $R_2 = R_3 = OH$, Figure1.1) and delphinidin-3-glucoside ($R_1 = R_2 = R_3 = OH$, Figure1.1). MV3G including its acetylated forms malvidin-3-(acetyl)glucoside ($R_3 = OCH_3CH$ Figure1.1) and malvidin-3-(coumaryl)glucoside ($R_3 = OC_9H_7O_2$ Figure1.1), is the predominant anthocyanin in *Vitis vinifera* grapes, comprising approximately 60 percent of the total anthocyanin content

(Wulf and Nagel, 1978; Piergiovanni and Volonterio, 1980). The anthocyanins leach into the must during skin contact in the winemaking process.

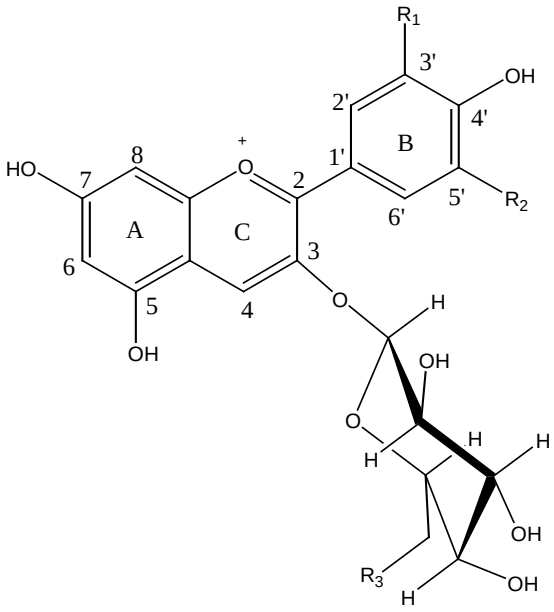

Figure 1.1 Anthocyanidin-3-glucoside

The structure of MV3G is dependent upon the pH of the medium it is in. It can exist in the following forms: flavylium cation, quinonoidal base, hydrated hemiketal which can tautomerise to a chalcone, quinonoidal anion and quinonoidal dianion (Figure 1.2). In the flavylium form (Figure 1.2 A), MV3G is a bright red colour, in the anion form (Figure 1.2 E) it is a purple colour and in the dianion form (Figure 1.2 F) it is a blue colour. Hydration of MV3G, at either the 2- or 4- positions, forms colourless compounds (Figure 1.2 C and D).

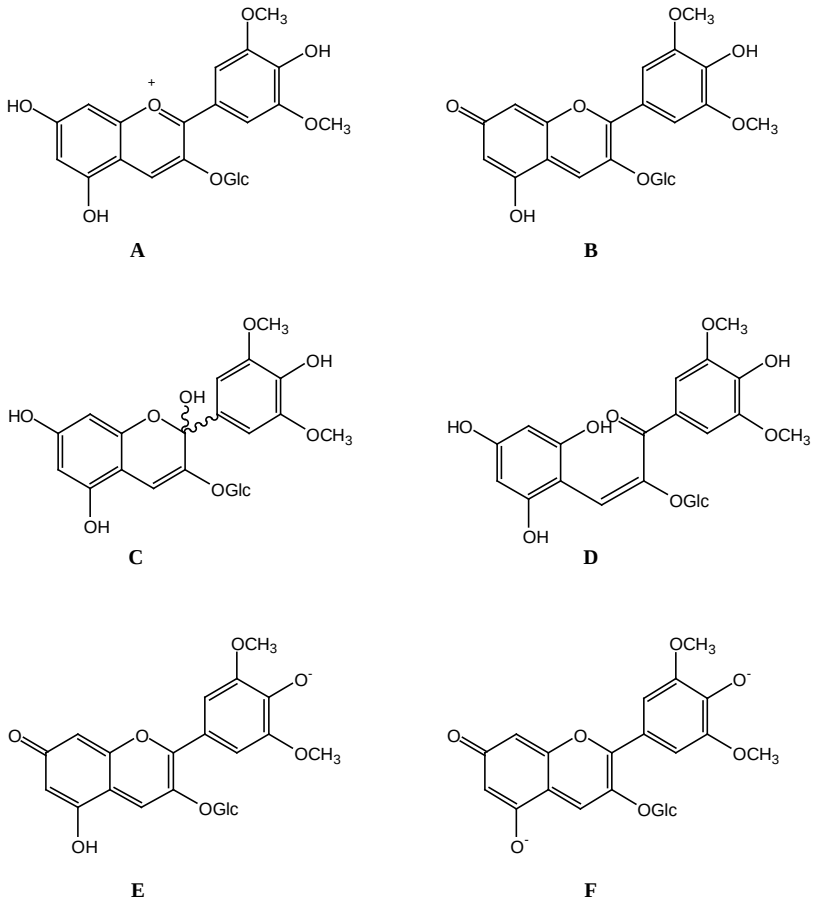

Figure 1.2. pH dependent structures of MV3G**. A** flavylium cation, **B** quinonoidal base, **C** hemiketal, **D** chalcone, **E** quinonoidal anion, **F** quinonoidal dianion (Glc = glucose).

Currently there are two postulated distribution profiles for MV3G. The first (Figure 1.3 (a)), as determined by (Brouillard and Delaporte, 1977), using UV-vis spectroscopy, proposes that the flavylium cation undergoes hydration (pK_H = 2.66) and at a slightly higher pH, the quinonoidal base is formed at low levels (pK_a = 4.25). The second (Figure 1.3 (b)), as determined by (Asenstorfer et al., 2003), using high-voltage paper electrophoresis and UV-vis spectroscopy, proposes that the flavylium cation undergoes deprotonation (pK_a = 1.76) to form the quinonoidal base before hydration occurs (pK_{H1} = 2.66). Asenstorfer et al. (2003) also proposes that the hydrated forms undergo dehydration (pK_{H2} = 5.90) to form the quinonoidal anion.

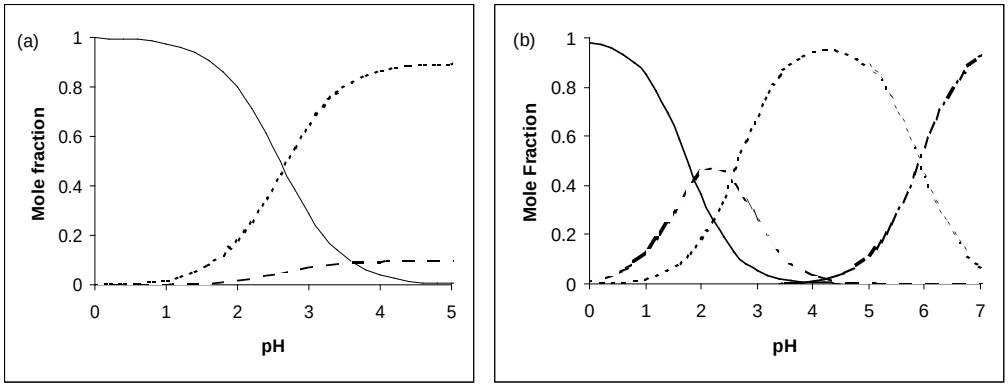

Figure 1.3. Species distributions profiles of MV3G as determined by a) Brouillard and Delaporte (1977) and b) Asenstorfer et al. (2003). (___ - flavylium cation, - quinonoidal base, _ _ _ _ - hydrated forms, _ . _ - quinonoidal anion)

Apart from hydration, anthocyanins can also be decolourised by sulphur dioxide bleaching which attaches as a bisulphite at position 4 (Berke et al., 1998). Substitution at position 4 of the anthocyanin increases the resistance to this sulphur dioxide bleaching (Timberlake and Bridle, 1968) and oxidation (Sweeny and Iacobucci, 1983). Resistance to decolourisation due to pH changes is also increased by substitution at position 4 (Brouillard et al., 1982).

It has been proposed that anthocyanins can undergo direct condensation, at position 4, with flavan-3-ols to create oligomeric and polymeric pigments (Somers, 1971) and orange xanthylium salts (Jurd, 1967). The oligomeric and polymeric pigments extracted from aged red wines have been found to be more resistant to sulphur dioxide bleaching (Somers, 1971) and have greater colour stability over a wider pH range (Somers, 1971).

1.3 Flavan-3-ols

The predominant monomeric flavan-3-ols in grapes are (-)-epigallocatechin, (-)-epicatechin-3-O-gallate and the diastereomers (+)-catechin (Figure1.4 A) and (-)-epicatechin (Figure1.4 B) (Singleton and Noble, 1976). It has been proposed that these flavan-3-ols undergo condensation to form proanthocyanidins and condensed tannins (Haslam, 1980). A number of oligomeric and polymeric proanthocyanidins have been found in the skins and seeds of grapes (Prieur et al., 1994), which predominantly have C4-

C8 or C4-C6 linkages (Balas and Vercauteren, 1994; Cheynier et al., 1992). The C4-C8 linked proanthocyanidin dimers include B1 (epicatechin-4-8-catechin, Figure1.4 C), B2 (epicatechin-4-8-epicatechin, Figure1.4 D), B3 (catechin-4-8-catechin, Figure1.4 E) and B4 (catechin-4-8-epicatechin, Figure1.4 F) whilst the C4-C6 linked proanthocyanidin dimers include B5 (catechin-4-6-epicatechin, Figure1.4 G), B6 (catechin-4-6-catechin, Figure1.4 H), B7 (epicatechin-4-6-catechin, Figure1.4 I) and B8 (epicatechin-4-6-epicatechin, Figure1.4 J). Further condensation reactions can take place in wine to form higher oligomers and condensed tannins. Monomeric flavan-3-ols, proanthocyanidins and condensed tannins are extracted from the seed into the must during the winemaking process. Flavan-3-ols are important contributors to the astringency and mouthfeel of red wines (Arnold et al., 1980)

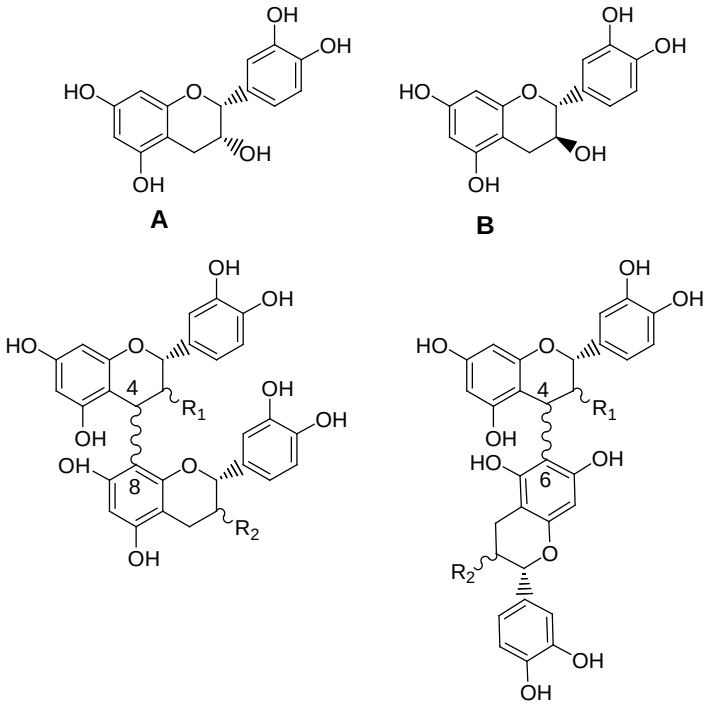

C R_1 = ▮OH , R_2 = ◄OH **G** R_1 = ◄OH , R_2 = ▮OH

D R_1 = ▮OH , R_2 = ▮OH **H** R_1 = ◄OH , R_2 = ◄OH

E R_1 = ◄OH , R_2 = ◄OH **I** R_1 = ▮OH , R_2 = ◄OH

F R_1 = ◄OH , R_2 = ▮OH **J** R_1 = ▮OH , R_2 = ▮OH

Figure 1.4. Monomeric (**A, B**), 4-8 linked dimeric (**C** to **F**) and 4-6 linked dimeric (**G** to **J**) flavan-3-ols.

1.4 Carbonyl compounds

Carbonyl compounds are integral components of yeast metabolism produced during the fermentation of wines and contribute to the odours and flavours of wines (Ebeler and Spaulding, 1998). Yeast strain (Romano et al., 1994), temperature, oxygen and SO_2 levels (Weeks, 1969), pH (Amerine and Ough, 1964) and yeast nutrient availability (Ough and Amerine, 1988; Millan et al., 1991) affect the amount of carbonyl compounds released into the wine.

Wildenradt and Singleton (1974) found that acetaldehyde is formed in wine and model solutions when vicinal di- or trihydroxypolyphenols were present in solution. They proposed that the di- or trihydroxypolyphenols were oxidised by oxygen to form orthoquinones, the orthoquinones reacting with water to form hydrogen peroxide, which in turn oxidised ethanol to form acetaldehyde. Carbonyl compounds can also be formed in wines by metal ion (such as iron and copper) catalysed oxidation of alcohols (Litchev, 1989).

1.5 Compounds formed by the reaction between polyphenols and carbonyl compounds

1.5.1 Reactions of acetaldehyde to form wine pigments

An increase in absorbance at 520 nm was noted by Singleton et al. (1964) when acetaldehydic heads were added to port wines. It was postulated that an acid-catalysed Baeyer reaction took place that formed anthocyanin-$CH(CH_3)$-polyphenol compounds. Due to the structures of the reacting compounds it was also postulated that the ethyl linkage occurred at positions 6 or 8 on the anthocyanin.

Whilst studying model solutions containing anthocyanins, flavan-3-ols and acetaldehyde, Timberlake and Bridle (1976) observed an increase in colour intensity and a change of colour from red to violet. They proposed that an ethyl-bridge was formed between position 8 of the anthocyanins and positions 6 or 8 of the flavanols (Figure1.5).

NOTE: This figure is included on page 7 of the print copy of the thesis held in the University of Adelaide Library.

Figure 1.5 Reaction mechanism for the formation of 8,8-methylmethine-catechin-MV3G (Timberlake and Bridle, 1976)

1.5.1.1 Methylmethine-flavan-3-ol-anthocyanin compounds

In solutions of low pH, a proportion of acetaldehyde is present as the protonated enolic form. Timberlake and Bridle (1976) postulated that the resulting carbonium ion underwent electrophilic addition on position 8 or 6 of the flavan-3-ol (Figure1.5). The alcohol formed lost water and underwent electrophilic addition, to form a methylmethine bridge (-$CH(CH_3)$-), at position 8 or 6 on the anthocyanin (Figure1.5).

Using HPLC, it has been possible to investigate the compounds formed in model wine solutions by the reactions between anthocyanins, flavan-3-ols and acetaldehyde. As the reaction progresses, two new peaks are observed at 520 nm (Roggero et al., 1987; Rivas-Gonzalo et al., 1995). When isolated and investigated by mass spectroscopy, the two compounds giving rise to the individual peaks have the same m/z value (Bridle et al., 1996; Es-Safi et al., 1999) corresponding to 8,8-methylmethine-flavan-3-ol-anthocyanin dimers. The two compounds have similar UV-visible spectra and it has been postulated that the two compounds differ in stereochemistry at the CH position on the ethyl-bridge. No 8,8-methylmethine pigments have been found that contain more than two anthocyanin units

(Es-Safi et al., 1999a). This would suggest that anthocyanins are the terminal units in 8,8-methylmethine oligomeric pigments.

The kinetics of loss of anthocyanins and flavan-3-ols, in the presence of acetaldehyde, has been determined to be first order with respect to anthocyanin loss (Baranowski and Nagel, 1983; Dallas et al., 1996a). The rate of flavan-3-ol loss increases with an increase in its degree of polymerisation (Dallas et al., 1996b). When investigating the reaction kinetics of MV3G and flavan-3-ols in the presence of acetaldehyde Dallas et al. (1996a) found that the rate for the loss of the proanthocyanidin trimer C_1 ($k = 0.439\ day^{-1}$) was more than four times than that of catechin ($k = 0.08\ day^{-1}$) and epicatechin ($k = 0.105\ day^{-1}$), slightly faster than that of the proanthocyanidin dimers B_1 ($k = 0.393\ day^{-1}$) and B_2 ($k = 0.35\ day^{-1}$) and more than twice than that of the proanthocyanidin dimer B_3 ($k = 0.148\ day^{-1}$).

Nuclear magnetic resonance (NMR) has been used to determine the location and type of linkages in oligomeric compounds formed with acetaldehyde. By using flavylium salts as model anthocyanins, Escribano-Bailon et al., (1996) were able to determine the possible structure of methylmethine-catechin-flavylium compounds. Using DEPT, HMQC and HMBC NMR methods it was possible to determine that a methylmethine bridge linked the monomers at position 8. The structure of 8,8-methylmethine-epicatechin-cyanidin-3-galactose has also been found to have the methylmethine bridge at the 8 positions on the moieties (Shoji et al., 2002). As yet however, no NMR studies have been undertaken on the 8,8-methylmethine-catechin-MV3G diastereomers.

Using liquid chromatography coupled with ion spray mass spectroscopy (LC-ISP-MS), Fulcrand et al. (1996) followed the reaction of acetaldehyde with either catechin or epicatechin. They found ethanol adducts on monomers, dimers and trimers that supported the mechanism postulated by Timberlake and Bridle (1976) as shown previously in Figure1.5.

Escribano-Bailón et al. (2001) isolated one of the 8,8-methylmethine-catechin-MV3G diastereomers and studied its properties. It was found to me more resistant to bisulfite bleaching and colour loss due to pH change than the parent anthocyanin. In model solutions stored at 30 ^{0}C the 8,8-methylmethine compound was found to have a faster rate of degradation than MV3G.

Duenas et al. (2006) isolated both diastereomers of 8,8-methylmethine-catechin-MV3G. Using UV-visible spectroscopic methods, and the methodology developed by (Brouillard and Delaporte, 1977), they determined that the 8,8-methylmethine compounds were more acidic that the parent MV3G and had a greater resistance to hydration. It was noted that MC1 underwent slight hydration whilst MC2 did not. In the experiments however, a ratio of molar absorption coefficients was required to achieve linearity to allow the calculations. As there is a discrepency between pK values for MV3G as determined by Brouillard and Delaporte, (1977) and Asenstorfer et al., (2003) further studies on the pK values of these compounds need to be undertaken. Duenas et al. (2006) also found that both pigments have greater resistance to bisulfite bleaching.

1.5.1.2 Vinyl-linked anthocyanin and flavan-3-ol compounds

A group of oligomeric pigments identified in wine and model systems have been found to be resistant to sulphur dioxide bleaching (Dallas and Laureano, 1994). These pigments are believed to be formed by the crosslinking of flavan-3-ol and anthocyanin with acetaldehyde. For a complex pigment to be linked at the 4 position of the anthocyanin, it has been proposed that the anthocyanin would need to undergo nucleophilic addition at this position to form a vinyl-linked compound (Figure1.6). Francia-Aricha et al., (1997) isolated an orange-red pigment (B2-III) from a model solution and from spectroscopic and other data suggested that it was a vinyl-linked anthocyanin-flavan-3-ol compound.

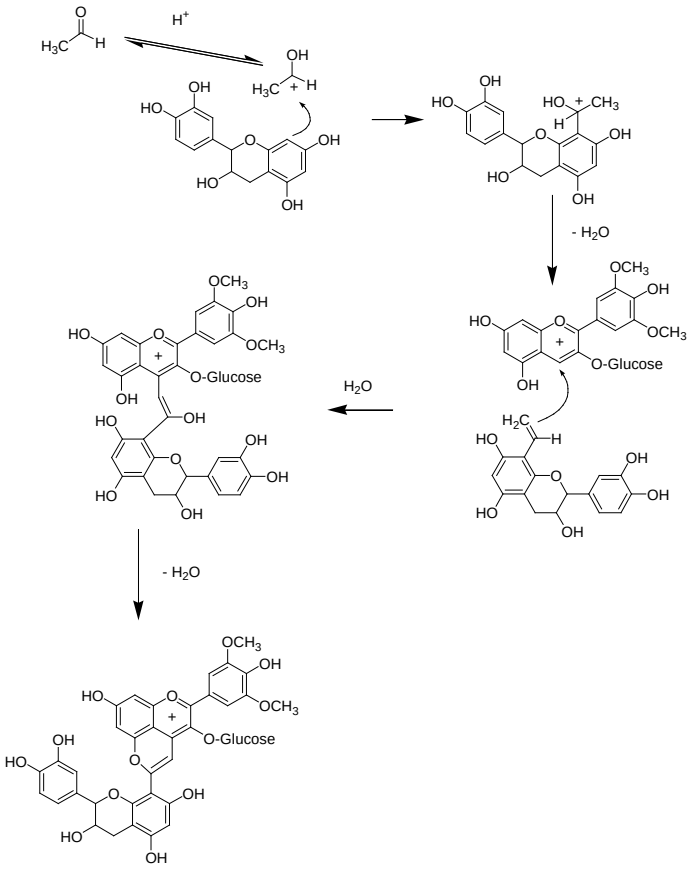

Figure 1.6 Proposed reaction mechanism for the formation of MV3G-4-vinyl-catechin (Francia-Aricha et al., 1997)

From the work of Timberlake and Bridle (1968) and Sweeny and Iacobucci (1983) it is expected that the ethyl and vinyl-linked compounds have different resistances to sulphur dioxide bleaching and oxidation. It is expected that due to the substitution at the 4 position for the vinyl-linked compounds they would have a greater resistance to bleaching than the 8,8-methylmethine compounds. However, (Duenas et al., 2006) have shown that MC1 and MC2 have high resistance to bisulfite bleaching.

1.5.2 Vitisins and related compounds

Vitisins and related compounds are formed when there is a ring closure involving a carbonyl compound (e.g. aldehyde, ketone etc), in its enol form, between positions 4 and the hydroxyl group on position 5 on MV3G forming a fourth ring (Figure1.7) (Benabdeljalil et al., 2000). Benabdeljalil et al. (2000) studied the formation and chromatographic properties of vitisin-type compounds formed via acetaldehyde, pyruvic acid, α-ketoglutaric acid, 3-hydroxybutan-2-one and acetone. They found that all of the vitisin compounds studied had a hypochromatic shift from 530 nm to the 480-514 nm region.

NOTE: This figure is included on page 11 of the print copy of the thesis held in the University of Adelaide Library.

Figure 1.7 Reaction mechanism proposed for the formation of vitisin B (Benabdeljalil et al., 2000)

Bakker and Timberlake (1997) studied the physical properties of vitisin A and vitisin B, isolated from port wine. A change in pH had a smaller effect on the colour expression of the vitisin compounds compared to MV3G. Further studies have shown that vitisins also have greater resistance to sulphur dioxide bleaching than MV3G (Berke et al., 1999).

1.5.3 Occurrence of vitisin-type and ethyl and vinyl-linked pigments in red wines

Grape anthocyanins are the major contributors to the colour of young wines. As wines age, the contribution of oligomeric and polymeric pigments to their colour increases (Somers, 1971). The formation of compounds by the reaction of anthocyanins, flavan-3-ols and carbonyl compounds has been extensively studied in model wine solutions. The use of HPLC and electrospray mass spectroscopy has also allowed the identification of these compounds in wines. 8,8-Methylmethine (Cheynier et al., 1997; Vivar-Quintana et al., 1999) and vinyl-linked (Hayasaka and Asenstorfer, 2002) anthocyanins and flavan-3-ols and vitisins (Bakker and Timberlake, 1997; Vivar-Quintana et al., 1999; Asenstorfer, 2001) have been identified in wines.

1.6 Isolation of grape anthocyanins and wine pigments

A number of methods have been used to isolate MV3G including recrystallisation from isoamyl alcohol (Willstatter and Zollinger, 1916), high-speed counter current chromatography (Degenhardt et al., 2000b), low-pressure liquid column chromatography (Kraemer-Schafhalter et al., 1998; Johnston and Morris, 1996) and semipressure liquid chromatography followed by preparative HPLC (Heredia et al., 1998).

Differential partitioning has been used to isolate MV3G and MV3GCOU (Willstatter and Zollinger, 1916). It was found however, that extraction with isoamyl alcohol produced low yields and repeated recrystallisations with diethyl ether were needed (Asenstorfer, 2001). The effectiveness of the recrystallisations depended upon the quality of the isoamyl alcohol, concentration of the anthocyanins and the presence of water. Furthermore, special refrigeration facilities are required as diethyl ether is used. High-speed counter current chromatography (HSCCC) has recently been used to isolate anthocyanins from red wine (Degenhardt et al., 2000b; Degenhardt et al., 2000a). Sample loads of up to 2 g have been used in HSCCC with run times of up to 300 minutes. Sulfoxyethylcellulose has been used to isolate grape anthocyanins (Spagna and Pifferi, 1992) and wine pigments (Hayasaka and Asenstorfer, 2002). Spagna and Pifferi (1992) encountered a problem whereby there was co-elution of the acetylated anthocyanins with the non-acetylated anthocyanins. Hayasaka

and Asenstorfer (2002) separated C-4 substituted wine pigments on the basis of their resistance to bisulfite bleaching.

To further improve the knowledge of the effect of grape and wine pigments on wine colour and sensory characteristics it is necessary to isolate them in large quantities. This will allow the study of their structures, their physiochemical properties, their physical and colour stabilities and their contribution to the mouthfeel of red wines.

1.7 Objectives

The objectives of this study were to determine the contribution made by 8,8-methylmethine-flavan-3-ol-MV3G compounds to red wine pigment development and to red wine colour. This was done by studying the pigment composition of model wines containing flavan-3-ols and MV3G. To further understand the contribution of 8,8-methylmethine-flavan-3-ol-MV3G compounds to red wine pigment development and to red wine colour, the colour and temporal stabilities of 8,8-methylmethine-(epi)catechin-MV3G compounds were studied. The colour stabilities were studied through colour change with respect to pH change. This was done by determining pK_a and pK_h using UV-visible spectroscopy and HVPE. Further colour stability studies were undertaken by determining their resistance to bisulfite bleaching. The temporal stability of these compounds were determined under anaerobic and aerobic conditions. To gain a further understanding of the colour and temporal stabilities of these compounds, their 3-dimensional structures needed to be determined. This was carried out through molecular modelling. As large quantities of 8,8-methylmethine-(epi)catechin-MV3G were required, new isolation techniques, using size-exclusion and ion exchange liquid chromatography, were developed for their isolation and also for the isolation of MV3G. Mass spectroscopy and NMR were used to identify the isolated compounds.

Chapter 2 - Materials and Methods

2.1 Isolation of MV3G

2.1.1 Grape skin extract preparation

Freeze-dried red grape skin extract (10 g, Waite 2001 Shiraz extracted as per p.78 Iland et al., 2000, kindly donated by the Australian Wine Research Institute) was dissolved in 150 mL aqueous 0.1% v/v TFA (Fluka). The solution was filtered (Whatman No. 1) and the filtrate washed with a further 50 mL aqueous 0.1% v/v TFA.

2.1.2 Size-exclusion chromatography

Toyopearl HW-40(F) (500 mL) was washed three times with 2000 mL 0.1% v/v aqueous TFA. The resin was poured into a column (57 cm x 3.6 cm) to a height of 46 cm and equilibrated with 2000 mL 0.1% v/v aqueous TFA at a flow rate of 4 mL/min using a LKB 12000 Varioperpex peristaltic pump.

The grapeskin extract (200 mL) was applied to the top of the column. Elution was carried out using the following solvents: (1) 0.1% v/v aqueous TFA (2000 mL), (2) 20% v/v aqueous ethanol (BDH) containing 0.1% v/v TFA (1750 mL), (3) 80% v/v aqueous ethanol containing 0.1% v/v TFA (1000 mL) and cleaned with (4) 70% v/v aqueous acetone (BDH) containing 0.1% v/v TFA (500 mL). The flow rate of the sample introduction and eluting solvents was controlled with a LKB 12000 Varioperpex peristaltic pump at 4 mL/min. The column was re-equilibrated with 500 ml of solvents (3) and (2) and 2000 mL solvent (1). The composition of the fractions obtained were monitored using analytical HPLC with a LiChrospher 100 RP18 column (Chapter 2.4.1).

The solvent from fraction (2) was removed by rotary evaporation at 40^0C to give a final volume of 1080 mL.

2.1.3 Cation-exchange chromatography

Sulfoxyethylcellulose (400 mL, Sigma) was prepared as per the method of Spagna and Pifferi (1992). The slurry was introduced to a glass column (32 cm x 3.6 cm) to a height of 27 cm. The resin was equilibrated with 1000 ml 0.02 mol dm^{-3} HCl (BDH) at a rate of 4 mL/min.

The de-alcoholised fraction (2) from the size exclusion chromatography was acidified to 0.02 mol dm^{-3} HCl and applied to the top of the sulfoxyethylcellulose column. Elution was carried out using the following solvents: (1) 0.02 mol dm^{-3} HCl (900 mL), (2) 0.2 mol dm^{-3} HCl in ethanol/water (20:80 v/v, 600 mL), (3) 0.2 mol dm^{-3} HCl in ethanol/water (45:55 v/v, 300 mL) and (4) 0.2 mol dm^{-3} HCl in methanol (1500 mL). 100 mL fractions were collected and stored at 4^0C for analytical HPLC analysis using a LiChrospher 100 RP18 column (Chapter 2.4.1). The sulfoxyethylcellulose column was re-equilibrated with 500 ml of solvents (3) and (2) and 2000 mL solvent (1).

Fractions containing MV3G were combined, diluted with 200 mL H_2O, rotary evaporated at 35^0C to remove the methanol, lyophilised and stored at -15^0C.

2.2 Synthesis of 8,8-methylmethine pigments

MV3G (500 mg, 0.001mol) as isolated in Chapter 2.1, (epi)catechin (500 mg, 0.002mol, Fluka) and 20% v/v aqueous acetaldehyde (1.0 mL, 0.01mol) were added to a 250 mL solution of 0.02 mol dm^{-3} tartaric acid (Ajax) adjusted to approximately pH 2 with concentrated HCl. The reaction mixture was stored in darkness at room temperature and monitored by analytical HPLC (using a LiChrospher 100 RP18 column, Chapter 2.4.1). Once the area of the 8,8-methylmethine compounds had reached a maximum, the solution was retained on a C18 Sep-pak (10 g, Waters). The reaction mixture was washed with aqueous TFA (0.1% v/v), eluted with 30 mL methanol (BDH) and diluted with water and TFA to give a ratio of methanol/water/TFA (50:49.9:0.1).

2.2.1 Isolation of 8,8-methylmethine pigments

2.2.1.1 Size exclusion chromatography

A slurry of Sephadex LH-20 (100 mL, Amersham Biosciences) in methanol/ water/TFA (50:49.9:0.1) was introduced to a glass column (36.5 cm x 1.9 cm) to a height of 33 cm. The column was equilibrated with 500 mL methanol/water/TFA (50:49.9:0.1) at a rate of 3 mL/min.

The crude reaction mixture from Chapter 2.2 was applied to the top of the column and eluted with 200 mL methanol/water/TFA (50:49.9:0.1). Once the red band had reached the bottom of the column 10 mL fractions were collected. Following the elution of the dense red band, further elution was continued with 100 mL methanol/water/TFA (60:39.9:0.1), 100 mL methanol/TFA (99.9:0.1) and acetone/water/TFA (70:29.9:0.1). The column was re-equilibrated with 100 mL methanol/TFA (99.9:0.1) and 500 mL methanol/water/TFA (50:49.9:0.1). The contents of the fractions were monitored using analytical HPLC using a LiChrospher 100 RP18 column (Chapter 2.4.1).

The fractions containing the 8,8-methylmethine compounds were combined, rotary evaporated at 35^0C to remove the methanol, lyophilised and stored at -15^0C.

2.2.1.2 Cation-exchange chromatography

As with the isolation of anthocyanins, the sulfoxyethylcellulose (400 mL, Sigma) was prepared as per the method of Spagna and Pifferi (1992). The slurry was introduced to a glass column (32 cm x 3.6 cm) to a height of 27 cm. The resin was equilibrated with 1000 ml 0.02 mol dm^{-3} NaCl (BDH) at a rate of 4 mL/min. NaCl was used instead of HCl to prevent hydrolysis of the isolated pigments.

The de-alcoholised fractions from the size exclusion chromatography (Chapter 2.2.1.1) were diluted with 0.02 mol dm^{-3} NaCl and applied to the top of the sulfoxyethylcellulose column. The 8,8-methylmethine pigments were eluted using the following solvents: (1) 0.02 mol dm^{-3} NaCl (900 mL), (2) 0.1 mol dm^{-3} NaCl in ethanol/water (10:90 v/v, 600 mL), (3) 0.2 mol dm^{-3} NaCl in ethanol/water (10:90 v/v, 300 mL), (4) 0.2 mol dm^{-3} NaCl

in ethanol/water (20:80 v/v, 300 mL), (5) 0.2 mol dm^{-3} NaCl in ethanol/water (50:50 v/v, 300 mL) and (6) 0.2 mol dm^{-3} NaCl in methanol (1500 mL). Fractions (10 mL) were collected and stored at 4^0C for analytical HPLC analysis using a LiChrospher 100 RP18 column (Chapter 2.4.1). The sulfoxyethylcellulose column was re-equilibrated with 200 mL of (5), (4), (2) and 900 mL of (1).

The fractions containing the particular 8,8-methylmethine diastereomer were combined, rotary evaporated at 35^0C and retained on a C18 Sep-pak cartridge (10g, Waters). The C18 Sep-pak cartridge was washed with 0.02 mol dm^{-3} HCl to remove the NaCl. The pigment retained on the Sep-pak cartridge was eluted with methanol. Aqueous TFA (0.1% v/v) was added to the solution and the methanol was removed by rotary evaporation (35^0C). The resultant aqueous solution was lyophilised and stored at $^-15^0$C.

2.3 Synthesis and isolation of proanthocyanidin dimers

2.3.1 Isolation of proanthocyanidins B1 and B2

Proanthocyanidins B1 and B2 were isolated in the laboratory from a commercial grape tannin extract (Grapex, Tarax Technologies Australia). The extract was dissolved in methanol:water (30:70) and applied to a reverse phase C18 column (Grace Chemicals, Melbourne, Australia). Elution was carried out with methanol:water (30:70). Repeated application and elution afforded fractions containing the desired proanthocyanidins. The fractions were monitored on TLC using Merck silica 60 F254 aluminium plates with toluene:acetone:acetic acid (3:3:1) as mobile phase. These fractions were combined and concentrated by applying to a LH20 column using methanol:water (10:90) as eluent. The concentrated proanthocyanidin fractions were separated on a reverse phase C18 column (eluting with a gradient of methanol:water (10:90) to methanol:water (40:60)) to afford fractions containing proanthocyanidins B1 and B2. The fractions were combined, the methanol was removed by rotary evaporation (35^0C) and the resultant aqueous solution was lyophilised and stored at $^-15^0$.

2.3.2 Synthesis and isolation of proanthocyanidins B3 and B4

Proanthocyanidins B3 and B4 were synthesised and isolated in the laboratory by dissolving 250 mg taxifolin (Sigma) and 250 mg (+)-catechin (Fluka, proanthocyanidin B3) or 250 mg (-)-epicatechin (Fluka, proanthocyanidin B4**)** (250 mg) in ethanol (previously purged with nitrogen). Sodium borohydride (300 mg) in ethanol was added over 30 minutes. The reaction mixture was stirred, under nitrogen, for 2 hours whereafter water was added. The pH was adjusted to 5.0 with 10% acetic acid and the reaction mixture was allowed to stand for 1 hour. The proanthocyanidins were extracted with ethyl acetate. Water was added to the ethyl acetate phase and the ethyl acetate was removed by rotary evaporation (35^0C). Proanthocyanidins B3 and B4 were isolated by consecutive liquid chromatography on Sephadex LH-20 (eluting with methanol:water (40:60)) and reverse phase C18 (eluting with a gradient of methanol:water (10:90) to methanol:water (40:60)). The methanol was removed by rotary evaporation (35^0C) and the resultant aqueous solution was lyophilised.

2.4 Analytical HPLC

Analytical HPLC was conducted using a Waters HPLC system (WISP 710 autosampler, 501 solvent delivery system, 996 diode array detector and a temperature control system) and the results analysed using Waters Millennium software. The columns used for HPLC analysis were: 1) LiChrospher 100 (Supelco) RP18 column (250 mm x 4.6 mm) and 2) Platinum EPS C18 Rocket (Alltech) column (53 mm x 7 mm). The column temperature was maintained at 30^0C. Detection was by a photodiode array detector covering the 250 nm – 700 nm range of wavelengths with the progress monitored at 280 nm and 520 nm.

The concentration of the anthocyanins and 8,8-methylmethine compounds were measured as equivalents of MV3G and MC2 respectively as determined by peak areas at 520 nm by comparison with previously established concentration curves. The purity of the anthocyanins and 8,8-methylmethine compounds were calculated from their peak areas at 280 nm. The concentration of pyranoanthocyanins were measured as equivalents of MV3G as determined by peak area at 520 nm by comparison with previously established concentration curves. The concentration of (epi)catechin, proanthocyanidins and other colourless compounds were measured as equivalents of catechin as determined by peak

area at 280 nm by comparison with previously established concentration curves. The concentration of other (unidentified) pigments was determined by subtracting the peak areas of known pigments from the total peak area at 520 nm and expressed as equivalents of MV3G.

2.4.1 LiChrospher 100 RP18

Analytical HPLC analysis was carried out on a LiChrospher 100 (Supelco) RP18 column (250 mm x 4.6 mm) protected by a LiChrospher RP18 guard column. A binary solvent system consisting of (A) 1% v/v aqueous formic acid and (B) formic acid/acetonitrile/water (1:50:49) using a linear gradient from 0% B to 100% B over 30 minutes and an isocratic elution of 100% B for 10 minutes at a flow rate of 1.0 mL/min. Injection volume was 10 μL (Rivas-Gonzalo et al., 1995).

2.4.2 Platinum EPS C18 Rocket

Analytical HPLC analysis was carried out on a Platinum EPS C18 Rocket (Alltech) column (53 mm x 7 mm) protected by a LiChrospher RP18 guard column. A binary solvent system consisting of (A) 2% v/v aqueous formic acid and (B) acetonitrile using an isocratic elution of 10% B for 2 minutes, a linear gradient from 10% B to 60% B over 8 minutes, 60% B to 100% B over 2 minutes and an isocratic elution of 100% B for 2 minutes at a flow rate of 1.5 mL/min. Injection volume was 10 μL.

2.5 Mass Spectrometry

Mass spectra were obtained using an API-300 mass spectrometer with an ionspray interface (PE Sciex, Thornhill, Ontario, Canada) connected to a HPLC (LC-MS) system. The ion spray and orifice potentials were 5.5 kV and 30 V for the positive ion mode and –4.5 kV and –30 V for the negative ion mode respectively. The samples were injected using a flow injector with a 5 μL loop coupled to a C18 reversed-phase HPLC column (2 x 150 mm, Nova-Pak, Waters) at a flow rate of 100 μL/min. A binary solvent system consisting of (A) 2.5% v/v aqueous acetic acid and (B) acetic acid/acetonitrile/water (2.5:90:7.5) was

used. The programme for the solvents was a linear gradient from 10% B to 70% B over 60 minutes and from 70% to 100% B from 60 to 70 minutes, with a flow rate of 5 μL/min. The mass spectral data were processed using Bio-Multiview software 1.2β3 (PE Sciex).

2.6 Nuclear Magnetic Resonance Spectroscopy

Spectra were recorded on a Varian Inova 600 MHz Spectrometer operating at 600 MHz for ^{1}H and 150 MHz for ^{13}C. One-dimensional ^{1}H and ^{13}C and two-dimensional spectra including DQCOSY, ROESY, HSQC and HMBC were recorded at 298 K. The freeze-dried samples (40 mg) were dissolved in D_2O acidified with 20% v/v HCl (9:1) immediately prior to analysis.

2.7 Molecular Modelling

CS Chem3D Pro® version 5.0 was used to determine the structural conformations and properties of MC1, MC2, ME1 and ME2. The energy states of the compounds was minimised using MM2. Physical dimensions were determined by measuring the distance between terminal atoms in the relevant dimension. The cubic volume was calculated by multiplying the three dimensions of the compounds. Dipole measurements were calculated using MOPAC molecular computations with AM1 theory, closed shell wave function and Mullikin charges.

2.8 Estimation of Ionisation Constants Using High Voltage Paper Electrophoresis (HVPE)

2.8.1 Calculations

The predicted mobility (m_p) can be estimated at each pH (Equation 2.1, Asenstorfer et al., 2003). The derivitisation of Equation 2.1 is outlined in Appendix 1. The number of terms in the numerator and the divisor is dependent upon the number of ionisations, e.g. for a single ionisation only the first two terms are required. It should be noted that Equation 2.1

is constrained by the number of variables, therefore due to experimental effects, e.g. buffer ion concentration, a slight deviation of the experimental data from the theoretical curve may occur.

$$m_p = \frac{m_0 + m_1.10^{pH-pK_1} + m_2.10^{2pH-pK_1-pK_2} + ...}{1+10^{pH-pK_1} + 10^{2pH-pK_1-pK_2} + ...}$$ Equation 2.1

The macroscopic pKa calculations were estimated for each buffer separately as it was not possible to obtain a continuous mobility profile across all of the buffers. This is due to discontinuities between the buffers used.

2.8.2 Apparatus

The apparatus used for HVPE was based on the immersed strip method (Tate, 1981). The elctrophoretogram was immersed in an inert liquid, tetrachloroethylene, to dissipate the heat (Tate, 1981). A water-cooling coil was used to maintain an operating temperature of approximately 25^0C.

2.8.3 Method for the Estimation of Ionisation Constants

The buffers, voltages and times (Table 2.1), were based on those used by Asenstorfer et al. (2003) for the determination of the ionisation constants of MV3G. The oxalate buffer consisted of 0.1 mol dm^{-3} oxalic acid (BDH) and the oxalate/citrate buffer was prepared my mixing 0.05 mol dm^{-3} oxalic acid (BDH) and 0.05 mol dm^{-3} citric acid (BDH). The buffers were pH adjusted with sodium hydroxide (BDH). An Activon Model 210 (Thornleigh, NSW, Aust.) pH meter was used to measure the pH values. The pH meter was calibrated using pH 4 and 7 buffers (BDH).

Table 2.1. Parameters used in HVPE measurements

pH	**Buffer**	**Volts (V)**	**Amps (mA)**	**Power (mW)**	**Time (min)**
1.4 – 3.0	oxalate	1850	80	150	45
3.2 – 4.6	oxalate	1850	80	150	60
3.0 – 5.0	oxalate / citrate	2000	75	150	60
5.2 – 7.4	oxalate / citrate	2000	75	150	75

The elctrophoretogram consisted of chromatography paper (Number 1, Whatman). The relative mobilities (Rm_{OG}) were compared to the neutral standard fructose and the anionic standard Orange G (Sigma, 1-phenylazo-3,5-disulphonate). A silver stain (2 g dm^{-3} silver nitrate, Sigma, in acetone) and 1 mol dm^{-3} sodium hydroxide (BDH) in 80% v/v ethanol was used to reveal the position of fructose (Tate, 1981).

Graphs were plotted from the calculated relative mobilities and the predicted mobility curve (Equation 2.1) was fitted using WinCurveFit version 1.1.8 (Kevin Raner Software, Aust.). The WinCurveFit software also calculated error and regression estimates.

2.9 Estimation of Hydration and Ionisation Constants using UV-visible Spectrophotometry

2.9.1 Calculations

The calculation of macroscopic pK values can be determined by applying Equation 2.2 to UV-visible spectroscopic data. The derivitisation of Equation 2.2 is outlined in Appendix 1 (Asenstorfer, 2001). As noted previously for Equation 2.1, Equation 2.2 is constrained by the number of variables. Therefore due to experimental effects a slight deviation of the experimental data from the theoretical curve may occur.

$$Abs_p = \frac{Abs_0 + Abs_1.10^{pH-pK_1} + Abs_2.10^{2pH-pK_1-pK_2} + ...}{1+10^{pH-pK_1} + 10^{2pH-pK_1-pK_2} + ...} \qquad \text{Equation 2.2}$$

2.9.2 Apparatus

A Carey 1 spectrophotometer was used to obtain the UV-visible spectra of the compounds. The pH of the solutions was obtained with a FET pH meter (pH Boy-P2; Shindigen, Japan).

2.9.3 Method for the Estimation of Ionisation Constants

The macroscopic hydration (pK_H) or ionisation (pK_a) constants of MC1, MC2, ME1 and ME2 were estimated by using two 10 mL equimolar solutions (38 mol dm^{-3}) prepared at

pH 0.7 (0.2 mol dm^{-3} HCl) and at pH 7.2 (0.2 mol dm^{-3} trisodium citrate, BDH). The citrate buffer was titrated with the hydrochloric acid solution to obtain a series of spectra ranging from pH 7.2 to pH 0.7. UV-visible spectra were taken using a 10 mm quartz cell covering the wavelengths from 250 nm to 750 nm. The spectra were post processed using GRAMS/32 software. An array basic program (Appendix 2) was written to obtain the absorbances at the chosen analytical wavelengths (450 nm, 480 nm and 540 nm).

Graphs were plotted from the determined absorbances and the predicted absorbances (Equation 2.1) were fitted using WinCurveFit version 1.1.8 (Kevin Raner Software, Aust.). The WinCurveFit software also calculated error and regression estimates.

2.10 UV-visible spectroscopy

UV-visible spectroscopy was carried out on either a Carey 1 spectrophotometer (Varian, Melbourne, Australia) with a 10 mm pathlength quartz cell maintained at approximately 25^0C or on a Helios α spectrophotometer (Thermo Scientific, Melbourne, Australia) using a 2 mm pathlength quartz cell with spectra recorded from 250 to 700 nm.

2.11 Estimation of the stability of 8,8-methylmethine-(epi)catechin-MV3G compounds to change in pH

Data obtained from the UV-visible spectroscopy determination of ionisation and hydration constants was used to determine the stability of MC1, MC2, ME1 and ME2 with regards to pH. The colour density (A_{420} + A_{520} adjusted to 10 mm pathlength, Somers, 1971) and Glories' colour density (A_{420} + A_{520} +A_{620} adjusted to 1 mm pathlength, Glories, 1984) were calculated for the solutions. The spectra were integrated in the visible region (400 nm to 700 nm) at the baseline using GRAMS/32 software to calculate the spectra area and the centre of mass of the spectra. The spectra areas were calculated as a percentage of the spectra area obtained at pH 1 and plotted against pH.

2.12 Estimation of the stability of 8,8-methylmethine-(epi)catechin-MV3G compounds to sulfur dioxide

Citrate (0.2 mol dm^{-3}) buffer solutions at pHs 2.8 and 3.3 containing $2x10^{-4}$ mol dm^{-3} MV3G, MC1, MC2, ME1 and ME2 were prepared. The spectra were taken using a Helios α spectrometer covering the wavelengths 250 nm to 700 nm using a 2 mm quartz cell. Sulfur dioxide (10 g/L) was added to a concentration of 50 mg/L and the solutions were allowed to stand for 30 minutes. The spectra were retaken using the above parameters. The colour density (A_{420} + A_{520} adjusted to 10 mm pathlength) was calculated for the solutions before and after the addition of sulfur dioxide.

2.13 Estimation of the stability of 8,8-methylmethine-(epi)catechin-MV3G compounds to oxidation

Model wine solutions consisted of 2.5 g/L potassium hydrogen tartrate (BDH) in 10% v/v aqueous ethanol. The pH was adjusted to 3.6 using tartaric acid (BDH). MC1 and MC2 were added to 60 mL of this solution to give a concentration of approximately 35 mg/L. This allowed an absorbance of approximately 1.0 at 535 nm. A much higher concentration of MV3G (230 mg/L) was required to achieve an absorbance of approximately 1.0 at 520 nm. Half of the solution was split into three open 10 mL vials. The other half was sparged thoroughly with nitrogen for 10 minutes and placed into three sealed vials containing a septum in the lid. The solutions were stored in the dark at room temperature (approximately 20^0C). The concentrations were measured regularly using analytical HPLC with a Platinum EPS C18 Rocket column. Colour density (A_{420} + A_{520}) and hue (A_{520}/A_{420}) was also obtained for each sample at regular intervals by visible spectroscopy, using a Helios α spectrometer, covering the wavelengths 350 nm to 750 nm.

The concentration [A] of the substance studied at time t, is dependent upon the order of the reaction and the rate constant k:

Zero order: $[A] = [A_0] - kt$ Equation 2.3

First order: $[A] = [A_0].e^{-kt}$ Equation 2.4

Second order: $[A] = \frac{[A_0]}{1 + kt[A_0]}$ Equation 2.5

where $[A_0]$ is the initial concentration.

The data obtained from the HPLC chromatograms was transformed and plotted using the formulae:

Zero order: $[A_0] - [A] = kt$ Equation 2.6

First order: $\ln \frac{[A]}{[A_0]} = -kt$ Equation 2.7

Equation 2.8

Second order: $\frac{1}{[A]} - \frac{1}{[A_0]} = kt$

The linearity of the plot indicates the order of the reaction and the slope afforded the rate constant. The error associated with k was calculated using linear regression analysis in Microsoft Excel.

Once the reaction order and the rate constant were determined the half-life was estimated using the relevant equation:

Zero order: $t_{1/2} = \frac{[A_0]}{2.k}$ Equation 2.9

First order: $t_{1/2} = \frac{\ln 2}{k}$ Equation 2.10

Second order: $t_{1/2} = \frac{1}{k.[A_0]}$ Equation 2.11

2.14 Wine Fermentations

2.14.1 Fermentation media

CDGJM in 1L contained: 200g glucose (BDH), 2.5g potassium tartrate (BDH), 0.44g calcium chloride (BDH), 2.78g ammonium sulfate (BDH), 2.5mL trace vitamin solution (400 x standard stock solution), 2mL trace mineral solution (500 x standard stock solution), 10mL salts (50 x standard stock solution).

2.14.2 Reagents

The reagents used in the winemaking processes were MV3G, proanthocyanidins B1 and B2, proanthocyanidin B3 and proanthocyanidin B4 which were isolated as previously discussed (Chapter 2.3), and commercially obtained catechin (Fluka).

2.14.3 Fermentation conditions

Flasks (100ml) containing CDGJM was inoculated with yeast (*Saccharomyces cerevisiae bayanas* EC1118) to a concentration of 1 x 10^6 cells/mL. The conditions used were: a) control, b) MV3G (400 mg dm^{-3}), c) MV3G (400 mg dm^{-3}) and catechin (300 mg dm^{-3}) e) MV3G (400 mg dm^{-3}) and proanthocyanidin B3 (580 mg dm^{-3}), f) MV3G (400 mg dm^{-3}) and proanthocyanidin B4 (580 mg dm^{-3}) and g) MV3G (400 mg dm^{-3}) and proanthocyanidins B1 and B2 (580 mg dm^{-3}). Fermentations were also carried out with the yeasts *Saccharomyces cerevisiae* Syrah and BDX with MV3G (400 mg dm^{-3}) and catechin (300 mg dm^{-3}). Each fermentation condition was carried out in triplicate.

The fermentations were conducted at 30^0C and the flasks containing MV3G were protected from light by aluminium foil. Refractive indices were taken to monitor the progress of the ferments. Once the refractive indices were below 6.5 a clinie test was used to verify that the ferment had gone to completion.

The ferments were centrifuged and the wine drained off the lees. Each wine was adjusted to approximately pH 3.6 using 10 mol dm^{-3} sodium hydroxide. Three samples (20 mL) of each wine were placed in sealed vials and stored in the dark at room temperature for aging.

Analysis of the samples was carried out regularly with HPLC using a Platinum EPS C18 Rocket column (Chapter 2.4.2) and UV-visible spectroscopy with a Helios α spectrometer (Chapter 2.10).

Chapter 3 - Isolation of anthocyanin monoglucosides and 8,8-methylmethine-(epi)catechin-MV3G and pigments

3.1 Introduction

Isolation of anthocyanins is necessary to further understand their properties and to synthetically prepare their condensation products found in red wine (Somers, 1971; Jurd, 1967; Timberlake and Bridle, 1976; Francia-Aricha et al., 1997; Bakker and Timberlake, 1997; Benabdeljalil et al., 2000) and to understand their properties and their contribution to red wine colour. A problem encountered by chemists in the isolation of anthocyanins from grape skins and wines is the complexity of the extracts obtained. Apart from the mixture of anthocyanin monoglucosides and acetylated anthocyanin monoglucosides, there are also their condensation products, monomeric, oligomeric and polymeric flavan-3-ols and sugars. Whilst anthocyanins may readily be separated from sugars by using an XAD-7 column (Kraemer-Schafhalter et al., 1998), the isolation, of large quantities, of individual anthocyanins is more complicated. Selective extraction and precipitation (Willstatter and Zollinger, 1916) and high speed counter current chromatography has been used in the isolation of MV3G and other anthocyanins (Degenhardt et al., 2000a; Degenhardt et al., 2000b).

The isolation of 8,8-methylmethine-epicatechin-cyanidin-3-galactoside compounds has been achieved eluting the compounds from a preparative ODS packed column followed by further purification on a preparative ODS packed column (Shoji et al., 2002). Escribano-Bailón et al. (2001) isolated one of the 8,8-methylmethine-catechin-MV3G diastereomers (MC2) using preparative HPLC. However, isolation of significant amounts of the other diastereomer (MC1) was not achieved using this method as it readily degraded. Recently, isolation of both diastereomers has been achived using semipreparative HPLC (Duenas et al., 2006).

In this study, size-exclusion liquid chromatography followed by cation-exchange liquid chromatography was investigated as a method for the large-scale isolation of anthocyanin monoglucosides (especially MV3G) and 8,8-methylmethine-(epi)catechin-MV3G compounds. Although the small-scale synthesis of 8,8-methylmethine compounds has been extensively studied, including their rates of formation under various conditions, little work has been done on their synthesis and isolation on a larger scale.

3.2 Results

3.2.1 Isolation of MV3G

The crude Shiraz grape skin extract contained numerous compounds including phenolic acids, flavan-3-ols of varying degrees of polymerisation and anthocyanins (Figure 3.1 (a)). The chromatogram recorded at 280 nm (Figure 3.1 (a)) also displays a "hump" (Wulf and Nagel, 1978) characteristic of HPLC chromatograms of grape and wine extracts. As a percentage of total anthocyanins (Figure 3.1 (b)), the extract consisted of 60.1% MV3G, 14.3% PT3G, 9.8% MV3GCOU, 5.6% DP3G and 5.4% MV3GACET. The purities of MV3G, PT3G, MV3GCOU, DP3G and MV3GACET, as peak area percentage measured at 280 nm, were determined as 8.4%, 1.3%, 2.7%, 0.7% and 1.1% respectively.

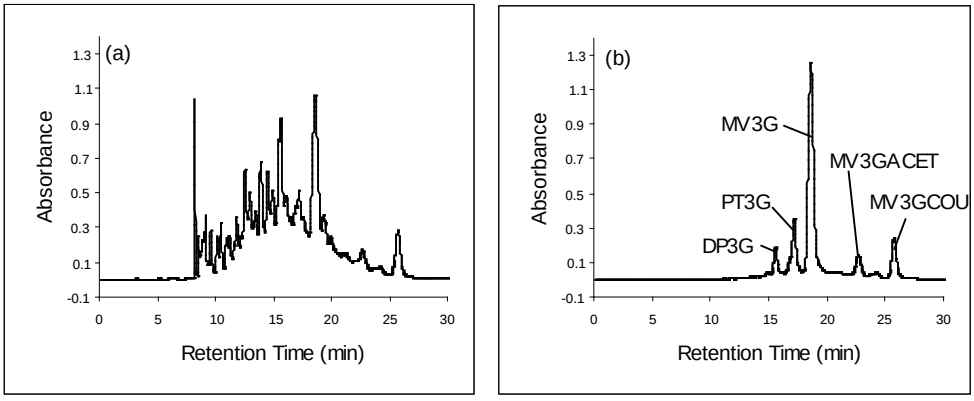

Figure 3.1. HPLC chromatograms of the crude grape extract recorded at (a) 280 nm and (b) 520 nm.

3.2.1.1Size-exclusion chromatography

The crude grape extract was subjected to size exclusion chromatography on a column containing HW-40(F) resin and four fractions were obtained. Fraction (1) was obtained with 0.1% aqueous TFA and contained a number of compounds that absorbed at 280 nm (Figure 3.2 (a)) but not at 520 nm (Figure 3.2 (b)). A peak (~17 minutes) was observed in the chromatogram that absorbed at 520 nm.

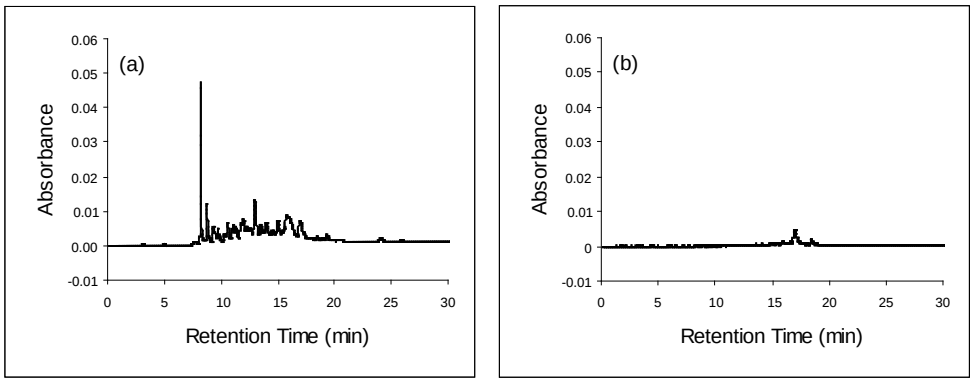

Figure 3.2. HPLC chromatograms of TSK HW-40(F) fraction (1) at (a) 280 nm and (b) 520 nm.

Elution of the HW-40(F) column with 20% aqueous ethanol (Fraction (2)) eluted the bulk of the anthocyanin monoglucosides (Figure 3.3 (b)), trace amounts of acylated anthocyanin monoglucosides (Figure 3.3 (b)) and some colourless polyphenols (Figure 3.3 (a)). The MV3G content of this fraction was 447 mg. As a percentage of total anthocyanins (Figure 3.3 (b)), the fraction consisted of 80% MV3G, 12.1% PT3G, 4.5% DP3G and 1.8% MV3GACET. The purities of MV3G, PT3G and DP3G, as peak area percentage measured at 280 nm, were determined as 53.4%, 10.4% and 2.6% respectively.

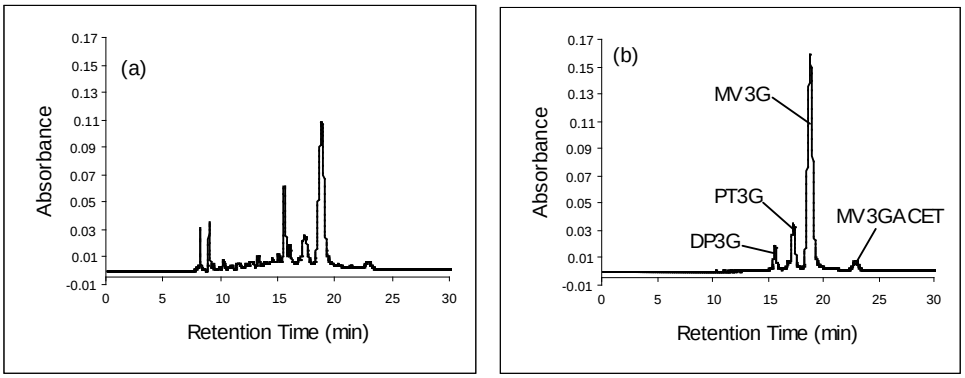

Figure 3.3. HPLC chromatograms of TSK HW-40(F) fraction (2) at (a) 280 nm and (b) 520 nm.

Further elution with 80% aqueous ethanol (Fraction (3)) eluted further colourless polyphenols (Figure 3.4 (a)), acylated anthocyanins (Figure 3.4 (b)) and part of the "hump" (Figure 3.4). The principle anthocyanins in this fraction were MV3GCOU and MV3GACET (Figure 3.4 (b)).

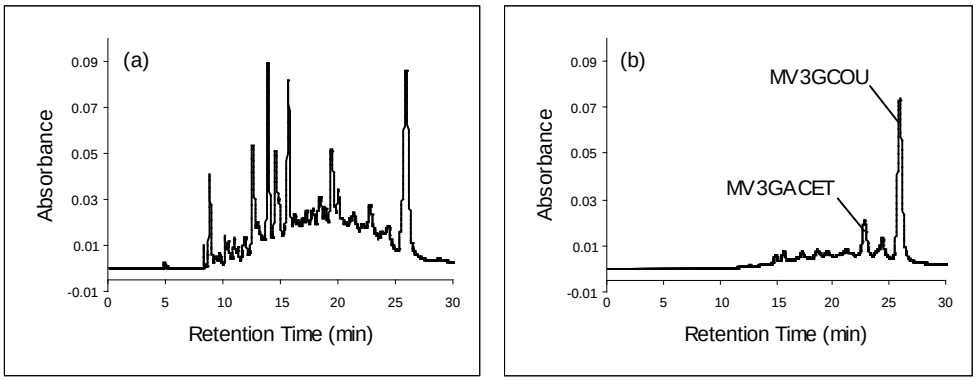

Figure 3.4. HPLC chromatograms of TSK HW-40(F) fraction (3) at (a) 280 nm and (b) 520 nm.

Finally, elution with 70% acetone (Fraction (4)) eluted the "hump" (Figure 3.5 (a)) which since it was slightly coloured (Figure 3.5 (b)).

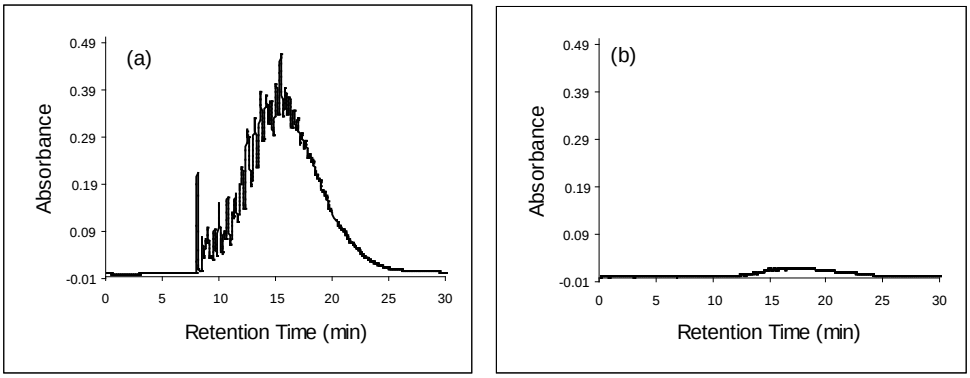

Figure 3.5. HPLC chromatograms of TSK HW-40(F) fraction (4), after the removal of acetone, at (a) 280 nm and (b) 520 nm.

3.2.1.2 Cation-exchange chromatography

The elution profile of the TSK HW-40(F) fraction (2) on sulfoxyethylcellulose is shown in Figure 3.6. Aqueous 0.02M HCl eluted the colourless neutral compounds. The samples had an orange-red colour due to small amounts of anthocyanins eluting (1-2 mg/L).

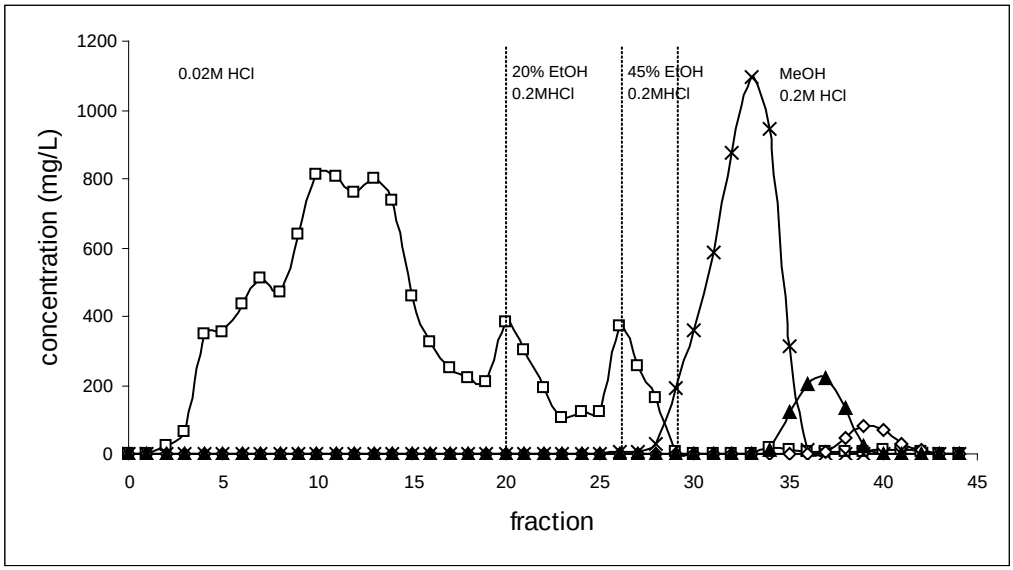

Figure 3.6. Elution profile of TSK HW-40(F) fraction (2) on sulfoxyethylcellulose. (□) Colourless products; (x) MV3G; (▲) PT3G; (◊) DP3G.

Further colourless compounds were eluted consecutively with 20% ethanol and 45% ethanol (Figure 3.6). The 20% ethanol fractions had a more intense pink-red colour, compared to the 0.02M HCl fraction, again due to small amounts of anthocyanins eluting (2-3 mg/L). The 45% ethanol fractions had a slightly deeper red colour (with a pink tint). The increase in colour was due to increased amounts of anthocyanins (5 mg/L increasing to 50 mg/L) including MV3GACET, which eluted just before MV3G.

Elution with 100% methanol eluted the anthocyanins in the following order (Figure 3.6): MV3G, PT3G and DP3G. PT3G eluted towards the end of the MV3G elution thereby causing a slight decrease in the purity of MV3G obtained. Fractions 29 to 35 (Figure 3.6) were combined and after lyophilisation, 402 mg MV3G chloride was obtained with a purity of 96%. PT3G chloride (46 mg, 88% purity) and DP3G chloride (27 mg, 82% purity) were isolated by combining fractions 36 to 38 and fractions 39 to 42 respectively (Figure 3.6).

Identification and purity of the isolated anthocyanins was confirmed by mass spectrometry. The *m/z* values of the isolated anthocyanins were 465.0 (aglycone fragment 303.2), 479.0 (aglycone fragment 317.2) and 493.2 (aglycone fragment 331.2), which correspond to DP3G, PT3G and MV3G respectively (Monagas et al., 2003).

3.3 Synthesis of 8,8-methylmethine-(epi)catechin-MV3G compounds

After 3 days the MV3G and catechin reaction mixture containing acetaldehyde consisted of 55mg MV3G (8%) and high levels of 8,8-methylmethine compounds MC1 (203 mg, 27%) and MC2 (281 mg, 35%) (Figure 3.7 (a)). The MV3G and epicatechin reaction mixture containing acetaldehyde consisted of 105mg MV3G (16%), 143 mg ME1 (21%) and 270 mg ME2 (36%) (Figure 3.7 (b)). In both reaction mixtures, further condensation had occurred with the presence of peaks eluting after MC1 and MC2 (ME1 and ME2) during HPLC analysis of the reaction mixtures (Figure 3.7). As can be seen in Figure 3.7, there is a slightly higher difference in retention times for ME1 and ME2 as compared to MC1 and MC2.

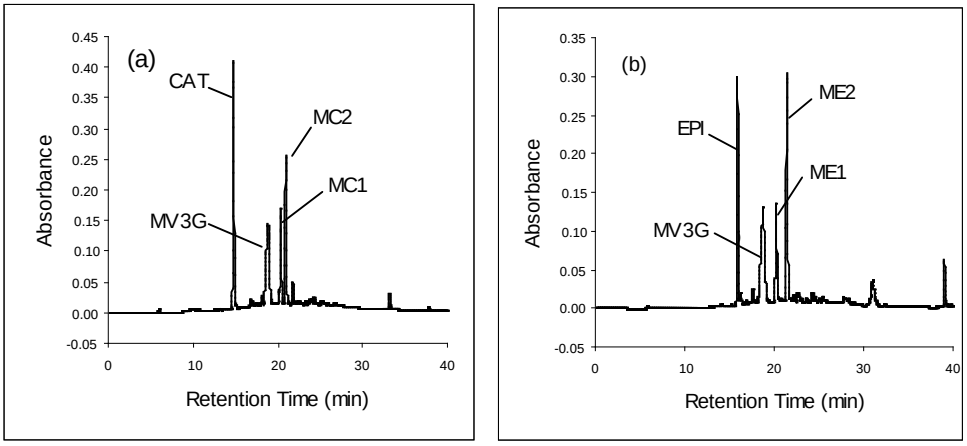

Figure 3.7. HPLC chromatogram of the MV3G and (a) catechin and (b) epicatechin reaction mixture recorded at 280 nm.

3.3.1 Isolation of 8,8-methylmethine-(epi)catechin-MV3G compounds

3.3.1.1 Size-exclusion chromatography

Chromatography on LH-20 allowed convenient separation of the 8,8-methylmethine compounds from MV3G and catechin as shown in Figure 3.8. Elution with methanol/water/TFA (50:49.9:0.1) eluted in the following order: MV3G, MC1 and MC2 and catechin. Further condensed compounds eluted after MC1 and MC2 and during and after catechin. A similar order of elution of MV3G, ME1 and ME2 and epicatechin was obtained when epicatechin was used as the reagent instead of catechin.

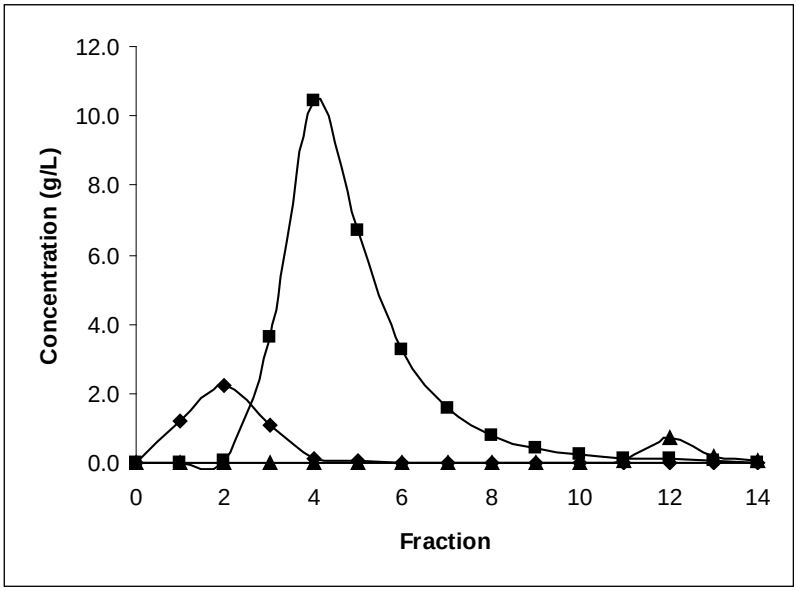

Figure 3.8. Fractions and compound concentration of the LH-20 chromatography of the MV3G, catechin and acetaldehyde reaction mixture. (♦) MV3G; (■) MC1 and MC2; (▲) catechin.

3.3.1.2 Cation-exchange chromatography

The fractions containing high concentrations of the 8,8-methylmethine compounds, with some co-eluting compounds (MV3G and catechin), (fractions 3 to 10, (Figure 3.8) were combined and applied to the sulfoxyethylcellulose column after the relevant treatment (Chapter 2.2.1). Elution with increasing concentrations of NaCl and ethanol afforded in the following order: MV3G, MC2 (ME2) and MC1 (ME1) (Figure 3.9). Although there was some co-elution between MC2 (ME2) and MV3G and between MC1 (ME1) and MC2 (ME2), it was possible to isolate the 8,8-methylmethine-(epi)catechin-MV3G diasteromers of sufficient purities (>80%).

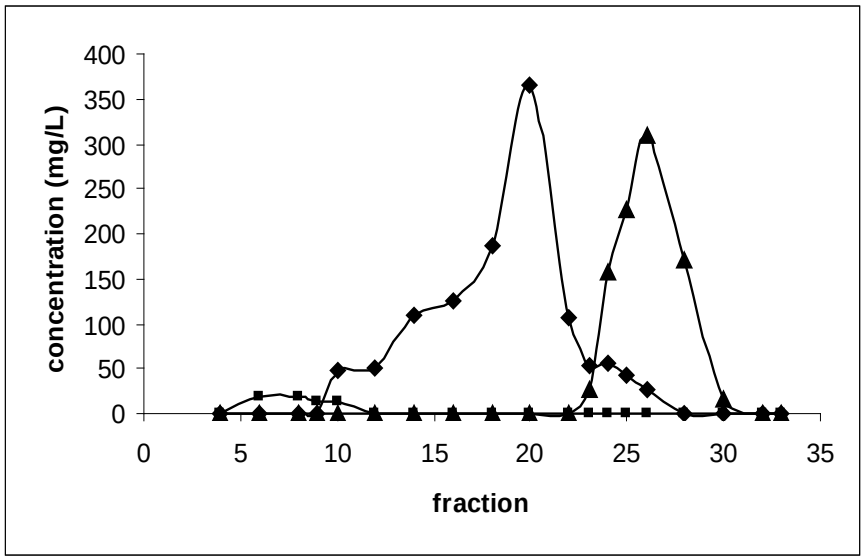

Figure 3.9. Elution profile on sulfoxyethylcellulose of LH-20 fractions 3 to 10, of the MV3G and catechin reaction mixture. (■) MV3G; (▲) MC1; (♦) MC2

After combining the relevant fractions and lyophilisation, the trifluroroacetate salts of the following 8,8-methylmethine compounds were obtained: MC1 (125 mg, 83% purity), MC2 (220 mg, 87% purity), ME1 (44 mg, 85% purity) and ME2 (79 mg, 90% purity).

3.4 Discussion

This study showed that size-exclusion liquid chromatography followed by cation exchange liquid chromatography proved an effective method for the isolation of large quantities of anthocyanin monoglucosides and 8,8-methylmethine-(epi)catechin-MV3G compounds. Previous methods used for the large scale isolation of anthocyanins have included size-exclusion liquid chromatography (Kraemer-Schafhalter et al., 1998), selective extraction and precipitation (Willstatter and Zollinger, 1916) and high speed counter current chromatography (Degenhardt et al., 2000b). The isolation 8,8-methylmethine-(epi)catechin-MV3G compounds has been achieved by preparative ODS packed columns (Shoji et al., 2002) and (semi)preparative HPLC (Escribano-Bailón et al., 2001; Duenas et al., 2006).

The use of TSK HW-40(F) afforded the isolation of anthocyanins from the bulk of polyphenols which has not been shown in the use of XAD-7 (Kraemer-Schafhalter et al., 1998). The high loading capacity of TSK HW-40(F) allowed the fractionation of large quantities of samples (up to 15 g on a 57 x 3.6 cm column). The large volumes of the fractions collected (500-2000 mL) ensured that the fractionation was not labour intensive. The hydrophobic groups on the TSK HW-40(F) allowed the fractionation of the grape skin extract in four broad fractions consisting of a) low molecular weight polyphenols with a small amount of PT3G, b) anthocyanin monoglucosides and monomeric and dimeric flavan-3-ols, c) acylated anthocyanin monoglucosides and oligomeric flavan-3-ols and d) polymeric flavan-3-ols. Size-exclusion chromatography enabled the separation of anthocyanin monoglucosides from the “hump” and increased the purity of MV3G, as measured at 280 nm, from 8.4% to 53.4%.

Sulfoxyethylcellulose has been used for the isolation of anthocyanins (Spagna and Pifferi, 1992). However, Spagna and Pifferi (1992) reported the co-elution of acetylated anthocyanin monoglucosides with anthocyanin monoglucosides. By carrying out size-exclusion chromatography beforehand, the levels of acetylated anthocyanin monoglucosides are decreased and thereby reduce the levels of co-eluting acetylated anthocyanin monoglucosides. Although separate bands could be observed on the sulfoxyethylcellulose column, there was some co-elution between the anthocyanin

monoglucosides. This involved the co-elution of PE3G with MV3G and CY3G with PT3G. Despite the co-elution, it was still possible to isolate the anthocyanin monoglucosides of sufficient purity. In grape extracts and wines, the co-eluting anthocyanins (PE3G and CY3G) only make a small contribution to the total anthocyanins (Wulf and Nagel, 1978; Piergiovanni and Volonterio, 1980). Due to the use of hydrochloric acid, there are losses of anthocyanins due to hydrolysis (Willstatter and Zollinger, 1916). Other acids such as trifluoroacetic acid and formic acid were investigated in an effort to reduce anthocyanin losses. However, these acids did not promote the elution of the compounds, which remained adsorbed to the solid phase. Sodium chloride could not be used in this instance as MV3G readily elutes and would co-elute with the colourless compounds, such as flavan-3-ols.

The synthesis of 8,8-methylmethine-(epi)catechin-MV3G compounds required a balance between levels of product formation, the time taken for this to occur, and the levels of by-products formed by further condensation. Garcia-Viguera et al. (1994) showed that in the pH rage of 2 to 5, the highest and most rapid levels of formation occurred at pH 2. A pH of 2 was used in this study as the reaction mixture afforded a rapid formation of significant amounts of 8,8-methylmethine-(epi)catechin-MV3G compounds with accepteable levels of by-products.

Size-exclusion chromatography on LH-20 separated the MV3G, (epi)catechin and acetaldehyde reaction mixture into three broad fractions. The three fractions were 1) MV3G, 2) 8,8-methylmethine-(epi)catechin-MV3G compounds (including some MV3G) and 3) (epi)catechin. The 8,8-methylmethine-(epi)catechin-MV3G compounds eluted immediately after the band of MV3G which made the complete separation between them and MV3G not possible. Although the 8,8-methylmethine-(epi)catechin-MV3G compounds eluted immediately after MV3G, they were highly concentrated (Figure 3.9) which facilitated their further isolation. The elution of (epi)catechin, the smallest molecule of interest, well after the concentrated bands of MV3G and the 8,8-methylmethine-(epi)catechin-MV3G compounds is in agreement with previous studies using LH-20 (Prior et al., 2001) where flavan-3-ols eluted after anthocyanin monoglucosides. This could be due to MV3G and the 8,8-methylmethine-(epi)catechin-MV3G compounds in their flavylium forms having a greater affinity for the acidic eluent compared to (epi)catechin, as

the separation of anthocyanins and flavan-3-ols is based on the number of phenolic hydrogens of the compounds bonding with hydrogen-bond acceptors in the gel (Kantz and Singleton, 1990).

Separation of the 8,8-methylmethine-(epi)catechin-MV3G diastereomers was achieved using cation-exchange chromatography on sulfoxyethylcellulose. This would suggest that the two diastereomers had different levels of attraction to the cation-exchange resin. This could be due to either the diastereomers having a large difference in pKa values, hence a different charge to mass ratio at a particular pH, or that if the pKa values are similar, the separation is due to differences in the dimensions or structures of the molecules.

An advantage by isolating the 8,8-methylmethine-(epi)catechin-MV3G diastereomers through size-exclusion liquid chromatography followed by cation exchange liquid chromatography is that it can be readily scaled-up for the isolation of larger quantities (e.g. for the use in sensory studies). The scale-up is easier and cheaper compared to semipreparative HPLC (Duenas et al., 2006). Although MV3G has been isolated using high speed counter current chromatography (Degenhardt et al., 2000b), as yet there have been no reports made for its use in the isolation of 8,8-methylmethine-(epi)catechin-MV3G compounds.

The use of sodium chloride as the ion in the solvent, instead of hydrochloric acid altered the order of elution of MV3G compared to the other compounds of interest. With hydrochloric acid, the order of elution went from the larger molecules to the smaller ones i.e.: MV3GACET (Mw 535 g/mol), MV3G (Mw 493 g/mol), PT3G (Mw 479 g/mol) and DP3G (Mw 465 g/mol). This is expected, as at low pH the anthocyanins are in the flavylium form (Asenstorfer et al., 2003) and the order of elution follows the increase in charge to mass ratio. With sodium chloride on the other hand, MV3G eluted before the larger 8,8-methylmethine-(epi)catechin-MV3G compounds. This could be due to the change in pH of the eluting solutions. With sodium chloride, the pH is higher so MV3G and the 8,8-methylmethine-(epi)catechin-MV3G compounds are in their anionic/neutral forms (quinonoidal anion, quinonoidal base and hydrated forms) so the order of elution follows the increase in mass/molecule size.

With greater emphasis of waste management being placed on laboratories and companies it is necessary to reduce the volume of waste produced in the isolation of the products of interest. Preparative HPLC and High Speed Counter Current Chromatography rely on eluents that are of either HPLC grade or are of a mixture that cannot be reused (Escribano-Bailón et al., 2001; Degenhardt et al., 2000b). The size-exclusion and cation-exchange chromatography methods used in this study for the isolation of anthocyanin monoglucosides and 8,8-methylmethine-(epi)catechin-MV3G compounds have the advantage that the eluents do not require to be of HPLC grade and that they can be recovered and reused (as was done in this study). Although the recovered eluents may have a slightly different concentration, as compared to the original, the elution gradient is such that this will have little effect on the elution profile and therefore the final purity of the compound of interest.

Chapter 4 - Characterisation of 8,8-methylmethine-(epi)catechin-MV3G pigments

4.1 Introduction

Nuclear magnetic resonance (NMR) has been used to determine the location and type of linkages in oligomeric compounds formed with acetaldehyde. By using flavylium salts as model anthocyanins, Escribano-Bailon et al. (1996) were able to determine the structure of 8,8-methylmethine-catechin-flavylium compounds. Using DEPT, HMQC and HMBC NMR methods they determined that an ethyl bridge linked the flavylium and catechin moieties at the 8-positions. The structure of 8,8-methylmethine-epicatechin-cyanidin-3-galactose has also been found to have the ethyl bridge at the 8-positions on the cyanidin-3-galactose and epicatechin (Shoji et al., 2002). Although the formation rates of 8,8-methylmethine-flavan-3-ol-MV3G compounds have been extensively studied (Baranowski and Nagel, 1983; Dallas et al., 1996b; Dallas et al., 1996a) the structures of these pigments have not been determined. To further understand the physico-chemical properties and the colour and temporal stabilities of these compounds, it is necessary to know their structures. The determination of the structures for 8,8-methylmethine-(epi)catechin-MV3G using mass spectrometry, 1- and 2-dimensional NMR spectroscopy and molecular modelling are discussed in this chapter.

4.2 Results

4.2.1 Mass Spectrometry

MC1 , MC2, ME1 and ME2 all gave a molecular ion *m/z* 809 amu (Figure 4.1) in the positive ion mode. Daughter ions of *m/z* 647, 519 and 357 were recorded which respectively corresponded to the cleavage of glucose (162 amu), catechin (290 amu) and glucose and catechin (162+290 amu).

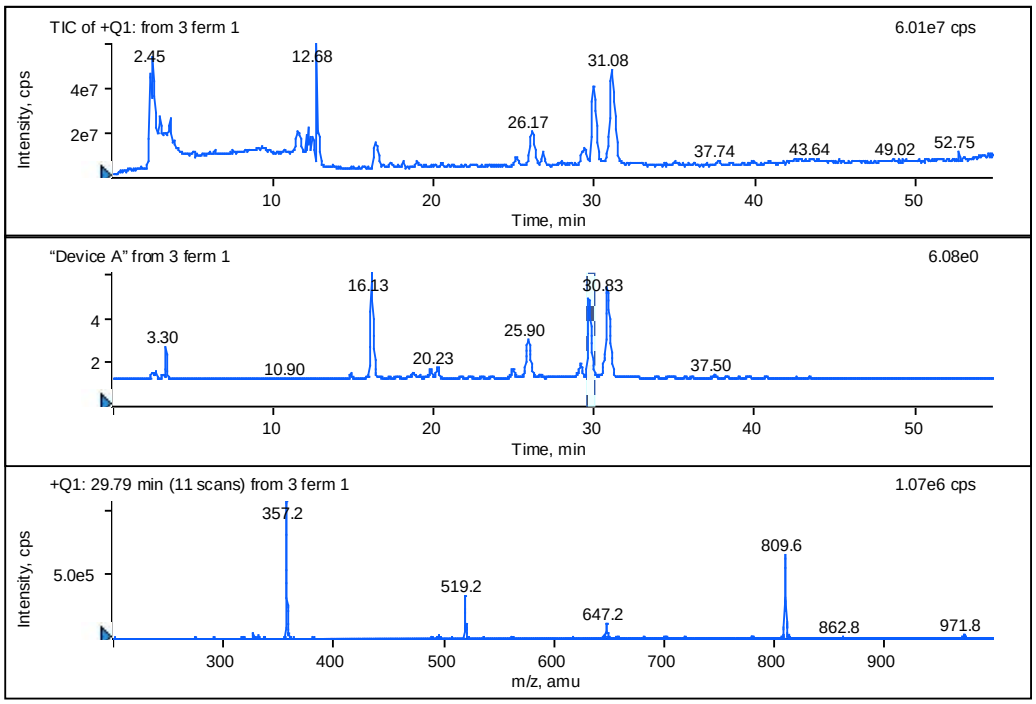

Figure 4.1. Mass spectra of MC1 obtained in the positive ion mode .

4.2.2 Nuclear magnetic resonance spectrometry

The numbering used for ^{1}H and ^{13}C assignments in the NMR analysis of MC1, MC2, ME1 and ME2, as discussed in this chapter, is shown in Figure 4.2.

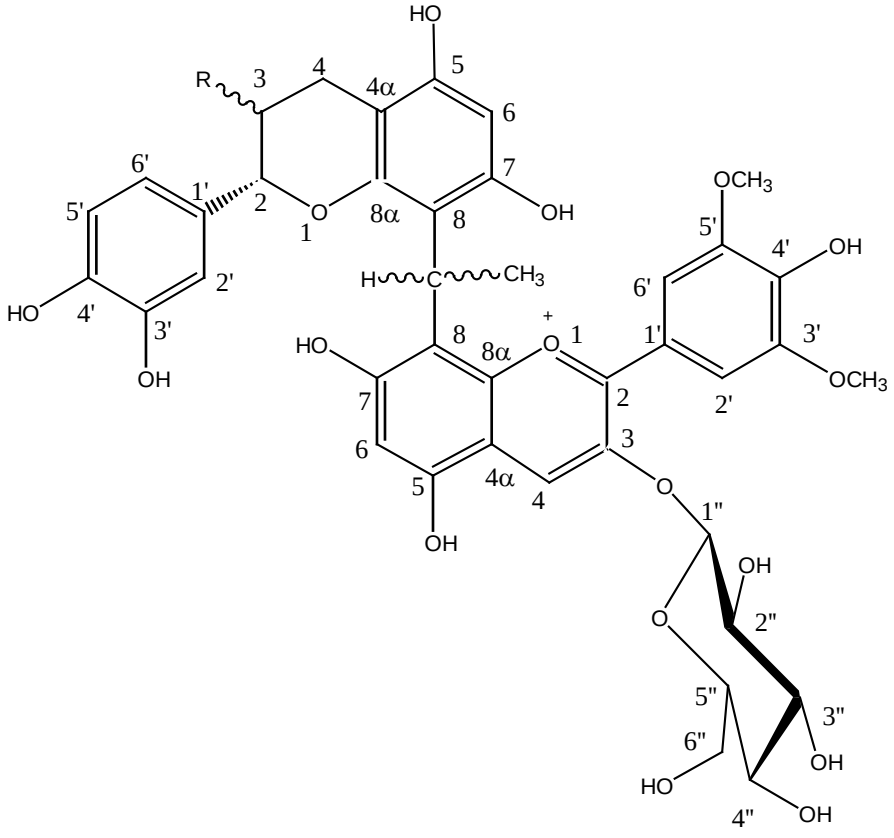

catechin R = OH

epicatechin R = OH

Figure 4.2. Structure and numbering of MC1, MC2, ME1 and ME2.

4.2.2.1 Solvent system

Initially deuterium chloride was used to acidify the solvent so that the structures of the compounds would be in their flavylium forms. However this caused the disappearance of the proton signal for MV3G H-6 (Figure 4.3 (b)). The proton signal for MV3G H-6 was visible when hydrochloric acid was used instead of deuterium chloride (Figure 4.3 (a)).

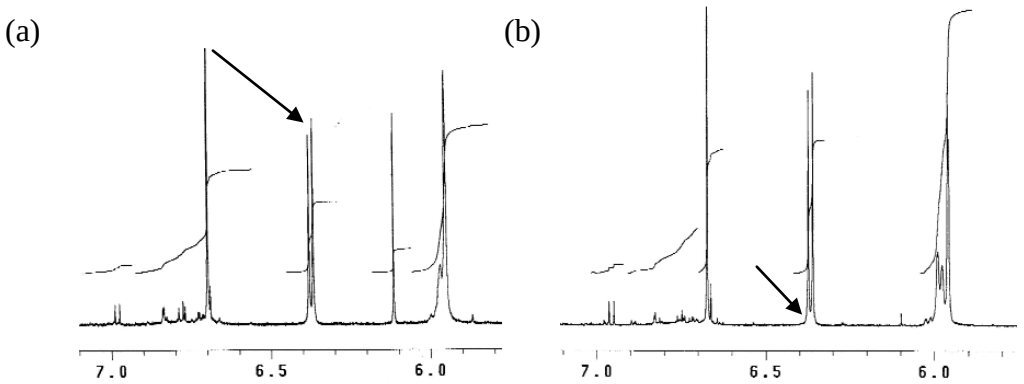

Figure 4.3. Proton signal for MV3G H-6 (arrowed) of MC2 with (a) HCl and (b) DCl in the solvent.

4.2.2.2 ^{1}H NMR

The ^{1}H NMR spectra of the four compounds showed seven aromatic proton signals, one of which when integrated indicated two protons (MC1: δ7.70; MC2: δ7.88; ME1: δ7.73; ME2: δ7.76). Based on previous ^{1}H NMR spectra of MV3G (Berke et al., 1999) these were assigned to the equivalent MV3G H-2',6'. The chemical shifts (MC1: δ8.67; MC2: δ8.77; ME1: δ8.70; ME2: δ8.85) and (MC1: δ6.75; MC2: δ6.67; ME1: δ6.76; ME2: δ6.70) were assigned to the MV3G H-4 and H-6 or H-8. The remaining aromatic singlet was assigned to the (epi)catechin H-6 or H-8 (MC1: δ6.17, MC2: δ6.11; ME1: δ6.17; ME2: δ6.20). The proton signals assigned to H-6 or H–8 could not definitely be assigned for MV3G and (epi)catechin as their chemical shifts are similar (Berke et al., 1999; Escribano-Bailon et al., 1996; Shoji et al., 2002). Three doublets were observed (MC1: δ5.91; MC2: δ5.96, 1.8 Hz; ME1: δ6.02; ME2: δ6.11), (MC1: δ6.34, 7.8 Hz; MC2: δ6.36, 7.8 Hz; ME1: δ6.32, 7.8 Hz; ME2: δ6.25, 7.8 Hz) and (MC1: δ5.94; MC2: δ5.98, 7.8 Hz; ME1: δ5.98; ME2: δ5.98) which are characteristic of catechin (Escribano-Bailon et al., 1996) and epicatechin (Shoji et al., 2002) and were assigned to H-2', H-5' and H-6' respectively. An absence of second proton signals for H-6/8 for the MV3G and (epi)catechin moieties indicates that the ethyl bridge is at either the 6- or 8-position of the constituent units.

A large singlet peak (MC1: δ3.83; MC2: δ3.90; ME1: δ3.83; ME2: δ3.90) corresponded to the methoxy groups at the 3'- and 5'-positions as previously determined by other authors (Berke et al., 1999). A doublet (MC1: δ5.35, 7.8 Hz; MC2: δ5.30, 7.8 Hz; ME1: δ5.30;

ME2: δ5.47, 7.2 Hz) was assigned as the anomeric proton H-1". DQCOSY coupling (Appendix 2) enabled the assignment of the glycosyl protons H-2" (MC1: δ3.71; MC2: δ3.68; ME1: δ3.70; ME2: δ3.73), H-3" (MC1: δ3.73; MC2: δ3.58; ME1: δ3.62; ME2: δ3.64), H-4" (MC1: δ3.59; MC2: δ3.48; ME1: δ3.60; ME2: δ3.62), H-5" (MC1: δ3.62; MC2: δ3.64; ME1: δ3.69; ME2: δ3.72), H-6"a (MC1: δ3.89; MC2: δ3.83; ME1: δ3.89; ME2: δ3.89) and H-6"b (MC1: δ4.03; MC2: δ4.01; ME1: δ3.99; ME2: δ3.99).

Two aliphatic doublet of doublets shared a common carbon and were assigned as (epi)catechin H-4a (MC1: δ2.84, 16.2 Hz, 5.4 Hz; MC2: δ2.94, 16.2 Hz, 6.0 Hz; ME1: δ2.72, 16.2 Hz, 4.0 Hz; ME2: δ2.78, 16.8 Hz, 4.2 Hz) and H-4b (MC1: δ2.34, 16.2 Hz, 9.6 Hz; MC2: δ2.37, 16.2 Hz, 9.6 Hz; ME1: δ2.58, 16.8 Hz, 2.4 Hz; ME2: δ2.65, 16.8 Hz, 2.4 Hz). The DQCOSY spectra showed that the protons at the 4-position were coupled to a multiplet that was assigned as H-3 (MC1: δ3.64; MC2: δ3.72; ME1: δ3.87; ME2: δ3.84), which in turn was coupled to a doublet assigned as H-2 (MC1: δ4.97; MC2: δ4.03, 8.4 Hz; ME1: δ4.38; ME2: δ4.59, 8.4Hz).

An aliphatic hydrogen doublet (MC1: δ1.62, 7.8 Hz; MC2: δ1.78, 7.8 Hz; ME1: δ1.70, 7.8 Hz; ME2: δ1.70, 8.4 Hz) which when integrated indicated three protons was assigned as the methyl group of the methylmethine bridge. The DQCOSY spectra indicated that this is coupled with a quartet (MC1: δ4.97; MC2: δ5.2, 15.0 Hz; ME1: δ5.08, 13.8 Hz; ME2: δ5.41, 15.6 Hz) which was assigned as the methine group of the methylmethine bridge.

4.2.2.3 ^{13}C NMR

HSQC spectra (Appendix 2) were used to assign the following MV3G carbon peaks: C-4 (MC1: δ135.3; MC2: δ135.5; ME1: δ135.5; ME2: δ135.0), C-6/-8 (MC1: δ104.1; MC2: δ103.8; ME1: δ103.7; ME2: δ104.4), C-2' (MC1: δ113.0; MC2: δ111.0; ME1: δ110.4; ME2: δ110.7), C-6' (MC1: δ110.5; MC2: δ111.0; ME1: δ110.4; ME2: δ110.6), C-1" (MC1: δ103.1; MC2: δ103.9; ME1: δ103.4; ME2: δ102.8), C-2" (MC1: δ75.4; MC2: δ75.7; ME1: δ75.4; ME2: δ75.4), C-3" (MC1: δ78.2; MC2: δ78.8; ME1: δ78.4; ME2: δ78.3), C-4" (MC1: δ71.1; MC2: δ71.4; ME1: δ71.1; ME2: δ71.0), C-5" (MC1: δ78.2; MC2: δ79.1; ME1: δ78.4; ME2: δ77.9), C-6" (MC1: δ62.2; MC2: δ62.7; ME1: δ62.2;

ME2: δ61.6) and methoxy-3' and –5' (MC1: δ57.6; MC2: δ57.5; ME1: δ57.7; ME2: δ57.4). As mentioned in the previous section, C-6/-8 could not be definitely assigned with this data.

The following (epi) catechin carbon signals were also assigned through HSQC: C-2 (MC1: δ83.2; MC2: δ84.0; ME1: δ80.5; ME2: δ81.0), C-3 (MC1: δ68.7; MC2: δ68.4; ME1: δ66.7; ME2: δ66.3), C-4 (MC1: δ29.6; MC2: δ30.4; ME1: δ29.7; ME2: δ29.2), C-6/-8 (MC1: δ97.4; MC2: δ96.7; ME1: δ97.0; ME2: δ97.1), C-2' (MC1: δ115.2; MC2: δ115.8; ME1: δ115.3; ME2: δ113.8), C-5' (MC1: δ116.7; MC2: δ117.0; ME1: δ116.7; ME2: δ115.4) and C-6' (MC1: δ119.8; MC2: δ120.4; ME1: δ120.4; ME2: δ119.8). As with MV3G, C-6/-8 could not be definitely assigned for the (epi)catechin moiety with this data.

The methine group (MC1: δ27.7; MC2: δ28.1; ME1: δ27.7; ME2: δ26.9) and the methyl group (MC1: δ20.6; MC2: δ20.6; ME1: δ20.8; ME2: δ19.2) of the methylmethine bridge carbons were also assigned through HSQC.

For the MV3G moiety, common HMBC correlations (Appendix 2) between H-4 and H-2'/-6' enabled the assignments of C-2 (MC1: δ161.9; MC2: δ162.7; ME1: δ162.1; ME2: δ161.0) and C-1' (MC1: δ120.5; MC2: δ120.3; ME1: δ120.4; ME2: δ120.5); between H-4 and H-6/-8 enabled the assignments of C-5 (MC1: δ155.2; MC2: δ157.0; ME1: δ155.5; ME2: δ155.8), C-4a (MC1: δ114.4; MC2: δ114.6; ME1: δ114.6; ME2: δ113.7) and C-8a (MC1: δ156.5; MC2: δ155.8; ME1: δ156.7; ME2: δ156.6); between H-4 and H-1" enabled the assignments of C-3 (MC1: δ145.5; MC2: δ146.6; ME1: δ145.4; ME2: δ145.8). Further common HMBC correlations between H-2'/-6' and the 3'/5' methoxy protons enabled the assignments of C-3' and C-5' (MC1: δ149.4; MC2: δ149.9; ME1: δ149.5; ME2: δ149.3). H-2'/-6' had a HMBC correlation which was assigned to C-4' (MC1: δ144.5; MC2: δ146.0; ME1: δ144.6; ME2: δ145.5) and H-6/-8 had a correlation which was assigned to C-6/-8 (MC1: δ113.0; MC2: δ113.7; ME1: δ113; ME2: δ113).

Common HMBC correlations (Appendix 2) were also used to further determine ^{13}C signals for the (epi)catechin moiety. Common correlations between H-2 and H-5' enabled the assignment of C-1' (MC1: δ130.0; MC2: δ131.4; ME1: δ132.4; ME2: δ131.7); between H-3, H-4a, H-4b and H-6/-8 enabled the assignments of C-4a (MC1: δ102.4; MC2: δ103.8; ME1: δ100.7; ME2: δ101.2); between H-4a, H-4b and H-6/-8 enabled the assignments of C-5 (MC1: δ155.0; MC2: δ155.7; ME1: δ156.0; ME2: δ156.6) and C-8a (MC1: δ155.2; MC2: δ155.5; ME1: δ156.6; ME2: δ156.7) and between H-2', H-5' and H-6' enabled the assignments of C-3' (MC1: δ145.3; MC2: δ146.7; ME1: δ145.4; ME2: δ145.6) and C-4' (MC1: δ145.3; MC2: δ146.7; ME1: δ145.6; ME2: δ145.5). H-6/-8 had further correlations which were assigned as C-7 (MC1: δ155.2; MC2: δ155.5; ME1: δ155.2; ME2: δ155.6) and C-6/-8 (MC1: δ110.5; MC2: δ108.7; ME1: δ110.6; ME2: δ108.7).

4.2.2.4 Determination of the position of the methylmethine bridge

Strong ROESY interactions were observed between the methyl group of the methylmethine bridge and H-6' and the methoxy group of the MV3G (Figure 4.4) which suggested a spatial proximity. To have such a spatial proximity the methylmethine bridge would need to be at the 8-position on the MV3G. Further confirmation of the position of the ethyl bridge was obtained by a HMBC correlation observed between the methine group of the methylmethine bridge and the C-8a position of the MV3G which had a connectivity to H-4 (Figure 4.4). A HMBC correlation between the methine group of the methylmethine bridge and the C-8a position of the (epi)catechin moiety indicated that the methylmethine bridge was on the 8-position on the (epi)catechin. Furthermore, no HMBC correlations were observed between the methine group and C-5 and C-7 of the MV3G and (epi)catechin which would occur if the linkage was at the 6-position (Saucier et al., 1998).

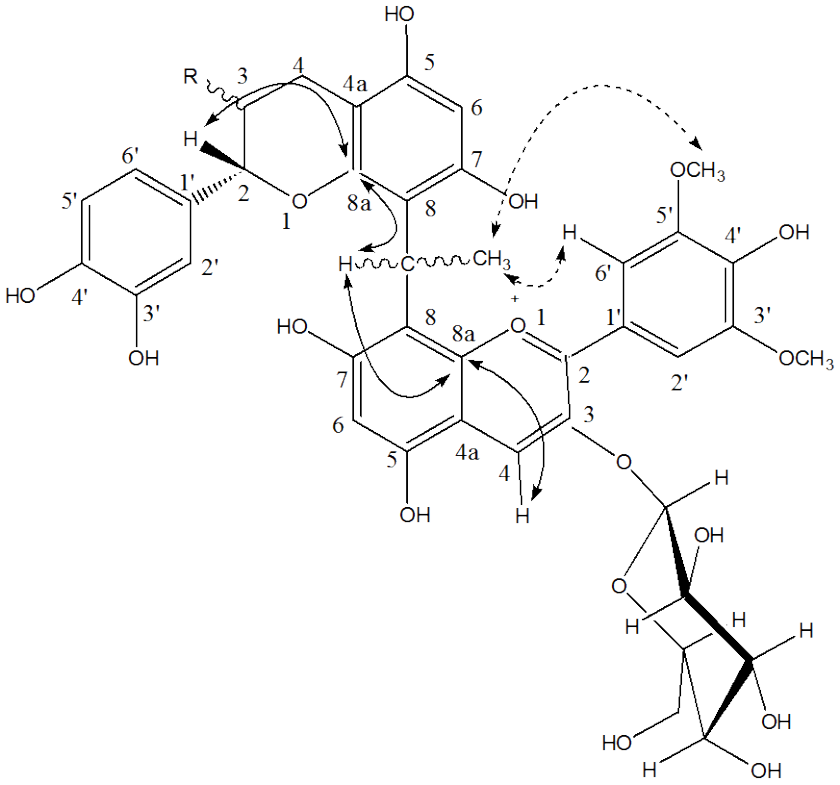

Figure 4.4. HMBC (solid lines) and ROESY (dashed lines) correlations for MC1, MC2, ME1 and ME2.

4.2.3 Molecular Modelling

ROESY interactions were observed between the (epi)catechin H-5' and the MV3G H-4 indicating that the B-ring of (epi)catechin moiety is above/under the C-ring of MV3G. For the compounds MC2 and ME2, ROESY interactions were observed between the (epi)catechin H-5' and the MV3G H-6"b indicating that the B-ring of the flavanol unit is in the vicinity of the glucoside. This would occur if the flavanol moiety was on the same as the glucoside with respect to the malvidin aglycone (Figure 4.5 (b) and (d)). Considering that for all four compounds that the methyl group of the methylmethine bridge projects towards the B-ring of MV3G, it is proposed that for MC1 and ME1 the (epi)catechin moiety is on the opposite side to the glucoside with respect to the malvidin aglycone (Figure 4.5 (a) and (c)). The proposed structures indicate that at the methine group on the methylmethine bridge, MC1 and ME1 are the R-diastereomers and MC2 and ME2 are the S-diastereomers.

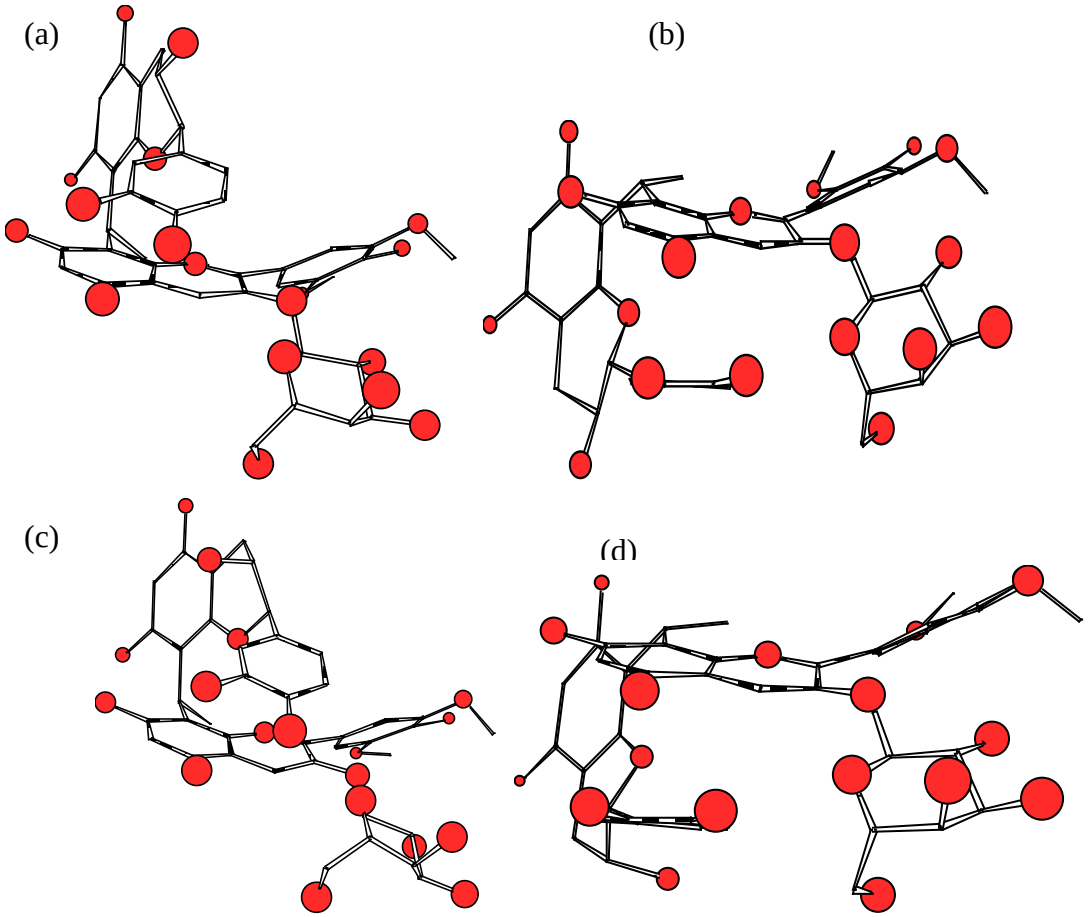

Figure 4.5. Proposed 3-dimensional structures for (a) MC1, (b) MC2, (c) ME1 and (d) ME2. Oxygen atoms are shown as solid spheres.

It should be noted however, that the glucoside could be on the opposite side with respect to the malvidin aglycone (Figure 4.6 (a) to (d)) and still give similar NMR spectra. Although the stereochemistry, at the methine group, of the compounds has reversed (i.e. MC1 and ME1 are the S-diastereomers and MC2 and ME2 are the R-diastereomers), the positioning of the flavan-3-ol moieties remain the same with respect to the glucoside groups.

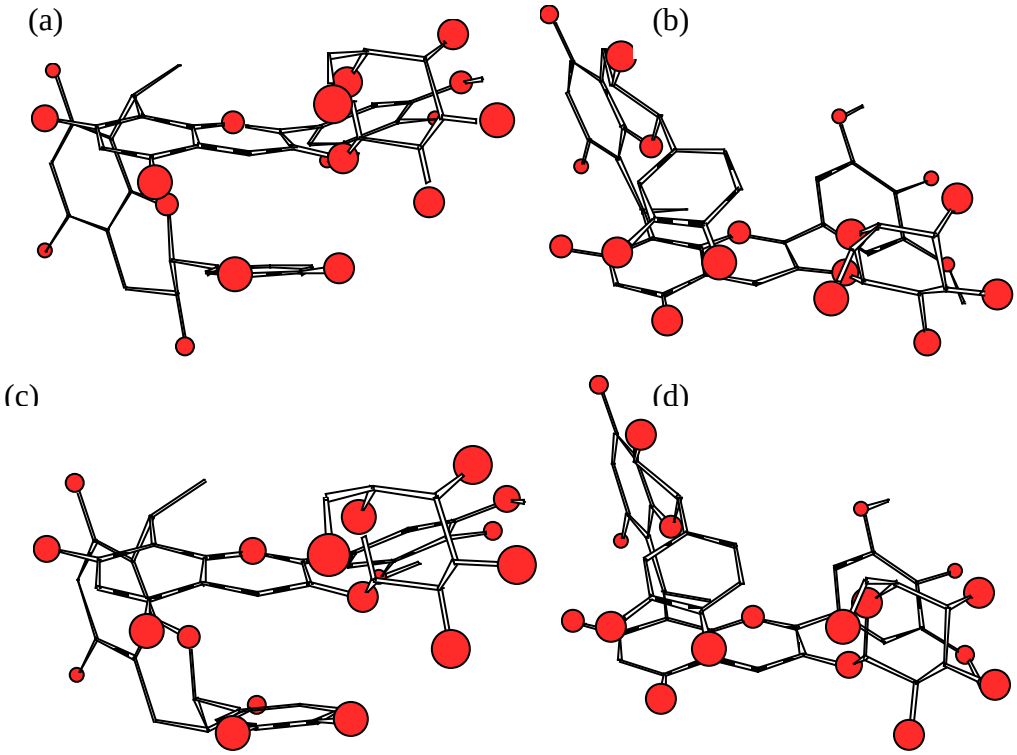

Figure 4.6. Alternative proposed 3-dimensional structures for (a) MC1, (b) MC2, (c) ME1 and (d) ME2. Oxygen atoms are shown as solid spheres.

The coordination used to determine the dimensions and dipole moments is shown in Figure 4.7. The dimensions and cubic volumes of the proposed structures are listed in Table 4.1. There is little difference in the dimensions along the X and Y-axis, whilst there are considerable differences along the Z-axis. For both the proposed structures and the alternative proposed structures, MC1 and ME1 are longer along the Z-axis than MC2 and ME2 respectively. Although the cubic volume is not the actual volume of the compounds, it gives a clear indication of the "space" occupied by the compounds. As with the Z-axis dimensions, the cubic volumes of the proposed and alternative structures of MC1 and ME1 are larger than that of MC2 and ME2 respectively.

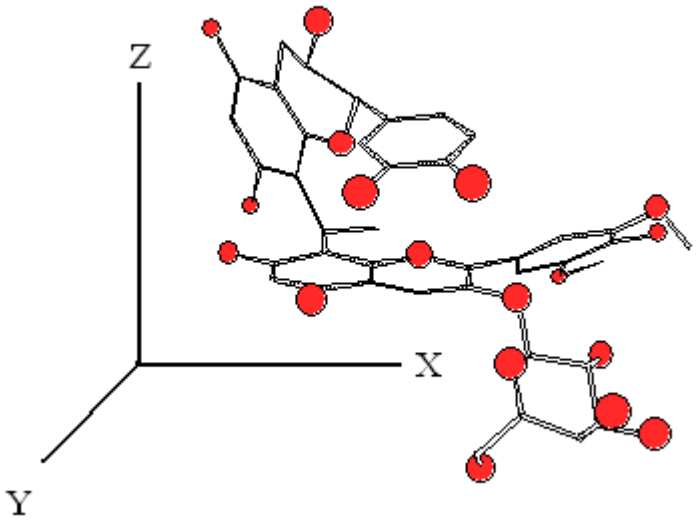

Figure 4.7. Coordinate system used in the molecular modelling of MC1, MC2, ME1 and ME2.

Table 4.1. Predicted dimensions and cubic volumes of the proposed structures

DIMENSION	**MC1**	**MC2**	**ME1**	**ME2**	alt **MC1**	alt **MC2**	alt **ME1**	alt **ME2**
X (Å)	12.6	12.7	12.4	11.8	11.8	12.8	11.9	12.7
Y (Å)	11.6	10.5	13.8	11.7	11.5	10.7	10.8	10.5
Z (Å)	9.9	7.5	9.6	6.9	9.4	6.7	8.7	6.9
Volume ($Å^3$)	1447	1000	1643	953	1276	918	1118	920

The polarity of the compounds was determined by calculating the dipole moments of the compounds using MOPAC molecular computations. The coordinations used in the calculations are the same as those used in the determination of the dimensions (Figure 4.7). The overall magnitude of the dipole moments for MC1 and ME1 are considerably greater than that of MC2 and ME2 indicating that MC1 and ME1 are more polar than MC2 and ME2 respectively. The magnitude of the dipole moments also shows that the polarity of ME2 is less than that of MC2. The dipole moments along the Y-axis are considerably greater in magnitude for MC1 and ME1 as compared to ME2 and ME2.

Table 4.2. Predicted dipole moments of the proposed structures

DIPOLE MOMENT	**MC1**	**MC2**	**ME1**	**ME2**	alt **MC1**	alt **MC2**	alt **ME1**	alt **ME2**
X (Debye)	-0.7	5.3	4.8	1.2	-1.1	5.0	-3.0	2.0
Y (Debye)	-10.6	2.4	-8.0	0.8	10.4	-2.5	7.3	-0.5
Z (Debye)	4.3	1.8	-0.2	3.3	7.6	5.6	9.5	4.6
Magnitude (Debye)	11.4	6.1	9.3	3.6	12.9	7.9	12.4	5.0

4.3 Discussion

Mass spectrometry, NMR and molecular modelling have afforded the structures and stereochemistries of MC1, MC2, ME1 and ME2. The postulated structures and stereochemistries would be expected to have an influence on the physico-chemical properties of these compounds.

The location of the bridge for the methylmethine-(epi)catechin-MV3G compounds was determined through HMBC and ROESY to be on the 8-position on both MV3G and (epi)catechin. This is in agreement with previous studies on 8,8-methylmethine-catechin-flavylium compounds (Escribano-Bailon et al., 1996) and 8,8-methylmethine-epicatechin-cyanidin-3-galactose (Shoji et al., 2002).

Although one- and two-dimensional NMR afforded the connectivity of the hydrogen and carbon atoms in the methylmethine-(epi)catechin-MV3G compounds, molecular modelling was required to determine the positioning of the (epi)catechin moiety with respect to the MV3G moiety. Molecular modelling has previously been used to propose a structure for one of the 8,8-methylmethine-catechin-flavylium diastereomers (Escribano-Bailon et al., 1996). However, the structure for the other diastereomer was not published. The structure proposed for MC2/ME2 closely resembles the structure proposed by (Escribano-Bailon et al., 1996). The proposed structures for MC1/ME1 differ to MC2/ME2 by the location of the (epi)catechin moiety with respect to the glucoside moiety of MV3G.

The linkage at the 8-positions allows the (epi)catechin moiety to fold over/under the A- and C-rings of MV3G (Figure 4.5). This was confirmed by ROESY interactions between (epi)catechin H-5' and MV3G H-4. The positioning of the (epi)catechin B-ring gives some protection, through steric hindrance, to the 2- and 4-positions of MV3G. This steric hindrance would be expected to afford the 8,8-methylmethine-(epi)catechin-MV3G compounds greater resistance to bisulfite bleaching at the 4-position and hydration at the 2- and 4-positions.

The stereochemistries of the 8,8-methylmethine-(epi)catechin-MV3G compounds are dependant upon the positioning of the methyl group in relation to (epi)catechin. Although the methyl group can rotate around the carbonium ion, molecular modelling indicates that minimal energy occurs when the methyl group is in an axial position with respect to the A-ring of (epi)catechin (Figure 4.8).

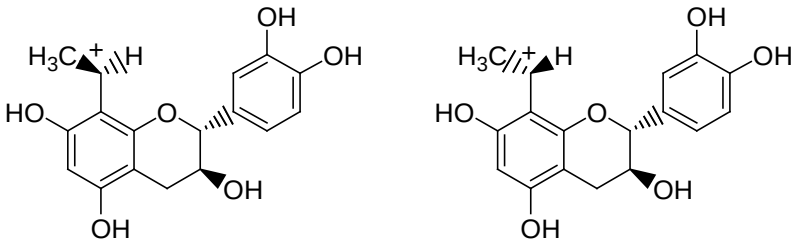

Figure 4.8. Minimal energy positioning of the methyl-group for the catechin carbonium ion.

The methyl group of the (epi)catechin carbonium ion has a slight negative charge making it slightly attracted to the positive C-ring of the MV3G flavylium ion. This results in the methyl-group for the four compounds pointing towards the B-ring of MV3G and thereby positioning the (epi)catechin above/below MV3G (Figure 4.9). From this, a chiral centre at the methylmethine bridge is obtained.

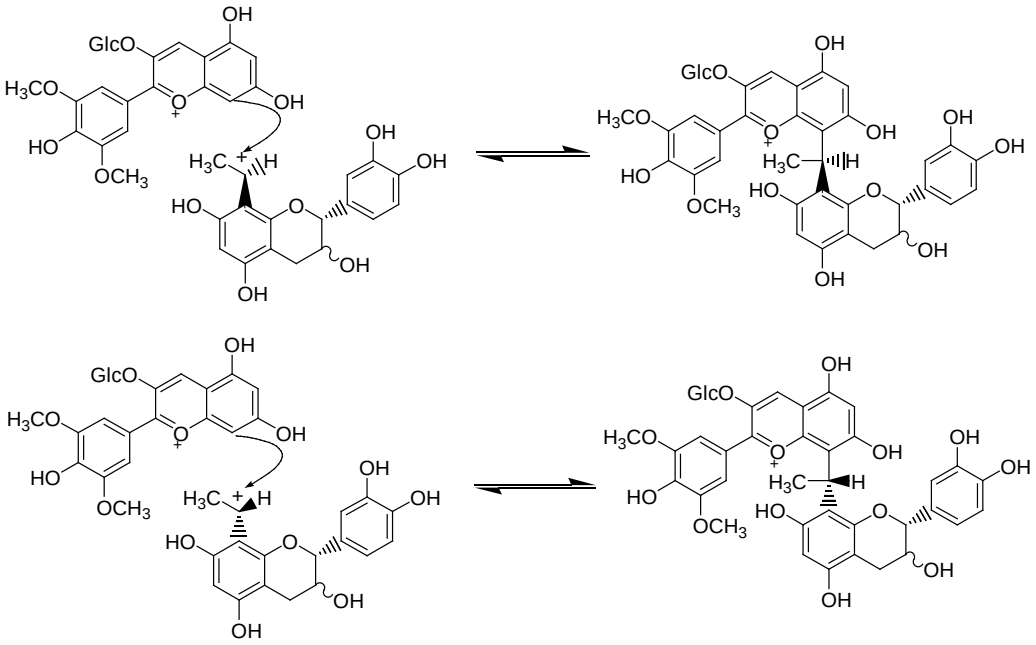

Figure 4.9. Proposed routes of formation of the 8,8-methylmethine MV3G and (epi)catechin diastereomers.

MV3G has been found to be the terminal unit in oligomeric 8,8-methylmethine-flavan-3-ol-MV3G compounds (Es-Safi et al., 1999b), indicating that the 6-position of MV3G is unavailable for further reaction. The 6-position of MV3G is still susceptible to electrophilic substitution as shown by the substitution when deuterium replaced hydrogen in the solvent (Figure 4.0.3). Although the 6-position of MV3G is susceptible to electrophilic substitution, steric hindrance of (epi)catechin limits further condensation at this position. Furthermore, molecular modelling of a methylmethine addition at this position indicates that the minimal energy occurs when the methyl group is in the equatorial position with respect to the A-ring of (epi)catechin which is not the minimal energy of the (epi)catechin carbonium ion as discussed previously. This would further explain the preference for substitution on the 8-position of MV3G for the initial addition. However, the 6-position of MV3G could be a site of further condensation as has been shown for 6,6-methylmethine-catechin-catechin dimers (Saucier et al., 1998).

The HPLC chromatographic separation on reversed-phase C18 columns of the 8,8-methylmethine-(epi)catechin-MV3G diastereomers has been observed in previous studies (Bakker et al., 1993; and in the previous chapter. The calculated size and polarities of MC1, MC2, ME1 and ME2 reflect these observed chromatographic properties. MC1 and ME1 are more polar than MC2 and ME2 so therefore elute earlier on reversed-phase columns. Molecular modelling indicates that MC2 and ME2 have similar cubic volumes, however ME2 is noticeably less polar than MC2. This would account for the larger differences in retention times on the reversed-phase columns for ME1 and ME2 compared to MC1 and MC2. The larger size of MC1 and ME1 compared to MC2 and ME2 accounts for the elution order on the sulfoxyethylcellulose column.

The stereochemistries of MC1, MC2, ME1 and ME2 were not determined in this study. A method to determine their stereochemistries involves x-ray crystallography. X-ray crystallography has been successfully used to study the structural conformations of anthocyanidins (Ueno and Saito, 1977a; Ueno and Saito, 1977b). As yet however, MV3G and other grape anthocyanins have not been crystallised, due to their amorphous nature through the glucoside, and studied with X-ray crystallography. Until either the 8,8-methylmethine-(epi)catechin-MV3G compounds, their anthocyanidin forms or MV3G are studied by X-ray crystallography it is not possible to determine the definitive structure of the 8,8-methylmethine-(epi)catechin-MV3G compounds and therefore their stereochemistries. Although the absolute stereochemistry of the 8,8-methylmethine-(epi)catechin-MV3G compounds has not been determined, the positioning of the (epi)catechin moiety with respect to the glucoside has been determined. The positioning of the (epi)catechin moiety in relation to the glucoside would be expected to have an influence on the physico-chemical properties and colour stability.

The proposed structures of MC1, MC2, ME1 and ME2 would be expected to have an influence on their chemical and colour stabilities, ionisations and hydrations. This is due to the substitution and the steric hindrance to nucleophilic attack of MV3G. The position of (epi)catechin in relation to MV3G would have an influence on the colour and chemical stabilities of MC1, MC2, ME1 and ME2 by exerting steric hindrance to the MV3G sites susceptible to nucleophilic attack. The substitution of MV3G and the proximity of (epi)catechin to the MV3G 5-OH group would be expected to have an influence on the ionisation constants, due to protonation, of the 8,8-methylmethine-(epi)catechin-MV3G compounds.

Chapter 5 - Stability of 8,8-methylmethine-(epi)catechin-malvidin-3-glucose pigments

5.1 Introduction

MV3G readily loses colour through change in pH (through hydration) and bleaching by sulfur dioxide. At wine pH (~3.6) the colourless hydrated species account for almost 90% of the MV3G content (Asenstorfer et al., 2003). The bleaching of MV3G occurs by sulfur dioxide attaching as a bisulphite ion at the 4-position (Berke et al., 1998). Oxidation of anthocyanins results in a number of products (Montreau et al., 1970) which are dependent upon the nature of the anthocyanin. Anthocyanin oxidation products include enol benzoates (Jurd, 1966), benzofurans (Jurd, 1964) and flavanols (Montreau et al., 1970). Substitution at the 4-position of the anthocyanin increases the resistance to this sulphur dioxide bleaching (Timberlake and Bridle, 1968) and oxidation (Sweeny and Iacobucci, 1983). Resistance to decolourisation due to pH changes is also enhanced by substitution at the 4-position (Brouillard et al., 1982).

8,8-methylmethine-(epi)catechin-MV3G compounds are not substituted at the 4-position on the anthocyanin. It would therefore be expected that they would have little resistance to bisulfite bleaching and loss of colour due to changes in pH. However, Escribano-Bailón et al. (2001) isolated one of the 8,8-methylmethine-catechin-MV3G diastereomers (MC2) and studied its properties. It was found to be more resistant to bisulfite bleaching and colour loss due to pH change than the parent anthocyanin. More recently, (Duenas et al., 2006) found that the other diastereomer (MC1) also displayed these properties. Furthermore, in model solutions stored at 30 ^{0}C MC1 was found to have a faster rate of degradation than MV3G (Escribano-Bailón et al., 2001). These studies have found that although MC1 is more colour stable compared to MV3G, to change in pH and bisulfite bleaching, they are more temporily unstable. To further understand the importance of 8,8-methylmethine-(epi)catechin-MV3G compounds to red wine colour and pigment development, the colour and chemical stabilities of MC1, MC2, ME1 and ME2 to change in pH, sulfur dioxide and oxidation were studied.

5.2 Results

5.2.1 Stability of 8,8-methylmethine-(epi)catechin-MV3G compounds to change in pH

The spectra of MV3G, MC1 and MC2, at pHs from 1.0 to 7.0 are shown in Figure 5.1. ME1 and ME2 have similar spectra, from pH 1.0 to 7.0, to those of MC1 and MC2. The absorption maxima in the visible region (λ_{max}) of MV3G at pH 1.0 is 517 nm. At pH 3.5 this has shifted slightly to a longer wavelength (519 nm) and has a dramatically decreased absorbance maxima. As the pH increases further, the λ_{max} shifts further to a longer wavelength (573 nm at pH 7.0) without any increase in the absorbance maxima. The λ_{max} of the 8,8-methylmethine compounds is in the vicinity of 534 nm at pH 1.0 which either slightly shifts to a longer wavelength of 536 nm (MC1 and ME1) or has a more pronounced shift to 541 nm (MC2 and ME2) at pH 3.5. Accompanying the shift in λ_{max} is a slight decrease in absorbance maxima and two isosbestic points are observed (575 and 410 nm for MC1 and ME1 and 567 and 420 nm for MC2 and ME2). As the pH increases further the minimum absorbance maxima occurs at pH 6.0 and λ_{max} has further shifted to 567 nm. Again, two isosbestic points are observed between pH 3.5 and 5.5 (565 and 414 nm for MC1 and ME1 and 565 and 432 nm for MC2 and ME2). Above pH 6.0 the absorbance maxima increases for all four 8,8-methylmethine compound with the λ_{max} shifting to 600 to 620 nm. The isosbestic points observed above pH 5.5 are 571 and 494 nm for MC1 and ME1, and 579 and 490 nm for MC2 and ME2.

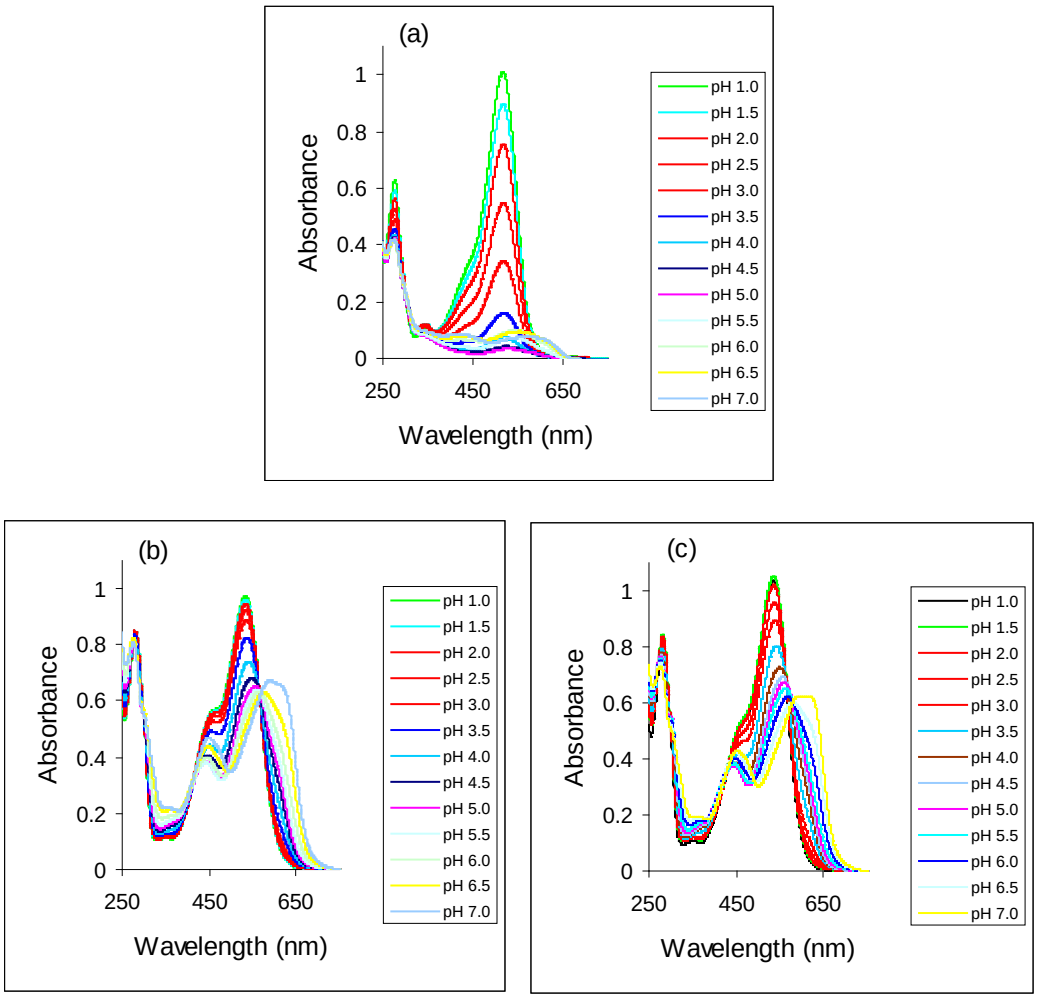

Figure 5.1. UV-visible spectra of (a) MV3G, (b) MC1 and (c) MC2 from pH 1.0 to 7.0.

The colour densities of the compounds at pH 1.0 and 3.6 are listed in Table 5.1. The 8,8-methylmethine-(epi)catechin-MV3G compounds had a far greater resistance to colour loss due to change in pH than MV3G.

Table 5.1. Colour densities ($A_{420} + A_{520}$) of MV3G, MC1, MC2, ME1 and ME2 at pH 1.0 and pH 3.6.

pH	MV3G	MC1	MC2	ME1	ME2
1.0	1.25	1.29	1.27	0.24	0.26
3.6	0.22	1.12	1.02	0.18	0.19
%	82.4	13.3	19.6	23.0	25.6
Decrease					

It should be noted however, that the 8,8-methylmethine-(epi)catechin-MV3G compounds have a greater absorbance at 620 nm, which continues to increase as the pH increases from 1.0 to 7.0 (Figure 5.1), than MV3G. The Glories' colour density takes this into account and the results are listed in Table 5.2. The decrease in colour density is reduced for the 8,8-methylmethine-(epi)catechin-MV3G compounds once the absorbance at 620 nm has been taken into account, whereas there is little change for MV3G.

Table 5.2. Glories' colour densities ($A_{420} + A_{520} + A_{620}$ 1mm pathlength) of MV3G, MC1, MC2, ME1 and ME2 at pH 1.0 and pH 3.6.

pH	**MV3G**	**MC1**	**MC2**	**ME1**	**ME2**
1.0	0.63	0.67	0.65	0.12	0.13
3.6	0.12	0.62	0.59	0.10	0.11
%	81.7	7.3	8.9	17.5	15.6
Decrease					

The evolution of the integrated spectra area and the centre of mass of MV3G, MC1 and MC2 from pH 1.0 to 7.0 are shown in Figure 5.2. The spectra areas of MC1 and MC2 gradually decreased (by 9.1% 11.1% respectively at pH 3.6) to a minima (85% of the initial area) at pH 5.0 whereafter they increased to the original levels by pH 6.7 and 7.3 respectively. The spectra area of MV3G dramatically decreased by 80% at pH 3.6, decreased to a minimum of 6.6% of the original area at pH 4.7 and increased after pH 5.5. The centre of mass for MC1 and MC2 remained steady at 514 nm and 517 nm respectively until pHs 3.0 (MC1) and 2.5 (MC2) where there was a noticeable increase which plateaued for both compounds at 535 nm (pH 5.1 and 4.6 respectively). A further noticeable increase in the centre of mass MC1 and MC2 started at pHs 5.8 and 5.5 respectively. The centre of mass for MV3G remained constant at 517 nm until pH 3.0 whereafter there is a steady increase (reaching 532 nm by pH 7.0).

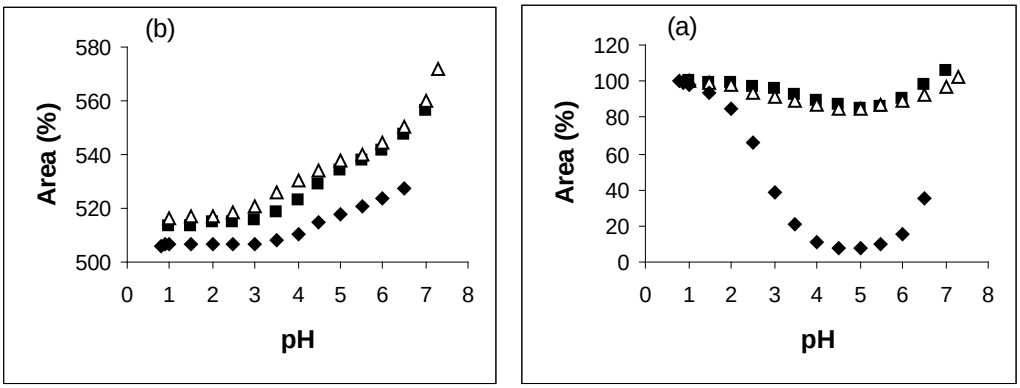

Figure 5.2. Evolution of (a) spectra area (400 nm to 700 nm) and (b) spectra centre of mass (400 nm to 700 nm) for MV3G (◆), MC1 (■) and MC2 (▲) in the pH range 1.0 to 7.0.

5.2.2 Stability of 8,8-methylmethine-(epi)catechin-MV3G compounds to sulfur dioxide

The colour densities before and after the addition of sulfur dioxide of MV3G, MC1, MC2, ME1 and ME2 are listed in Table 5.3. The 8,8-methylmethine compounds had a far greater resistance to bleaching by sulfur dioxide than MV3G. At both pHs studied, MC1 and ME1 had a slightly greater resistance to bisulfite bleaching than MC2 and ME2 respectively. There was little change in the percentage decrease, compared to the colour density, when Glories' colour density is used (Table 5.2).

Table 5.3. Colour densities ($A_{420} + A_{520}$) of MV3G, MC1, MC2, ME1 and ME2 before and after the addition of sulfur dioxide at pH 2.8 and pH 3.3.

[SO2] (ppm)	**MV3G**		**MC1**		**MC2**		**ME1**		**ME2**	
	pH 2.8	**pH 3.3**	**pH 2.8**	**pH 3.3**	**pH 2.8**	**pH 3.3**	**pH 2.8**	**pH 3.3**	**pH 2.8**	**pH 3.3**
0	3.6	0.85	5.5	5.1	6.0	5.4	4.5	3.8	3.7	3.1
50	0.2	0.08	4.0	3.1	2.7	1.9	2.7	1.8	1.7	1.0
(%) Decrease	95	90	28	40	56	65	41	53	53	67

Table 5.4. Glories' densities (A_{420} + A_{520} + A_{620} 1mm pathlength) of MV3G, MC1, MC2, ME1 and ME2 before and after the addition of sulfur dioxide at pH 2.8 and pH 3.3.

[SO2] (ppm)	**MV3G**		**MC1**		**MC2**		**ME1**		**ME2**	
	pH 2.8	**pH 3.3**	**pH 2.8**	**pH 3.3**	**pH 2.8**	**pH 3.3**	**pH 2.8**	**pH 3.3**	**pH 2.8**	**pH 3.3**
0	0.38	0.09	0.61	0.58	0.68	0.64	0.51	0.44	0.41	0.38
50	0.02	0.01	0.43	0.34	0.30	0.23	0.30	0.22	0.20	0.13
(%) Decrease	95	88	29	40	56	65	40	51	53	67

5.2.3 Stability of MC1 and MC2 to oxidation

The compositions of the model wine solutions for studying the degradation of MV3G, MC1 and MC2 under anaerobic conditions are shown in Figure 5.3. MC1 and MC2 degraded to form MV3G, and other pigments (Figure 5.3 (b) and (c)) which were observed as a "hump" in the chromatogram (not shown). Furthermore, the other diastereomer, present as an impurity, maintained its concentration throughout. LC-MS of the solutions containing MC1 and MC2 at 100 days revealed only trace amounts (<1 μg) of vinyl-linked MV3G and catechin, 8,8-methylmethine-proanthocyanidin-MV3G and further polymerised products such as MV3G-et-catechin-et-catechin. The degradation rates of MV3G, MC1 and MC2 were determined to be first order. The degradation rates and half-lives are listed in Table 5.5. MC1 and MC2 had significantly greater degradation rates and shorter half-lives than MV3G.

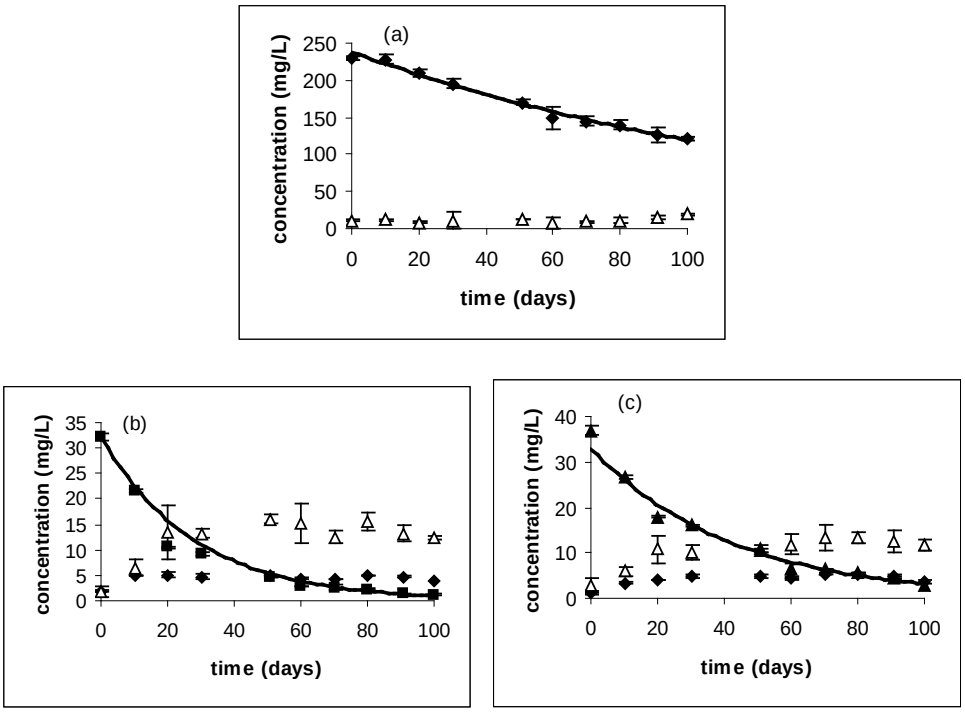

Figure 5.3. Solution composition for the degradation of (a) MV3G (◆), (b)MC1 (■) and (c) MC2 (▲) in model wines under anaerobic conditions at 20^0C. Evolution of other pigments (Δ) is also included.

Table 5.5. Rates of degradation and half-lives of MV3G, MC1 and MC2 in model wines (pH 3.6) under anaerobic conditions at 20^0C.

	MV3G	MC1	MC2
k (day^{-1})	0.0064±0.0001	0.035±0.001	0.0251±0.0007
$t_{1/2}$ (day)	108	19	28

The colour densities and hues of model wine solutions for the degradation studies of MV3G, MC1 and MC2 under anaerobic conditions are shown in Figure 5.4. MC1 and MC2 had a significantly greater decrease in colour density as compared to MV3G. After 90 days the colour densities of MC1 and MC2 had decreased by 50% and 43% respectively compared to 15% for MV3G. However, the hue of MV3G increased by 68% whereas there was little change in hue for MC1 and MC2 (0% and +8% respectively).

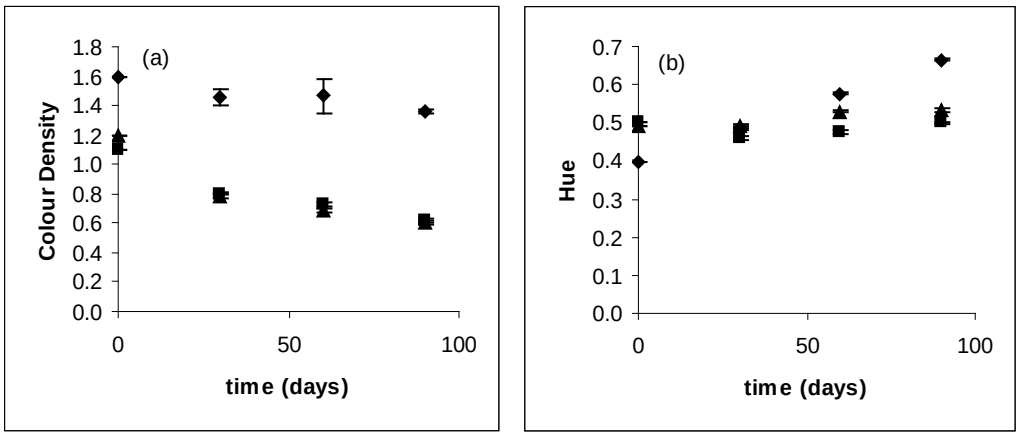

Figure 5.4. Change in (a) colour density and (b) hue of MV3G (◆), MC1 (■) and MC2 (▲) in model wines under anaerobic conditions at 20^0C.

The composition of the model wine solutions for studying the degradation of MV3G, MC1 and MC2 are under aerobic conditions is shown in Figure 5.5. MC1 and MC2 rapidly degraded to form MV3G and other pigments (Figure 5.5 (b) and (c)) which were observed as a "hump" in the chromatogram. As with the degradation under anaerobic conditions, the other diastereomer, present as an impurity, maintained its concentration. LC-MS of the solutions containing MC1 and MC2 at 50 days could not detect vinyl-linked MV3G and catechin, 8,8-methylmethine-proanthocyanidin-MV3G and further polymerised products, such as MV3G-et-catechin-et-catechin, which were detected under anaerobic conditions. The degradation rates were determined to be first order after linear transformation. The degradation rates and half-lives are listed in Table 5.6. MC1 and MC2 had significantly greater degradation rates than MV3G.

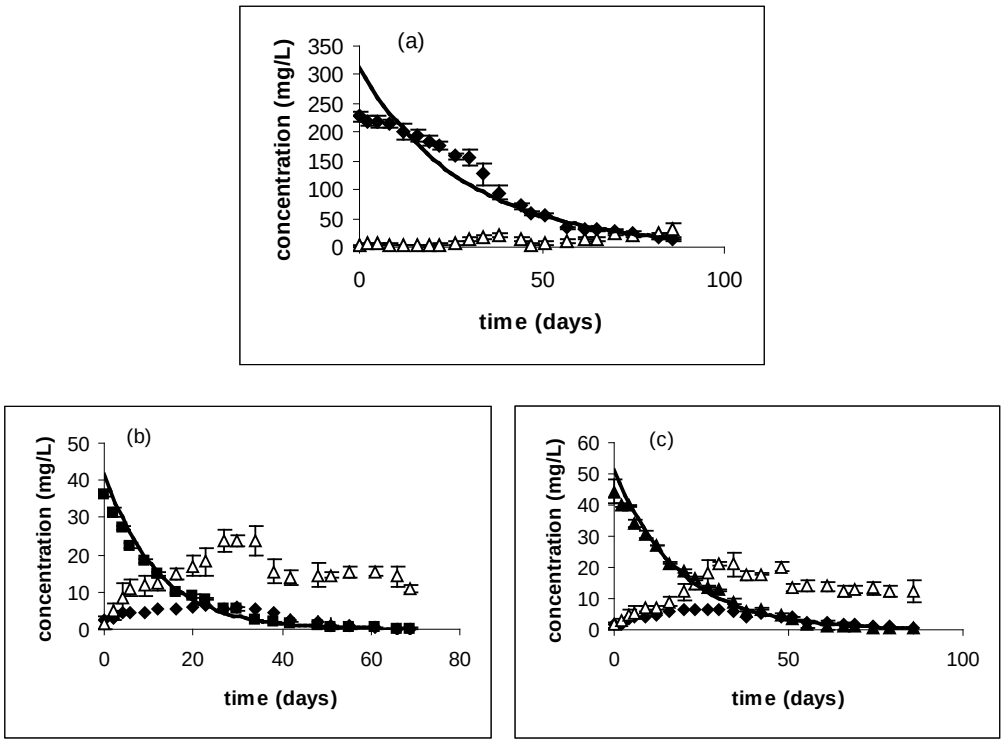

Figure 5.5. Solution composition for the degradation of (a) MV3G (◆), (b) MC1 (■) and (c) MC2 (▲) in model wines under aerobic conditions at 20^0C. Development of other pigments (Δ) is also included.

Table 5.6. Rates of degradation and half-lives pigments at 20^0C in model wines (pH 3.6) under aerobic conditions.

	MV3G	**MC1**	**MC2**
k (day^{-1})	0.025±0.002	0.080±0.001	0.052±0.001
$t_{1/2}$ (day)	28	9	13

The colour densities and hues of model wine solutions for studying the degradation of MV3G, MC1 and MC2 under aerobic conditions are shown in Figure 5.6. MC1 and MC2 had significantly greater decreases in colour densities as compared to MV3G. After 90 days the colour densities of MC1 and MC2 had decreased by 93% and 88% respectively compared 62% for MV3G. However, for the hue, MV3G increased by 208% whereas there was no change for MC2 (0%). There was little change in hue for MC1 until 50 days where it started to dramatically increase to be slightly more than double in value after a further 40 days. This corresponded to the degradation of MV3G and other pigments (Figure 5.5).

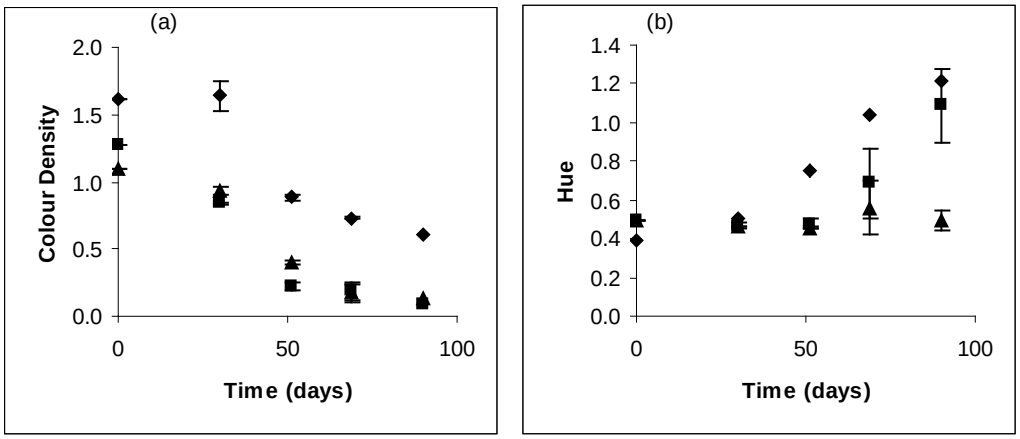

Figure 5.6. Change in (a) colour densities and (b) hues of MV3G (◆), MC1 (■) and MC2 (▲) in model wines under aerobic conditions at 20^0C.

5.3 Discussion

MC1, MC2, ME1 and ME2 have greater colour stability, compared to MV3G, to change in pH and to bisulfite bleaching. This is possibly due to steric hindrance of the (epi)catechin moiety to nucleophilic attack. Although MC1 and MC2 have greater colour stability, compared to MV3G, they have much lower temporal stabilities.

It has been observed that MV3G loses colour through hydration (Brouillard and Delaporte, 1977) whilst MC1 and MC2 have greater colour stability, with respect to pH change and bisulfite bleaching (Duenas et al. 2006). This study found that all of the 8,8-methylmethine-(epi)catechin-MV3G pigments have a greater resistance to colour loss due to change in pH than the parent MV3G. Whereas at pH 3.5, MV3G has a decrease in colour intensity of greater than 80%, the 8,8-methylmethine-(epi)catechin-MV3G pigments only decrease by 13% to 26%. This is reduced even further if the Glories' colour density is used. The small decrease in colour density indicates that little or no hydration is occurring to form colourless hydration products.

Duenas et al. (2006) proposed that MC2 does not undergo hydration whilst MC1 undergoes slight hydration (pK_H 4.17). However, the presence of isosbestic points in the visible region of the spectra for the 8,8-methylmethine-(epi)catechin-MV3G compounds indicates that very little/no hydration is occurring. The isosbestic points are the wavelengths where the absorbance is the same for two species. If hydration was occurring in the 8,8-methylmethine-(epi)catechin-MV3G pigments, the isosbestic points would be absent as in the case of MV3G. Further evidence that little/no hydration is occurring is that the change in the area of the spectra in the visible region of MC1 and MC2 both reach the same minima (approximately 85% of the original) whilst that of MV3G decreased to 20% of the original.

The change in colour intensity, with a change in pH, of the 8,8-methylmethine-(epi)catechin-MV3G pigments (observed as a change in the area of the spectra in the visible region) is concurrent with a change in colour (observed as an increase in the wavelength of the centre of mass of the spectra in the visible region). This indicates that there is a difference in molar absorptivity between the flavylium cation, quinonoidal base and quinonoidal anion forms of the 8,8-methylmethine-(epi)catechin-MV3G pigments. A large decrease in spectra area for MV3G is observed with no change in the centre of mass of the spectra indicating hydration is occurring. As this is not observed for the 8,8-methylmethine-(epi)catechin-MV3G pigments, this indicates that little or no hydration is occurring for the 8,8-methylmethine-(epi)catechin-MV3G pigments.

A possible explanation for the reduced decrease in colour is intramolecular copigmentation. Catechin and epicatechin are relatively poor copigments (Cai et al., 1990), significantly higher concentrations of the flavan-3-ols are required to increase the absorbance and to bathochromatically shift λ_{max}. A molar ratio of 2:1 of flavan-3-ol to malvin chloride is required to increase the absorbance by 18% and to shift λ_{max} by 0.8 nm (Mistry et al., 1991). Copigmentation is postulated to be through 'π π' stacking where the copigment is parallel to the anthocyanin. However, in the case of the 8,8-methylmethine-(epi)catechin-MV3G pigments, only the B-ring of the flavan-3-ol is in a position to act as a copigment for the MV3G chromophore. This is equivalent to catechol being the copigment. Catechol is a worse copigment than (epi)catechin requiring a molar ratio of 21:1 to malvin to increase the absorbance by 26% and to shift λ_{max} by 2.0 nm (Liao et al., 1992). Therefore it is unlikely that intramolecular copigmentation is making a significant contribution to the colour of the 8,8-methylmethine-(epi)catechin-MV3G compounds.

The 8,8-methylmethine-(epi)catechin-MV3G pigments change colour with a change in pH. As the pH increases from a low pH (1.0), the colours of the compounds change from red to red with a noticeable purple tint. As the pH increases from approximately 3.5 the colour becomes purple and as the pH increases from 5.0, the colour becomes blue. These changes in colour could correspond to transformation of the flavylium cation to the neutral quinonoidal base, which transforms to the quinonoidal anion, which transfoms into the quinonoidal dianion

At wine pH the 8,8-methylmethine-(epi)catechin-MV3G pigments are red with a purple tint. Furthermore, the 8,8-methylmethine-(epi)catechin-MV3G pigments retain their colour and have a significant absorbance at 620 nm. When present in wine, the 8,8-methylmethine-(epi)catechin-MV3G pigments would make a significant contribution to the red wine colour and to the purple tint associated with young red wines. The purple tint associated with red wines has been previously attributed to copigmentation of flavan-3-ols (monomeric, dimeric and oligomeric) and other polyphenols (e.g. quercetin) with grape anthocyanins (Liao et al., 1992). However, it should be noted that although the flavan-3-ols are in abundance, they are relatively poor copigments and the effective copigments such as quercetin are only present in low concentrations.

MC1 and MC2 have been shown to greater resistance to bisulfite bleaching compared to the parent MV3G (Duenas et al. 2006). Similar results have been observed in this study for MC1 and MC2 and have also been observed for ME1 and ME2. The greater resistance to bisulfite bleaching to 8,8-methylmethine-(epi)catechin-MV3G compounds can be explained by steric hindrance of the MV3G 4-position by the (epi)catechin and glucoside moieties. Direct attack by the bisulfite ion from one direction is sterically hindered by the (epi)catechin and glucoside moieties as shown by the location of the bisulfite ion in relation to the MV3G 4-position in Figure 5.7. Although the (epi)catechin and glucoside moieties sterically hinder bisulfite bleaching from one direction, the other direction is still susceptible to attack. Bisulfite addition results in the loss of planarity of the MV3G C-ring which would require extra energy to overcome the inertia of the (epi)catechin moiety.

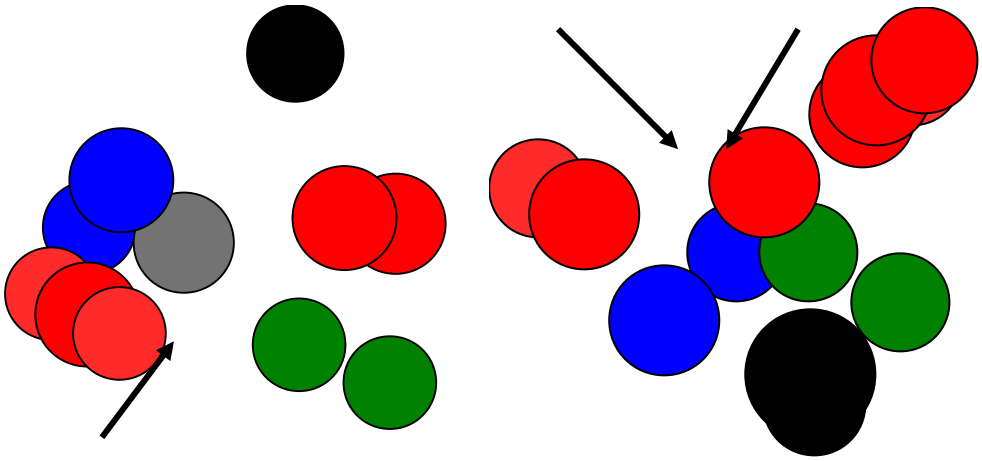

A **B**

Figure 5.7. Steric hindrance of the 4-position to bisulfite bleaching. The bisulfite molecule and the 4-position are in black.

The structural conformations of the 8,8-methylmethine-(epi)catechin-MV3G compounds, as proposed in Chapter 4, explain the differences in bisulfite bleaching between MC1/ME1 and MC2/ME2. For MC1 and ME1, the (epi)catechin and glucoside moieties are on opposite sides of the MV3G aglycone and limit nucleophilic attack to the 4-position (arrow Figure 5.7 A). The (epi)catechin and glucoside moieties are on the same side of the MV3G aglycone for MC2 and ME2 allowing greater access to the 4-position (arrows Figure 5.7 B). Given further time than the experimental conditions, it would be expected that the 8,8-methylmethine-(epi)catechin-MV3G compounds would undergo greater bisulfite bleaching, as there would be greater chances for the bisulfite ions to attack the 4-position of the MV3G aglycone from the necessary direction.

Escribano-Bailón et al. (2001) determined that in model solutions stored at 30 ^{0}C MC1 had a faster rate of degradation than MV3G. This study found that both MC1 and MC2 are far more chemically unstable than the parent MV3G under anaerobic and aerobic conditions in model wine solutions. The degradation products included MV3G and other pigments. However, catechin was not observed in the HPLC analysis. The formation of MV3G and other pigments indicates that the methylmethine bridge is being cleaved and that polymerisation is occurring.

The products formed via the degradation of MC2 and MC1, under anaerobic conditions, include MV3G, the other diastereomer and trace amounts of the vinyl-linked MV3G and catechin and the 8,8-methylmethine-MV3G-MV3G dimers. This indicates that the bridge is preferentially being split between the ethyl-group and MV3G (Figure 5.8). The products formed are a quinone ethide form of catechin and MV3G. The formation of the quinone ethide form of catechin would explain the lack of catechin observed as a degradation product. It should be noted that the quinone ethide would be very susceptible to polymerisation.

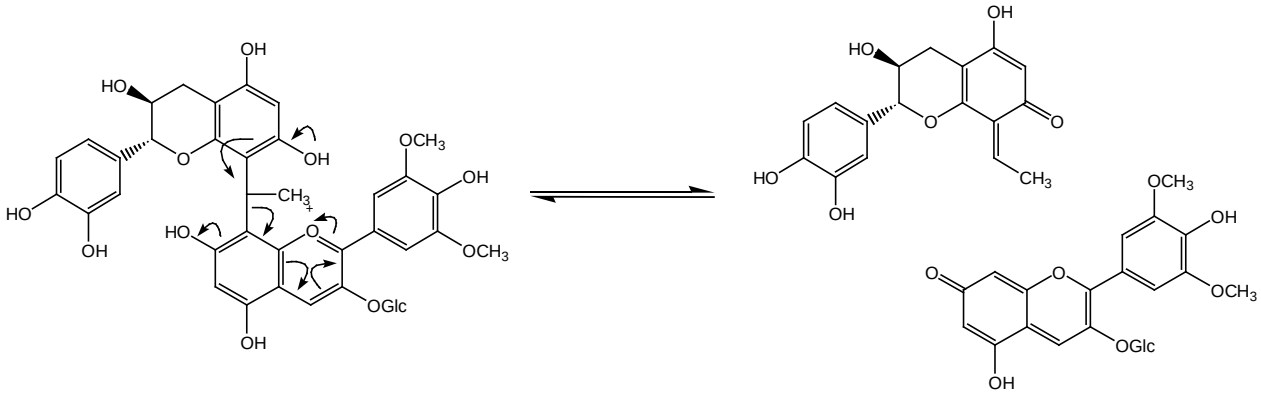

Figure 5.8. Postulated bridge cleavage mechanism of MC1 and MC2.

MC2 is considerably more stable than MC1. For complete degradation of the 8,8-methylmethine pigments, the catechin and MV3G moieties need to move sufficiently away from each other. The catechin moiety of MC2 is sterically hindered in moving in one direction by the glucoside (Figure 5.9 (b)) whereas MC1 had a greater degree of movement (Figure 5.9 (a)). Furthermore, hydrogen bonding between the catechin moiety and the glucoside would retard the movement of the catechin moiety away from MV3G.

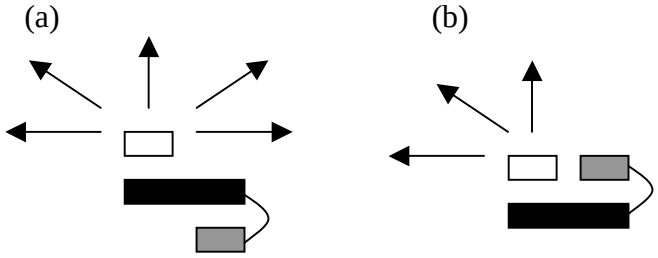

Figure 5.9. Schematic representation of the degree of movement for catechin of (a) MC1 and (b) MC2 after cleavage of the methylmethine-linkage. Malvidin aglycone – black, catechin – white, glucoside – grey.

There are a number of mechanisms whereby the formation of other compounds can occur including polymerisation. The first mechanism of polymerisation is the addition of the carbonium cation onto the 8,8-methylmethine-catechin-MV3G compound. As discussed in Chapter 4, this would not occur on the MV3G moiety, due to steric hindrance, however this could occur on the 6-position of the catechin moiety. Another mechanism of polymerisation is the formation of interflavan bonds between the catechin moieties as occurs with proanthocyanidin formation (Haslam, 1980).

Under anaerobic conditions, trace amounts of the vinyl-linked MV3G and catechin pigment was formed. The small amounts of the vinyl-linked pigment formed suggests that the mechanism of vinyl-linked MV3G and catechin pigment formation through the degradation of MC1 and MC2, as proposed by Francia-Aricha et al. (1997), is not the preferred mechanism for the formation of significant amounts of these compounds. The presence of oxygen interferes with the formation of vinyl-linked MV3G and catechin pigments as shown by the lack of vinyl-linked MV3G and catechin pigment present in the degradation of MC1 and MC2 under aerobic conditions.

The 8,8-methylmethine-(epi)catechin-MV3G pigments have significant colour at wine pH due to their lack of hydration and their resistance to bisulfite bleaching. Therefore these pigments would be effective at low concentrations in contributing to the colour of young red wines. Although 8,8-methylmethine-(epi)catechin-MV3G pigments have greater colour stabilities than MV3G, they have lower temporal stabilities which would allow them to contribute to the formation of further colour and temporally stable pigments in red wines.

Chapter 6 - pH-Dependent equilibria of 8,8-methylmethine-(epi)catechin-MV3G pigments

6.2 Introduction

High voltage paper electrophoresis (HVPE) has been used to determine the ionisation constants, with good correlations with literature values, of several low molecular weight compounds including: adenine, adenosine, 5'-adenosine monophosphate, 5'-adenosine diphosphate and 5'-adenosine triphosphate (Tate, 1981). More recently, Asenstorfer et al. (2003) used HVPE to determine the ionisation constants of MV3G. It was found that MV3G was more acidic (pKa_1 1.76) than previously determined using UV-visible spectroscopy (pKa 4.25, Brouillard and Delaporte, 1977).

Hydration of anthocyanins is dependent upon the structure of the anthocyanin (Brouillard and Lang, 1990, Mazza and Brouillard, 1987, Timberlake and Bridle, 1967). The hydration constant of MV3G has been determined, using UV-visible spectroscopy, as 2.6 (Brouillard and Delaporte, 1977) and 2.66 (Asenstorfer et al., 2003). The greater resistance to colour loss due to pH for MC2 (Escribano-Bailón et al., 2001) should indicate that the 8,8-methylmethine compounds either have a higher hydration constant than the parent anthocyanin or that hydration is not occurring. Recently, Duenas et al., (2006) proposed that MC2 does not undergo hydration whilst MC1 undergoes slight hydration (pK_H 4.17). It was also proposed that MC2 had ionisation constants of pKa_1 3.29 and pKa_2 5.38 and MC1 had ionisation constants of pKa_1 3.53 and pKa_2 5.04. The determination of the ionisation/hydration constants of 8,8-methylmethine-(epi)catechin-MV3G compounds, using HVPE and UV-visible spectroscopy, are investigated in this chapter to explain their greater resistance to colour loss due to pH.

6.2 Results

6.2.1 HVPE determination of ionisation constants

An oxalate buffer was used to cover the pH range pH 1.4 to 4.6 and an oxalate/citrate buffer for pH 3.0 to 7.0. The buffers used did not present a contiguous mobility profile. However, overlapping of the buffers allowed the development of a profile covering the pH range from 1.4 to 7.0.

Equation 2.1 (see Chapter 2) was fitted to the HVPE data for each of the compounds in the two buffers (Figure 6.1 and Figure 6.2). Due to the electro-osmotic flow of the buffer towards the cathode and the adsorption of the neutral species to the cellulose, the plateau for the neutral species does not coincide with the neutral reference compound (fructose) (Figure 6.1). Estimates of the pKa values as determined using Equation 2.1 are listed in Table 6.1.

Table 6.1. Macroscopic pKa values for MC1, MC2, ME1 and ME2 as derived using HVPE.

Ionisation constant	Compound			
	MC1	**MC2**	**ME1**	**ME2**
pKa_1	2.44±0.05	2.33±0.05	2.35±0.04	2.37±0.04
pKa_2	4.10±0.04	3.76±0.05	4.14±0.06	3.67±0.07
pKa_3	6.53±0.05			

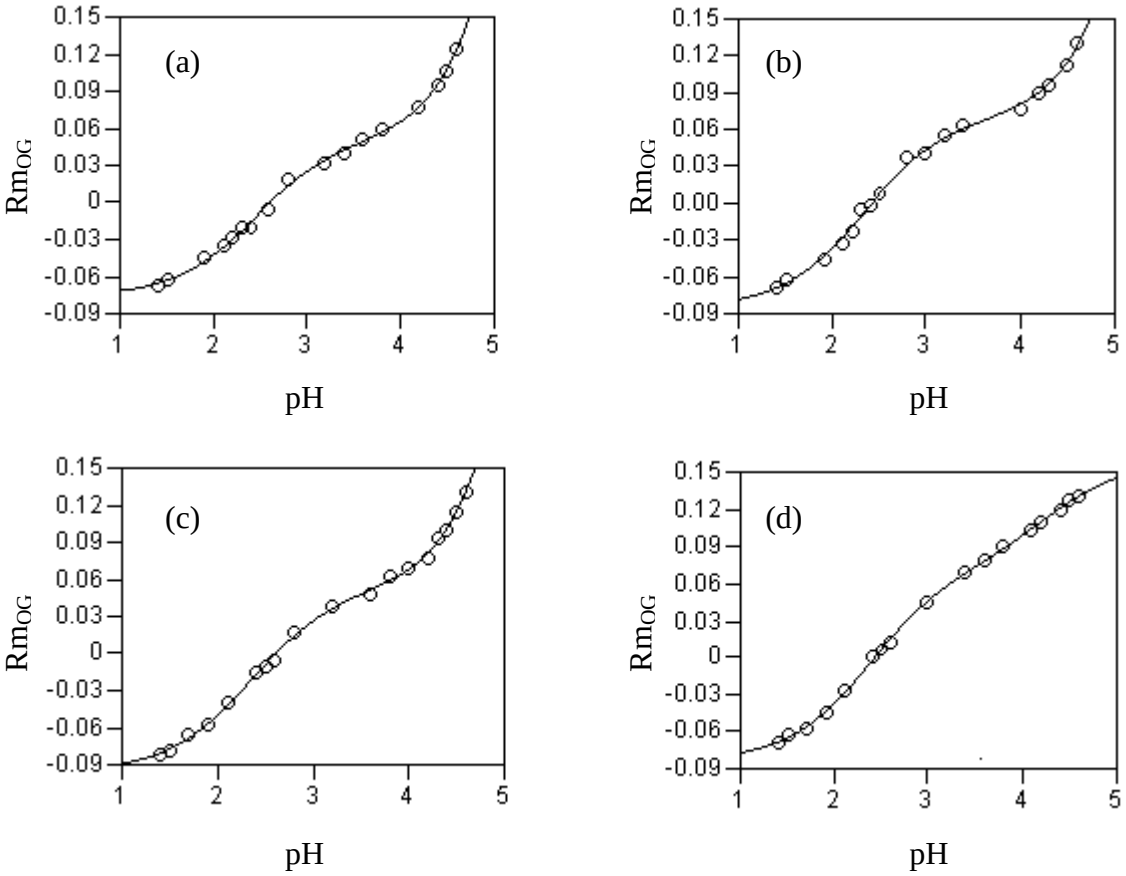

Figure 6.1. Relative mobilities of (a) MC1, (b) MC2, (c) ME1 and (d) ME 2 in an oxalate buffer as a function of pH. Equation 1.1 has been fitted for the estimation of pKa values. The coefficients of determination (r^2) for the four curves are (a) 0.99785, (b) 0.99703, (c) 0.99891 and (d) 0.99948.

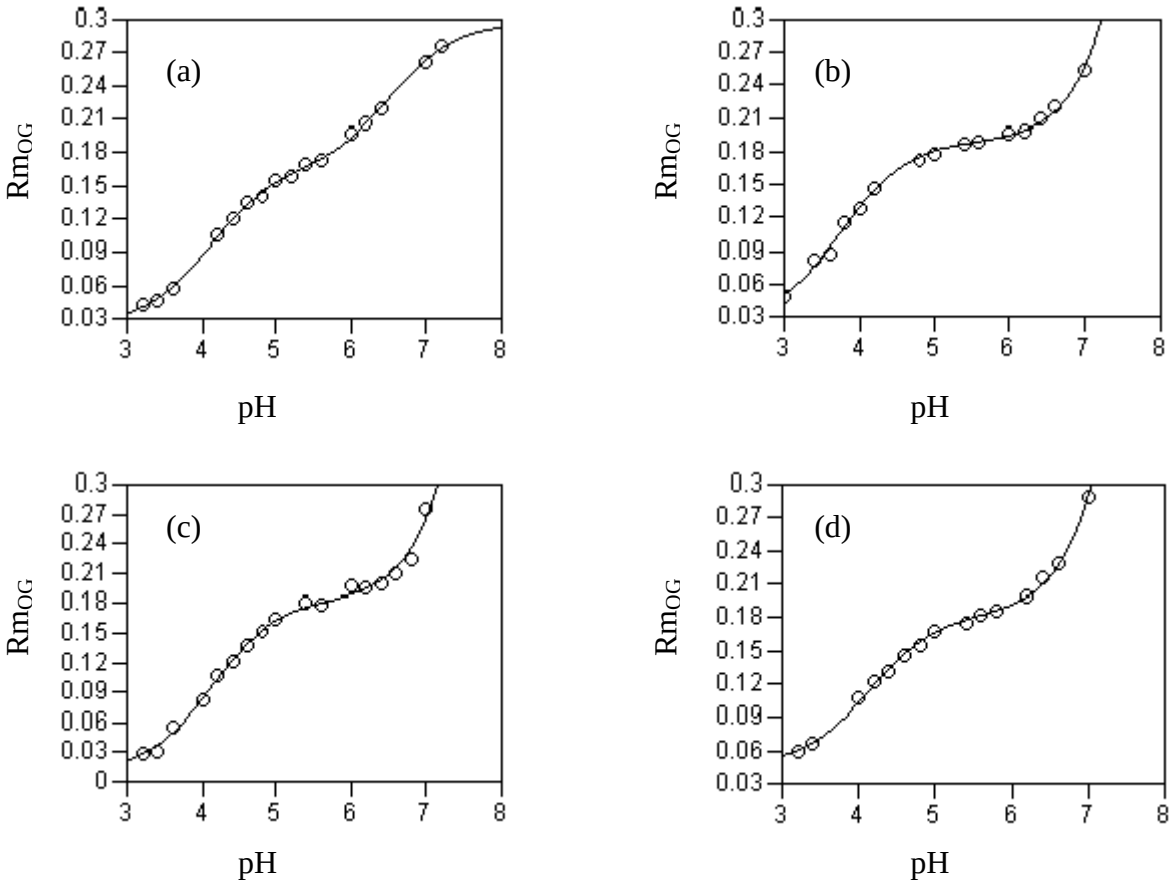

Figure 6.2. Relative mobilities of (a) MC1, (b) MC2, (c) ME1 and (d) ME2 in an oxalate/citrate buffer as a function of pH. Equation 1.1 has been fitted for the estimation of pKa values. The coefficients of determination (r^2) for the four curves are (a) 0.99901, (b) 0.99636, (c) 0.99470 and (d) 0.99746.

The plateau regions in Figure 6.1 and Figure 6.2 correspond to the optimum pHs for particular ionisation states. Table 6.2 lists the estimated optimum occurrences for particular ionisation states. From the electrophoretograms, the colours of the different forms of MC1, MC2, ME1 and ME2 were: flavylium ion – red, quinonoidal base – red with a purple tint and quinonoidal anion – purple.

Table 6.2. Estimated optimum pHs for the occurrences of ionisation states for MC1, MC2, ME1 and ME2.

Ionisation state	**Compound**				**Colour**
	MC1	**MC2**	**ME1**	**ME2**	
Flavylium ion	<1.4	<1.3	<1.3	<1.3	red
Quinonoidal base	3.3	3.1	3.2	3.0	red/purple
Anion	5.6	5.3	5.6	5.2	purple

6.2.2 UV-visible spectrophotometric determination of ionisation constants

The analytical wavelengths chosen for the determination of pK values were 480 nm, 500 nm, 535 nm and 620 nm. These wavelengths afforded the greatest difference in absorbances between different species. By fitting Equation 1.2 to the data from the four analytical wavelengths (Figure 6.3, Appendix 4), the macroscopic pK values were calculated (Table 6.3). The first two ionisation constants correlated to those obtained via HVPE and were assigned as pKa_1 and pKa_2 rather than hydration constants. A third ionisation constant (pKa_3) was also obtained via spectroscopic methods.

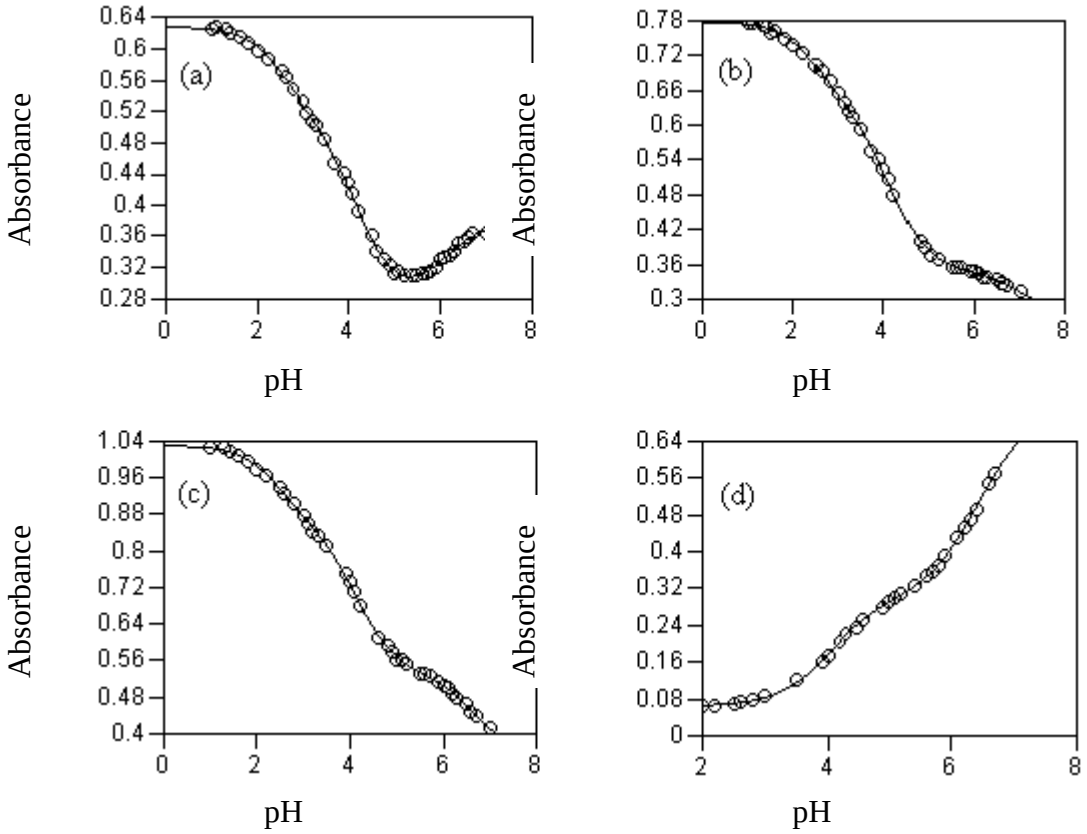

Figure 6.3. Absorbance of MC1 as a function of pH with Equation 1.2 fitted for the estimation of ionisation constants. The analytical wavelengths used were (a) 480 nm, (b) 500 nm, (c) 535 nm and (d) 620 nm. The coefficients of determination (r^2) for the four curves were (a) 0.99901, (b) 0.99636, (c) 0.99470 and (d) 0.99760.

Table 6.3. Macroscopic pKa values for MC1, MC2, ME1 and ME2 as derived using spectroscopic methods.

Ionisation Constant	**Analytical Wavelength (nm)**	**MC1**	**MC2**	**ME1**	**ME2**
pKa_1	480	2.53±0.07	2.51±0.06	2.56±0.06	
	500	2.50±0.06	2.50±0.06	2.51±0.07	2.58±0.08
	535	2.47±0.06	2.56±0.06	2.53±0.06	2.50±0.08
	average	**2.50**	**2.52**	**2.53**	**2.54**
pKa_2	480	4.15±0.04	3.71±0.04	4.12±0.04	
	500	4.13±0.03	3.70±0.04	3.99±0.05	3.54±0.06
	535	4.14±0.03	3.78±0.07	3.94±0.04	3.46±0.05
	620	4.05±0.03	3.56±0.04	4.08±0.05	3.39±0.04
	average	**4.12**	**3.69**	**4.03**	**3.46**
pKa_3	480	6.09±0.08	6.05±0.03	6.01±0.04	
	535	6.68±0.09	6.27±0.03		6.56±0.03
	620	6.38±0.03	6.49±0.02	6.55±0.03	6.35±0.02
	average	**6.38**	**6.27**	**6.28**	**6.46**

6.2.3 Determination of ionisation constants using spectra area and centre of mass

As the HVPE and UV-visible data indicate that hydration is not occurring for the 8,8-methylmethine-(epi)catechin-MV3G compounds, Equation 2.2 was applied to the spectra area and centre of mass curves (refer Chapter 5) for MV3G, MC1 and MC2 and are listed in Table 6.4. The pK values calculated for MC1 and MC2 closely correlate to those obtained via HVPE and UV-visible determinations. The pK values for MV3G obtained consisted of pK_{H1} (2.71, from spectra area) and pK_{H2} (6.05, from centre of mass) are consistent with the values (2.66 and 5.90 respectively) obtained by Asenstorfer et al. (2003).

Table 6.4. pKa values obtained from spectra area and centre of mass curves for MV3G, MC1 and MC2.

Compound	pK Value	
	Spectra Area	Centre of Mass
MC1	2.41±0.06	
	4.21±0.06	4.27±0.01
MC2	2.33±0.05	
	3.64±0.08	3.77±0.03
MV3G	2.71±0.07	4.15±0.07
		6.05±0.07

6.2.3.1 Distribution profiles

The average of the ionisation constants as determined through HVPE and UV-visible spectroscopy are listed in Table 6.5. The averages were used to plot distribution diagrams of MC1, MC2, ME1 and ME2 (Figure 6.4). At red wine pH (approximately 3.6), the predominant species of MC1, MC2, ME1 and ME2 are the red quinonoidal base and the purple quinonoidal anion (Figure 6.4).

Table 6.5. Average macroscopic pKa values for MC1, MC2, ME1 and ME2 as derived using HVPE and spectroscopic methods.

Ionisation Constant	**MC1**	**MC2**	**ME1**	**ME2**
pKa_1	2.47	2.43	2.44	2.46
pKa_2	4.11	3.73	4.09	3.57
pKa_3	6.46	6.27	6.28	6.46

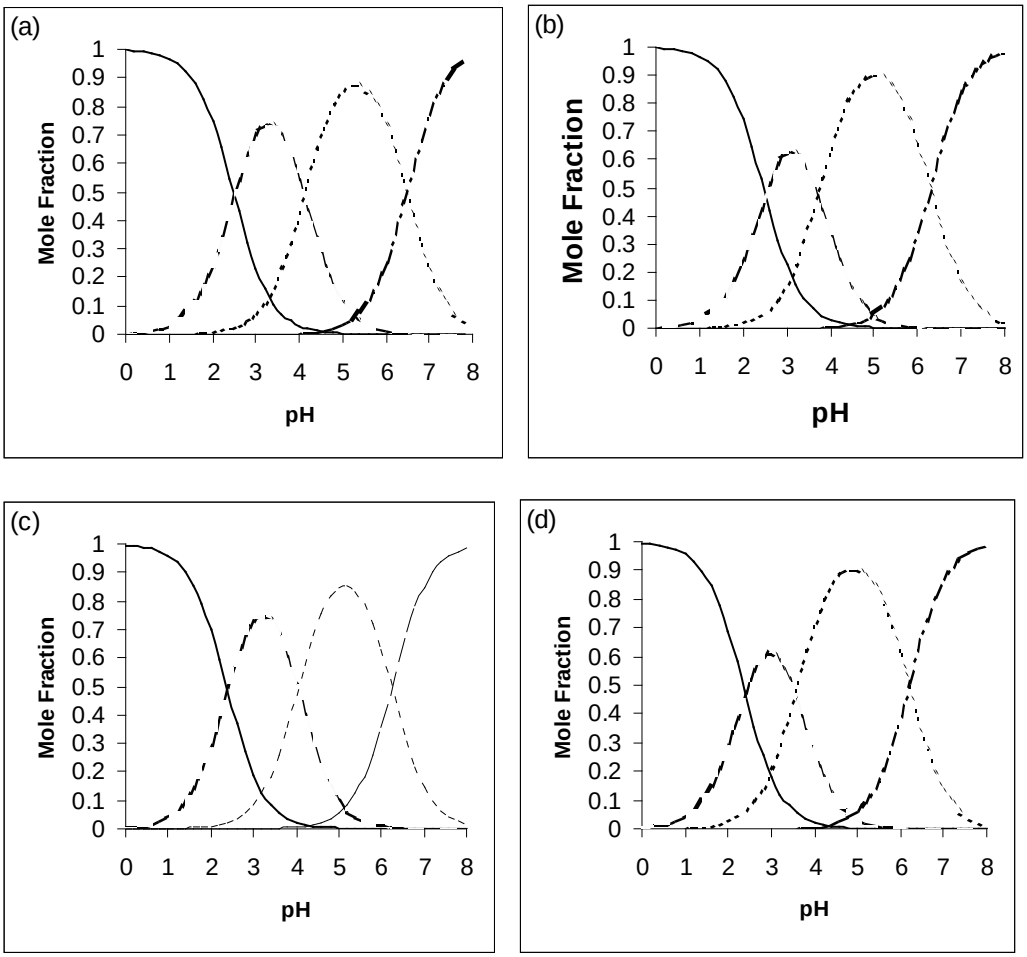

Figure 6.0.4. Species distribution as a function of pH for (a) MC1, (b) MC2, (c) ME1 and (d) ME2 (ionisation constants from Table 6.5). (—— - flavylium ion, ····· - quinonoidal base, - - - - - quinonoidal anion, _ . _ - quinonoidal dianion)

6.4 Discussion

Duenas et al. (2006) has reported that MC2 does not undergo hydration whilst MC1 undergoes slight hydration (pK_H 4.17). Duenas et al. (2006) also proposed that MC2 has ionisation constants of pKa_1 3.29 and pKa_2 5.38 and MC1 has ionisation constants of pKa_1 3.53 and pKa_2 5.04. In this study, covering a wider pH range, the macroscopic ionisation/hydration constants of MC1, MC2, ME1 and ME2, determined through HVPE and UV-Vis spectroscopy, correlated and therefore can be regarded as ionisation constants rather than hydration constants. The ionisation constants (pKa_1, pKa_2 and pKa_3) of MC1, MC2, ME1 and ME2 were found to be significantly different to those of MV3G, as determined by Asenstorfer et al. (2003) and to those determined by Duenas et al. (2006) (pKa_1 and pKa_2 for MC1 and MC2).

The differences in results obtained in this study to those of Duenas et al. (2006) can be attributed to the methodology used. In this study, both HVPE and UV-Vis spectroscopy were used to determine the ionisation constants whereas Duenas et al. (2006) relied solely upon UV-Vis spectroscopy. Also, the pH range used (1.0 to 7.0) was more extensive than that used by Duenas et al. (2006) (2.7 to 4.7). Another possible factor involved in the differences in ionisation/hydration constants is the distribution profile of MV3G. In this study, the distribution profile as determined by Asenstorfer et al. (2003) was used, whereas Duenas et al. (2006) used the distribution profile as determined by Brouillard and Delaporte (1977).

The method of plotting $A_0/(A_0 - A)$ versus 10^{-pH} (Brouillard and Delaporte, 1977) to determine the pK value of an anthocyanin is reliant upon the assumption than only two transformations are occurring for the compound studied, i.e. ionisation and hydration. However, in this study, two ionisations are occurring in the pH range studied by Duenas et al. (2006). This could explain the loss of linearity observed by Duenas et al. (2006) in their determinations of the pK values for MC1 and MC2. It is worth noting that the pK values determined for MC1 and MC2 by Duenas et al. (2006) are midway between pKa_1 and pKa_2 values determined in this study.

Further evidence that little/no hydration is occurring for MC1, MC2, ME1 and ME2 is the presence of isosbestic points and the similar minima in the spectra area as observed in the previous chapter. Also, a change in wavelength in the isobetic point is also observed between different ionisation states (e.g. 575 nm for flavylium ion/quinonoidal base and 565 nm for quinonoidal base/quinonoidal anion).

The first ionisation constant (pKa_1) involves the loss of a proton from the MV3G flavylium ion moiety to form the quinonoidal base. Deprotonation of the hydroxyl group can occur, as with MV3G, at the 5-, 7- or 4'-positions (Figure 6.5). Asenstorfer et al. (2003) determined pKa_1 of MV3G as 1.76 (c.f. 4.25 as determined by Brouillard and Delaporte (1977)). The pKa_1 values of MC1, MC2, ME1 and ME2 were slightly higher (by 0.6-0.7 units) than that of MV3G as determined by Asenstorfer et al. (2003). This indicates that they are either slightly less acidic than the parent MV3G. The change in pKa_1 indicates that substitution on the 8-position of MV3G by the flavan-3-ol moiety has an effect on the deprotonation of the MV3G moiety.

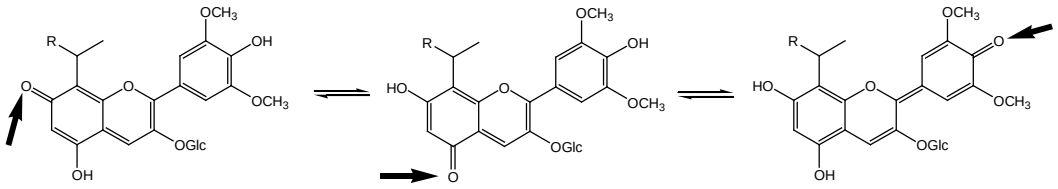

R = (epi)catechin

Figure 6.5. Quinonoidal base forms of MC1, MC2, ME1 and ME2. Arrows indicate locations of deprotonation of the flavylium form.

The second ionisation constant (pKa_2) involves deprotonation of the MV3G quinonoidal base moiety to form the quinonoidal anion. As with the first deprotonation, the second deprotonation can occur at the 5-, 7- or 4'-positions depending upon the location of the first deprotonation. For example, if the first deprotonation occurs at the 4'-position, the subsequent deprotonation can occur at the 5- or 7-positions (Figure 6.6). Asenstorfer et al. (2003) determined the pKa_2 value of MV3G as 5.36. Previous studies have shown (Perrin et al., 1981) that the substitution of a *p*-hydroxyphenylmethine group at the electrophilic 8-position is expected to facilitate the loss of a proton, particularly on the A-ring, thereby lowering pKa_2. This is supported by the significantly lower values of MC1, MC2, ME1 and ME2 (by 1.2 to 1.7 units) than that of MV3G.

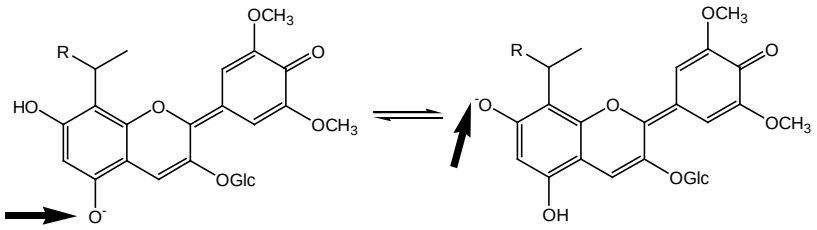

R = (epi)catechin

Figure 6.6. Quinonoidal anion forms of MC1, MC2, ME1 and ME2 where the first deprotonation has occurred at the 4'-position. Arrows indicate locations of the second deprotonation.

The third ionisation constant (pKa_3) involves the deprotonation of the final hydroxyl group of the MV3G moiety to form the quinonoidal dianion. As with the second ionisation constant (pKa_2), substitution of a *p*-hydroxyphenylmethine group at the electrophilic 8-position is expected to facilitate the loss of a proton, thereby lowering pKa_3 (Perrin et al., 1981). This is supported by the significantly lower pKa_3 values of MC1, MC2, ME1 and ME2 (by 1.6 to 1.8 units) than that of MV3G (8.08, Asenstorfer et al., 2003).

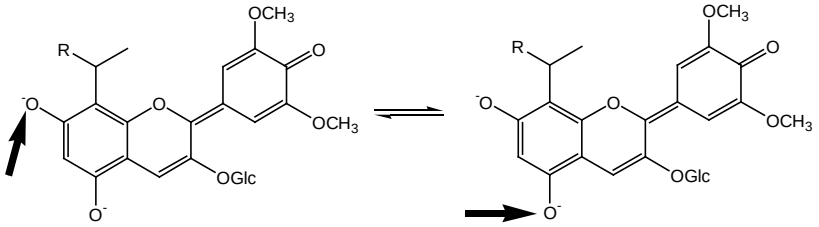

R = (epi)catechin

Figure 6.7. Quinonoidal dianion forms of MC1, MC2, ME1 and ME2. Arrows indicate locations of the third deprotonation.

The ionisation constants (pKa_1, pKa_2 and pKa_3) of MC1, MC2, ME1 and ME2 were ascribed to deprotonations of the MV3G moiety. The (epi)catechin moiety can also be deprotonated, however the macroscopic ionisation constants for (epi)catechin are 8.79, 9.44, 11.18 and 13.25 (Slabbert, 1977), which are well above the pH ranges studied.

The correlation between HVPE and UV-vis spectroscopy indicates that either hydration is not occurring or occurring to a very small extent within the pH range studied. This can be partly explained by steric hindrance to the nucleophilic addition of the water molecule. The (epi)catechin moiety folding over the B-ring offers steric hindrance to nucleophilic attack, by water, to the 2- and 4-positions of the MV3G moiety (Figure 6.8).

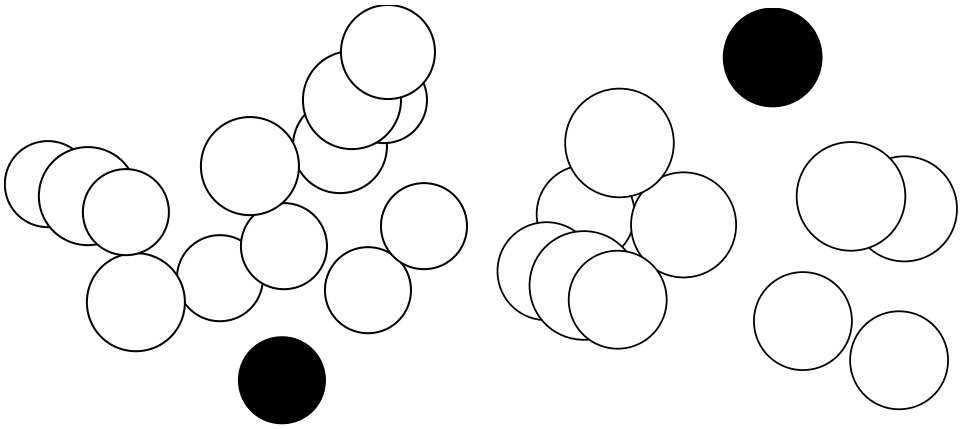

Figure 6.8. Steric hindrance of the 2- and 4-positions of the MV3G moiety to hydration. The water molecule and the 2- and 4-positions of the MV3G moiety are in black.

Although steric hindrance protects the 8,8-methylmethine compounds from hydration from one direction (Figure 6.8), the other direction is still open to nucleophilic attack. This is especially true for MC2 and ME2 where the flavan-3-ol is on the same side as the glucoside (refer Chapter 4). Two possible methods of preventing hydration from the other aspect are steric hindrance and self-association/dimerisation. Hydration results in the loss of planarity of the MV3G C-ring resulting in movement of the B-ring and the glucoside. Depending upon the direction of the movements, this would force the B-ring or the glucoside closer to the flavan-3-ol. Furthermore, the loss of planarity in the MV3G C-ring would move the A-ring. To move the flavan-3-ol attached to the A-ring would require extra energy to overcome the inertia. Self-association/dimerisation, would afford protection from the other direction (Figure 6.9).

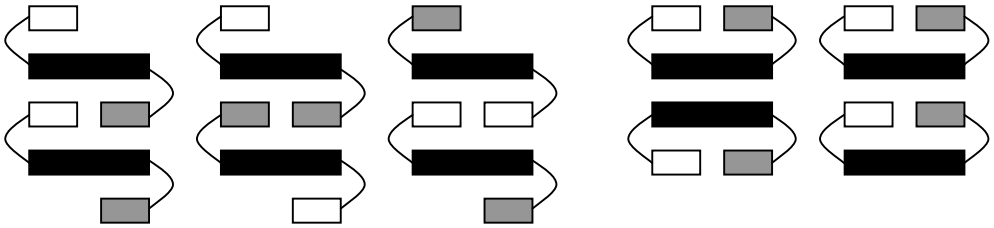

A B

Figure 6.9. Possible self-association/dimerisation structures of (A) MC1/ME1 and (B) MC2/ME2. Malvidin aglycone – black, epi(catechin) – white, glucoside – grey.

This study has shown that hydration is not occurring or occurring to a very small extent within the pH range studied. Therefore the distribution of MC1, MC2, ME1 and ME2 will be regarded as ionisation states. MC1, MC2, ME1 and ME2 at low pH are predominately in the red flavylium ion form. As the pH increases, deprotonation occurs to form the red, quinonoidal base forms. The quinonoidal base predominates in the pH range of approximately 2.5 to 4.0. As the pH further increases, the quinonoidal base is deprotonated to form the purple quinonoidal anion. The quinonoidal anion predominates in the pH range of approximately 4.0 to 6.2. At wine pH (3.0 – 4.0), the red quinonoidal base and purple quinonoidal anion forms predominate. These forms are red/purple in colour and, when present, could make an important contribution to the purple tint associated with young red wines.

Chapter 7 - Fermentations incorporating added MV3G and flavan-3-ols

7.1 Introduction

Grape anthocyanins are the major contributors to the colour of young red wines. As wines age, these anthocyanins undergo reactions to form oligomeric and polymeric pigments (Somers, 1971; Jones and Asenstorfer, 1997). The use of fractionation (Asenstorfer et al., 2001), HPLC and electrospray mass spectroscopy has allowed the identification of some of these compounds in wines. 8,8-Methylmethine-flavan-3-ol-anthocyanin compounds (Cheynier et al., 1997; Vivar-Quintana et al., 1999) and vinyl-linked flavan-3-ols and anthocyanins (Hayasaka and Asenstorfer, 2002) and vitisins (Bakker and Timberlake, 1997; Vivar-Quintana et al., 1999; Asenstorfer, 2001) have been identified in wines.

A hindrance to the understanding of pigment evolution in red wines is the complexity of the pigment composition found in red wines. To further understand the evolution of pigments in young red wines it is necessary to simplify the number of compounds involved during fermentation. Therefore, model wine fermentations involving MV3G in the presence of different flavan-3-ol compositions and commercial yeast strains were studied.

7.2 Results

7.2.1 Fermentation Details

A preliminary fermentation using CDGJM containing MV3G (640 mg/L) and catechin (590 mg/L) inoculated with EC1118 yeast was conducted. The fermentation took nine days and the resultant wines had an alcohol content of 10.3±0.8 % v/v. At the end of fermentation the concentration of MV3G decreased to 96 mg/L (Table 7.1). After 80 days of storage, the concentration of MV3G continued to decrease, at a slower rate, to a level of 9 mg/L. MC1 and MC2 were the major pigments formed during fermentation (Table 7.1). The levels of the 8,8-methylmethine-catechin-MV3G pigments were 171 mg/L at the end of fermentation and reached a maxima of 200 mg/L after 1-2 weeks of storage whereafter they decreased to 103 mg/L after 80 days of storage (Table 7.1). The level of other pigments increased from 43 mg/L (MV3G eq) to 96 mg/L (MV3G eq) after 80 days of storage.

Table 7.1. Development of MV3G, MC1 and MC2 and other pigments during preliminary fermentation and maturation of model wines

Day	MV3G (mg/L)	MC1 & MC2 (mg/L MV3G eq)	Other Pigments (mg/L MV3G eq)
0	642	0	0
9	96	171	43
16	81	201	53
23	53	197	53
30	37	191	54
61	15	153	78
90	9	103	96

The length of fermentation, alcohol content and pH of the wines resulting from the fermentations is listed in Table 7.2. The fermentations using the yeast strain EC118 were very rapid in duration in lasting 2-3 days whereas the other yeasts (Syrah and BDX) were more widespread in duration (2-5 days).

Table 7.2. Constituents, yeast strain, duration, alcohol content and pH of model wines resulting from fermentations carried out at 30^0C.

Constituents	Yeast Strain	Ferment Duration (days)	Adjusted pH
Control	EC1118	2	3.60±0.03
Control	Syrah	4	3.58±0.02
Control	BDX	4	3.57±0.01
MV3G & Catechin	EC1118	2	3.58±0.02
MV3G & Catechin	Syrah	5	3.60±0.01
MV3G & Catechin	BDX	2	3.60±0.01
MV3G & Proanthocyanidin B3	EC1118	2	3.59±0.02
MV3G & Proanthocyanidin B4	EC1118	2	3.57±0.01
MV3G & Procyan. B1 & B2	EC1118	2	3.58±0.01
MV3G	EC1118	3	3.59±0.01

7.2.2 Influence of Yeast Strain on Wine Pigment Formation

During fermentation there was a rapid decline in MV3G (Table 7.3) with the Syrah and BDX wines having significantly lower (190-200 mg/L) amounts at the end of fermentation than EC1118 (380 mg/L). The levels of MV3G decreased during storage with BDX and EC1118 decreasing at a more rapid rate than Syrah. By 60 days (from the start of the fermentation) virtually all of MV3G had disappeared for Syrah whereas after 159 days there were still noticeable levels present for EC1118 (44 mg/L) and BDX (16 mg/L). The rates of loss of MV3G, through degradation and reaction, was determined to be first order with rates of 0.0133 day^{-1}, 0.0146 day^{-1} and 0.0452 day^{-1} for the EC1118, BDX and Syrah wines respectively. The rates of loss for MV3G were significantly higher than that determined under anaerobic conditions (0.0064 day^{-1}) in Chapter 5.

Table 7.3. Concentration of MV3G (mg/L) for model wines formed from the fermentations involving the yeasts EC1118, Syrah and BDX.

day	EC118	Syrah	BDX
0	413	417	433
2	379	318	192
5		202	
20	241	124	92
44	177	43	63
60	143	4	55
91	92	1	36
125	62	1	21
159	45	0	17

The major pigments formed during fermentation were MC1 and MC2 with levels by the end of fermentation (Table 7.4) of 39 mg/L for the EC1118 wine, 60 mg/L for the Syrah wine and 45 mg/L for the BDX wine. MC1 and MC2 continued to be produced (at a first order rate of 0.011 day^{-1}) for the Syrah wine reaching levels of 92 mg/L after 44 days before a rapid decrease to 3 mg/L after 91 days (at a first rate order of 0.0372 day^{-1}). The rapid decrease in MC1 and MC2 in the Syrah wine coincided with the formation of pigmented precipitate. The EC1118 wine also showed an increase in levels of MC1 and MC2 (at a first order rate of 0.011 day^{-1}) reaching a maximum concentration of 72 mg/L after 60 days before decreasing to 42 mg/L after 159 days (at a first rate order of 0.005 day^{-1}). The levels of MC1 and MC2 for the BDX wine remained at constant levels of 39 to 46 mg/L for the first 91 days whereafter it gradually decreased to 33 mg/L after 159 days (at a first rate order of 0.003 day^{-1}).

Table 7.4. Concentration of MC1 and MC2 (mg/L MV3G eq) for model wines formed from the fermentations involving the yeasts EC1118, Syrah and BDX.

day	EC118	Syrah	BDX
0	0	0	0
2	39	56	45
5		60	
20	49	67	39
44	64	91	43
60	72	31	46
91	58	3	46
125	52	2	38
159	42	1	34

After 20 days a new, although small, peak was observed in the HPLC chromatograms of the Syrah wines. This peak was also observed after 44 days in the HPLC chromatograms of the EC1118 and BDX wines. Analysis of the peak gave it an m/z of 805 amu which was in accord with the mass of the vinyl-linked MV3G and catechin dimer. In the Syrah wine, there was a rapid increase in concentration reaching a maximum, after 60 days, of 1.5 mg/L (MV3G eq) (Table 7.5). This was followed by a rapid decrease similar to that of MC1 and MC2. The rate of formation in the EC1118 and BDX wines was slower, with the pigment only being noticeable on the chromatograms after 44 days where it reached levels of 1.0 mg/L (MV3G eq). Thereafter the concentration of the pigment gradually increased to levels of 1.5 mg/L (MV3G eq) and 2 mg/L (MV3G equivalent) after 159 days for the BDX and EC1118 wines respectively

Table 7.5. Concentration of pyranoanthocyanins (mg/L MV3G eq) for model wines formed from the fermentations involving the yeasts EC1118, Syrah and BDX.

day	EC118	Syrah	BDX
0	0	0	0
2	0	0	0
5		0	
20	0	1	0
44	1	1	1
60	1	1	2
91	2	1	1
125	2	0	1
159	2	0	2

The levels of other pigments was determined by subtracting the peak areas of MV3G and the vinyl- and 8,8-methylmethine-catechin-MV3G pigments from the total peak area at 520 nm on the chromatograms. The level of other pigments gradually increased from approximately 10 mg/L (MV3G eq) at the end of fermentation to approximately 40 mg/L (MV3G eq) for BDX and EC1118 after 159 days (Figure 7.5). The Syrah wine had a more rapid increase in other pigments increasing from 8 mg/L (MV3G eq) at the end of fermentation to 60 mg/L (MV3G eq) after 60 days. The levels of other pigments in the Syrah wine remained at approximately 60 mg/L (MV3G eq) until 91 days whereafter there was a dramatic decrease to 16 mg/L (MV3G eq) after a further 159 days. The decrease in other pigments in the Syrah wine corresponded to the formation of pigmented precipitate.

Table 7.6. Concentration of other pigments for model wines formed from the fermentations involving the yeasts EC1118, Syrah and BDX.

day	EC118	Syrah	BDX
0	0	0	0
2	8	11	8
5		11	
20	27	28	24
44	26	44	23
60	42	59	29
91	62	65	42
125	59	28	39
159	44	17	40

The Syrah and BDX wines had a significant decrease in total pigments during fermentation (Table 7.7), due mainly to loss of MV3G**.** Thereafter the total pigments in the Syrah wine continued to decrease to 18 mg/L after 159 days. In the BDX wine the total pigments decreased to 125 mg/L after 44 days where it remained relatively constant until 91 days. Thereafter the total pigments gradually decreased to 92 mg/L by 159 days. The EC1118 wine had no decrease in total pigments during fermentation but during storage the concentration of total pigments decreased to 132 mg/L by 159 days.

Table 7.7. Concentration of total pigments (mg/L) for model wines formed from the fermentations involving the yeasts EC1118, Syrah and BDX.

day	EC118	Syrah	BDX
0	413	417	433
2	426	385	245
5		273	
20	318	221	155
44	267	179	130
60	258	96	132
91	212	70	125
125	174	31	99
159	133	18	92

7.2.3 Influence of Yeast Strain on Wine Colour

The spectra of the wines at the start of fermentation (Figure 7.1) were consistent with that of MV3G (at pH 3.6) with a peak at 522 nm. After the fermentations and during storage the spectra of the wines all displayed the influence, of different timing and area, of the 8,8-methylmethine compounds on wine colour. In all cases a noticeable shoulder was formed at 450 nm (consistent with the spectra of MC1 and MC2 at pH 3.6 as discussed in Chapter 5). At the end of fermentation the spectra of the EC1118 wine (Figure 7.1 (a)) increased in area (by 14%) and had a slight increase of 3 nm in λ_{max}. By day 46 the area of the spectra had decreased (by 10%), λ_{max} had increased by a further 3nm and the influence of the 8,8-methylmethine on the compounds was noticeable. The area of the spectra continued to decrease (by a further 6%) by day 126 whereafter it remained constant and λ_{max} remained constant at 530 nm. The area of the spectra of the Syrah wine (Figure 7.1 (b)) decreased at the end of fermentation (by 26%) and λ_{max} showed a significant increase of 7 nm. This was followed by a significant increase in area (by 46%) by day 46, a further significant increase in λ_{max} of 10 nm and the spectra showed characteristics of the 8,8-methylmethine compounds. This was followed by a dramatic decrease (of 52%) in the area of the spectra by day 91, with a slight increase in λ_{max} of 2nm. The area of the spectra continued to decrease, to a lesser degree (by a further 56%), by day 159 and λ_{max} showed a dramatic

decrease of 14 nm to 527 nm. The area of the spectra of the BDX wine (Figure 7.1 (c)) had a large decrease (by 53%) at the end of fermentation and λ_{max} showed a significant increase of 6 nm. By day 46 the spectra showed the characteristics of the 8,8-methylmethine compounds. The area of the spectra had also increased (by 20%) with little change in λ_{max}. By day 91 the area of the spectra had further increased slightly (by 12%), λ_{max} increased by 4 nm whereafter both remained relatively constant throughout to day 159.

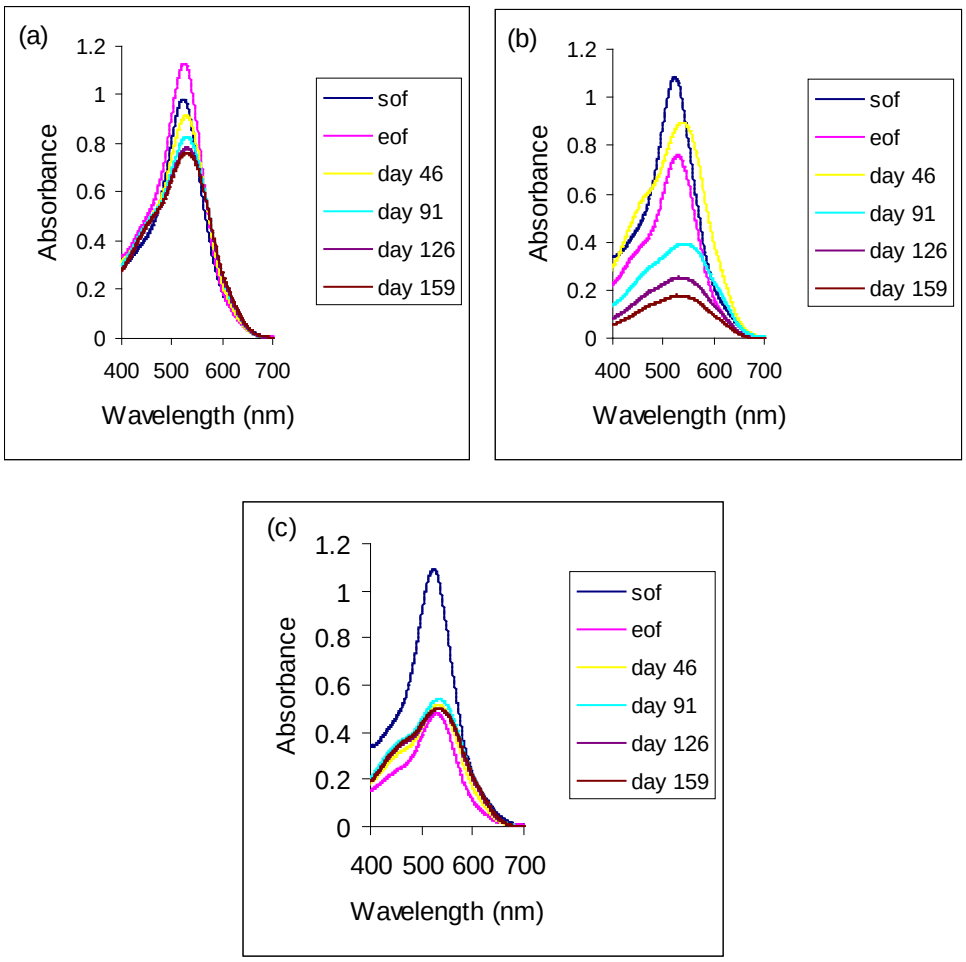

Figure 7.1. Spectra evolution of the wines formed from the fermentations involving (a) EC1118, (b) Syrah and (c) BDX. sof = start of fermentation, eof = end of fermentation, day No. refers to the number of days from the start of fermentation.

The three different wines showed different evolutions in colour density (Figure 7.2). The colour density for the wine from the yeast EC1118 had an 11% increase at the end of fermentation. Thereafter by day 91 the colour density decreased by 23% whereafter it gradually decreased by a further 9% by day 159. The Syrah wine had a significant

decrease (26%) in colour density at the end of fermentation. The colour density then increased (by18%) at day 46 whereafter it dramatically decreased by 57% by day 91 whereafter it continued to significantly decrease (by a further 53%) by day 159. The dramatic decrease in colour density corresponded to significant levels of with the formation of pigmented precipitate. At the end of fermentation, the BDX wine had the highest decrease (55%) in colour density. Thereafter the colour density increased by 11% by day 46 whereafter the colour density remained relatively stable.

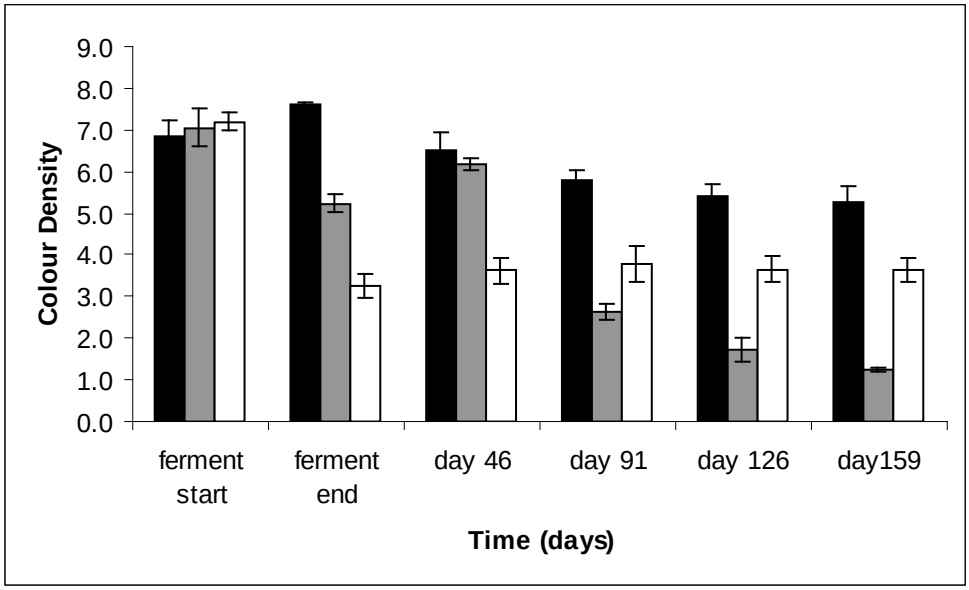

Figure 7.2. Colour density evolution for wines formed from the fermentations involving the yeasts (■) EC1118, (■) Syrah and (□) BDX.

The Glories' colour densities (A_{420} + A_{520} + A_{620} 1mm pathlength) of the wines (Figure 7.3) followed a similar trend to the colour densities although the magnitude of the changes differed slightly. The Glories's colour density increased by 9% by the end of fermentation for the EC1118 wines. Thereafter the densities decreased at a steadily (0.1% day^{-1} to 0.2% day^{-1}) by day 126 (decrease of 17%) whereafter they remained constant. By the end of fermentation for the Syrah wines the densities decreased by 26% which was followed by a 29% increase by day 46. Thereafter there was a dramatic decrease of 54% by day 91 and the densities further decreased by 35% from day 91 to day 126 and 29% from day 126 to day 159. There were dramatic decreases of 55% in colour densities for the BDX wines by the end of fermentation. This was followed by a steady increase of 23% by day 91 whereafter the densities remained constant.

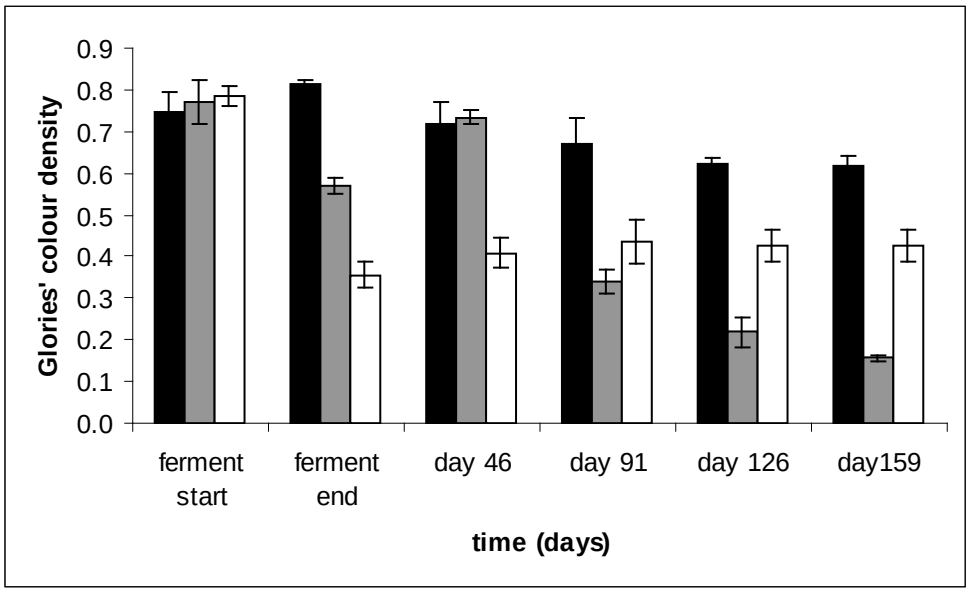

Figure 7.3. Changes in Glories' colour density with time for wines formed with the yeasts (■) EC1118, (■) Syrah and (□) BDX.

The development of hues were, as with colour density, different for the three wines (Figure 7.4). Although the hues increased for all the wines, this occurred at different rates and levels. The hue for the EC118 wine was the same (0.34) at the end of fermentation compared to the start of fermentation. The hue increased by 32% in 91 days whereafter it remained constant. Both the Syrah and BDX wines had slightly increased hues at the end of fermentation (0.37 and 0.40 respectively). The hue for the Syrah wine reached a maximum after 46 days (0.45) whereafter it remained constant. The BDX wine had the highest hue (0.51) after 91 days of maturation which remained similar after a further 34 days.

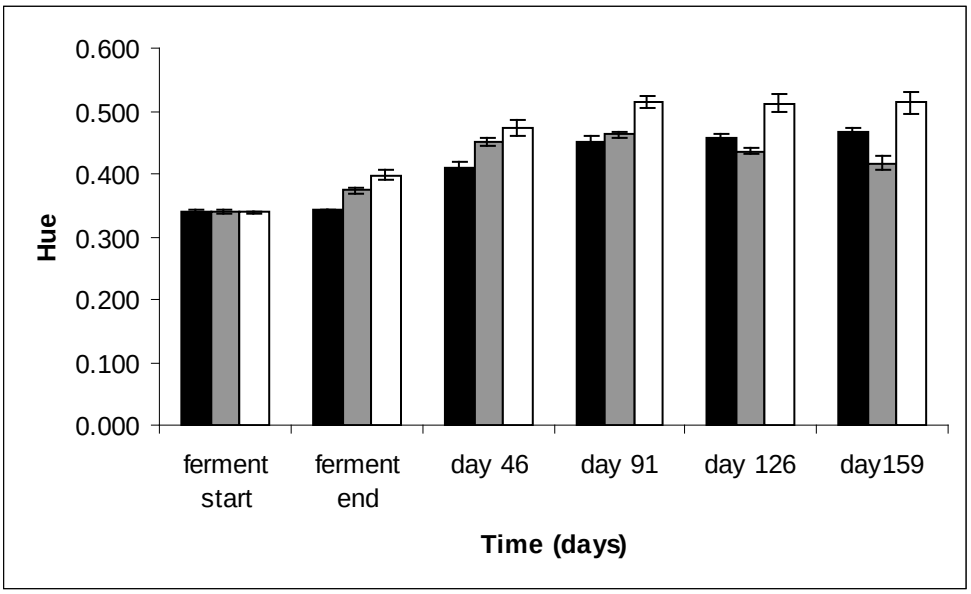

Figure 7.4. Hue evolution for wines formed from the fermentations involving the yeasts (■) EC1118, (■) Syrah and (□) BDX.

7.2.4 Influence of Flavan-3-ols on Wine Pigment Formation

At the end of fermentation the concentration of MV3G decreased from approximately 400 mg/L to 360-390 mg/L with the wine having no flavan-3-ols present having the lowest concentration (Table 7.8). During maturation the concentration of MV3G decreased in all the wines at varying first-order rates. The rate constants were determined as 0.013 day^{-1}, 0.010 day^{-1}, 0.011 day^{-1}, 0.035 day^{-1} and 0.038 day^{-1} for the wines containing catechin, proanthocyanidin B3, proanthocyanidin B4, proanthocyanidins B1 & B2 and no flavan-3-ols respectively. For the wines containing proanthocyanidins B1 & B2 and containing no flavan-3-ols, MV3G had decreased to levels of 24 mg/L and 8 mg/L by 90 days respectively and for both wines it had decreased to 2 mg/L by 159 days. In the wines containing no flavan-3-ols, the HPLC chromatograms consisted of a "hump" with two discernable peaks. Significant levels of MV3G at concentrations of 45 mg/L, 79 mg/L and 65 mg/L after 159 days occurred in the wines containing catechin, proanthocyanidin B4 and proanthocyanidin B3 respectively.

Table 7.8. Concentration of MV3G (mg/L) for model wines formed from the fermentations involving the flavan-3-ols catechin, proanthocyanidin B3, proanthocyanidin B4, proanthocyanidins B1 & B2 and no flavan-3-ols.

Day	Catechin	Proantho-cyanidin B3	Proantho-cyanidin B4	Proantho-cyanidins B1 & B2	No Flavan-3-ols
0	413	408	406	389	427
2	379	391	384	404	427
3					358
20	241	289	267	243	242
44	177	233	220	142	130
60	143	197	207	89	62
91	92	142	127	24	8
125	62	101	87	8	3
159	45	79	65	2	1

8,8-Methylmethine-flavan-3-ol-MV3G pigments were the major pigments formed by the end of fermentation (Table 7.9) for the wines containing flavan-3-ols. In the wines containing proanthocyanidins, mass spectra analysis revealed that apart from the 8,8-methylmethine-proanthocyanidin-MV3G compounds, significant amounts of 8,8-methylmethine-(epi)catechin-MV3G. The wines containing proanthocyanidins B3 and B4 contained approximately 23 mg/L (MC2 eq) at the end of fermentation whereas the wines containing catechin and proanthocyanidins B1 & B2 had higher levels of approximately 38 mg/L (MC2 eq). In the wine containing catechin, the concentration of 8,8-methylmethine-catechin-MV3G pigments reached a maximum of 72 mg/L (MC2 eq) after 90 days (at a first order rate of 0.011 day^{-1}) whereafter it decreased to 42 mg/L (MC2 eq) after 159 days (at a first order rate of 0.005 day^{-1}). At the end of fermentation the wine containing proanthocyanidin B3 contained 22 mg/L (MC2 eq) 8,8-methylmethine-flavan-3-ol-MV3G pigments. The concentration of the 8,8-methylmethine-flavan-3-ol-MV3G pigments reached 36 mg/L (MC2 eq) after 44 days (at a first order rate of 0.009 day^{-1}) where it remained constant until day 159 where it decreased to 30 mg/L (at a first order rate of 0.003 day^{-1}). The wine containing proanthocyanidin B4 contained 23 mg/L (MC2 eq) 8,8-methylmethine-flavan-3-ol-MV3G pigments at the end of fermentation. The levels of

these pigments increased to 45 mg/L (MC2 eq) after 60 days (at a first order rate of 0.011 day^{-1}) whereafter the concentration decreased to 22 mg/L (MC2 eq) after 159 days (at a first order rate of 0.008 day^{-1}). The wine containing proanthocyanidins B1 & B2 contained high levels of 8,8-methylmethine-flavan-3-ol-MV3G pigments at the end of fermentation (37 mg/L MC2 eq) which increased to 57 mg/L (MC2 eq) at 44 to 60 days (at a first order rate of 0.008 day^{-1}) and decreased to 11 mg/L (MC2 eq) after 159 days (at a first order rate of 0.017 day^{-1}). The decrease in the 8,8-methylmethine-flavan-3-ol-MV3G pigments corresponded to the the formation of pigmented precipitate. At the end of fermentation for the wines containing no flavan-3-ols, a new peak (1 mg/L MC2 eq) was observed after MV3G. Mass spectra analysis of the peak revealed it to be an 8,8-methylmethine-MV3G-MV3G dimer. The concentration of the 8,8-methylmethine-MV3G-MV3G dimer increased to a maximum of 3 mg/L (MC2 eq) at 44 to 60 days whereafter it decreased to 0.5 mg/L (MC2 eq) by 159 days.

Table 7.9. Concentration of 8,8-methylmethine pigments (mg/L MV3G eq) for wines formed from the fermentations involving catechin, proanthocyanidin B3, proanthocyanidin B4, proanthocyanidins B1 & B2 and no flavan-3-ols.

Day	Catechin	Proantho-cyanidin B3	Proantho-cyanidin B4	Proantho-cyanidins B1 & B2	No Flavan-3-ols
0	0	0	0	0	0
2	39	22	24	37	0
3					1
20	49	27	30	46	2
44	64	36	35	57	3
60	72	37	46	58	3
91	58	38	35	38	0
125	52	36	27	23	0
159	42	31	22	11	0

After 44 days (20 days for the wines containing proanthocyanidins B1 & B2) a peak corresponding to the vinyl-linked MV3G and (epi)catechin dimer was observed in the HPLC chromatograms of the wines containing flavan-3-ols. In the wine containing catechin, the levels of the vinyl-linked MV3G and catechin dimer increased from 1.0 mg/L

(MV3G eq) at 44 days to 2 mg/L (MV3G eq) at 159 days (Table 7.10). At 44 days, the wines containing proanthocyanidin B3 had double the amount of the vinyl-linked MV3G and (epi)catechin dimer (2 mg/L MV3G eq) compared to the wines containing catechin. The levels of the vinyl-linked pigments increased to 7 mg/L (MV3G eq) by 159 days. The wines containing proanthocyanidin B4 had a similar vinyl-linked MV3G and catechin dimer evolution profile to the wines containing catechin. The pigments increased from 1.0 mg/L (MV3G eq) at 44 days to 2 mg/L (MV3G eq) at 159 days. As mentioned previously, the vinyl-linked MV3G and (epi)catechin dimer was observed in the wines containing proanthocyanidins B1 & B2 at 20 days of a concentration of 1.5 mg/L (MV3G eq). The levels increased to 2 1.0 mg/L (MV3G eq) by 91 days whereafter they decreased to 0.2 mg/L (MV3G eq) at 159 days. After 20 days a significant peak (10 mg/L MV3G eq) was observed in the HPLC chromatograms of the wines containing no flavan-3-ols. Mass spectroscopy revealed this peak had a m/z value of 517 which correlated to vitisin B. The vitisin B concentration increased to 21 mg/L (MV3G eq) whereafter it dramatically decreased to 7 mg/L (MV3G eq) by 91 days and continued to decrease to 1 mg/L (MV3G eq) by 159 days.

Table 7.10. Concentration of pyranoanthocyanins (mg/L MV3G eq) for model wines formed from the fermentations involving catechin, proanthocyanidin B3, proanthocyanidin B4, proanthocyanidins B1 & B2 and no flavan-3-ols.

Day	Catechin	Proantho-cyanidin B3	Proantho-cyanidin B4	Proantho-cyanidins B1 & B2	No Flavan-3-ols
0	0	0	0	0	0
2	0	0	0	0	0
3					0
20	0	0	0	1	10
44	1	2	1	2	19
60	1	3	1	2	22
91	2	5	2	2	7
125	2	5	1	1	2
159	2	7	2	0	1

The levels of other pigments were determined by subtracting the peak areas of MV3G, the 8,8-methylmethine-flavan-3-ol-MV3G pigments and pyranoanthocyanins from the total peak area at 520 nm on the HPLC chromatograms. At the end of fermentation all the wines had similar levels of other pigments (8-11 mg/L MV3G eq, Table 7.11). During maturation the rate of formation and levels of other pigments varied, although in all wines the levels reached a maximum after 91 days. At 91 days, the wines containing proanthocyanidins B1 & B2 and no added flavan-3-ols contained the highest levels of 123 mg/L (MV3G eq) and 106 mg/L (MV3G eq) respectively. These levels decreased to 42 mg/L (MV3G eq) and 80 mg/L (MV3G eq) at 159 days for the wines containing proanthocyanidins B1 & B2 and no added flavan-3-ols respectively. The wines containing catechin, proanthocyanidin B3 and proanthocyanidin B4 had lower levels of other pigments at 91 days (64 mg/L, 65 mg/L and 76 mg/L MV3G eq respectively). These levels decreased slightly over the period to 159 days to 44 mg/L (MV3G eq) for the wines containing catechin whereas in the wines containing proanthocyanidin B3 and proanthocyanidin B4 the levels slightly increased to 68 mg/L and 81 mg/L (MV3G eq) respectively.

Table 7.11. Concentration of other pigments (mg/L MV3G eq) for model wines formed from the fermentations involving the flavan-3-ols catechin, proanthocyanidin B3, proanthocyanidin B4 and proanthocyanidins B1 & B2 and no flavan-3-ols.

Day	Catechin	Proantho-cyanidin B3	Proantho-cyanidin B4	Proantho-cyanidins B1 & B2	No Flavan-3-ols
0	0	0	0	0	0
2	8	9	8	11	8
3					8
20	27	38	43	44	30
44	26	25	36	90	42
60	42	46	55	90	69
91	62	60	76	123	106
125	59	56	72	68	84
159	44	68	81	42	80

By the end of fermentation the wine containing no flavan-3-ols had a significantly lower concentration in total pigments (367 mg/L) than the wines with flavan-3-ols (416-451 mg/L) (Table 7.12). For all the wines, the levels of total pigments decreased. At 159 days, the wines with no flavan-3-ols and with proanthocyanidins B1 & B2 had significantly lower levels of total pigments (82 and 55 mg/L respectively) than the other wines. At 159 days the wines containing catechin contained levels of total pigments of 133 mg/L whilst the wines containing proanthocyanidin B3 and proanthocyanidin B4 contained levels of 184 mg/L and 168 mg/L respectively.

Table 7.12. Concentration of total pigments (mg/L) for model wines formed from the fermentations involving the flavan-3-ols catechin, proanthocyanidin B3, proanthocyanidin B4 and proanthocyanidins B1 & B2 and no flavan-3-ols.

Day	Catechin	Proantho-cyanidin B3	Proantho-cyanidin B4	Proantho-cyanidins B1 & B2	No Flavan-3-ols
0	413	408	406	389	427
2	426	422	416	451	435
3					367
20	318	354	340	333	283
44	267	296	291	289	193
60	258	282	307	238	155
91	212	246	239	185	121
125	174	197	186	99	90
159	133	184	168	55	82

7.2.5 Influence of Flavan-3-ols on Wine Colour

The spectra of the wines at the start of fermentation (Figure 7.5) were consistent with that of MV3G (at pH 3.6) with a peak at 522 nm. After the fermentations and during storage the spectra of the wines all displayed (except for the wines containing no flavan-3-ols) the influence, of different timing and area, of the 8,8-methylmethine-flavan-3-ol-MV3G compounds on wine colour. In all cases a noticeable shoulder is formed at 450 nm (consistent with the spectra of 8,8-methylmethine-flavan-3-ol-MV3G compounds). At the end of fermentation the spectra of the wine containing catechin (Figure 7.5 (a)) increased

in area and had a slight increase of 3 nm of λ_{max}. By day 46 the area of the spectra had decreased, λ_{max} had increased by a further 3nm and the influence of the 8,8-methylmethine-flavan-3-ol-MV3G compounds was noticeable. The area of the spectra continued to decrease by day 126 whereafter it remained constant and λ_{max} remained constant at 530 nm. The spectra of the wines containing proanthocyanidins B3 and B4 (Figure 7.5 (b) and (c)) showed little change at the end of fermentation. This was followed by a significant decrease by day 46 followed by a gradual decrease by day 126 whereafter the spectra of the wines remained stable. By day 91 the spectra of both wines series showed characteristics of the 8,8-methylmethine-flavan-3-ol-MV3G compounds with a noticeable shoulder at 450 nm. The area of the spectra of the wines containing proanthocyanidins B1 & B2 increased slightly (by 7%) and λ_{max} increased by 4nm. The area of the spectra continued to increase by day 91 (by a further 30%) with λ_{max} decreasing by 5 nm at day 91. Thereafter the area of the spectra decreased dramatically by day 159 (by 58%) and λ_{max} continued to decrease to 512 nm. In the wines containing no flavan-3-ols the area of the spectra decreased by 33% with little change in λ_{max}. By day 46 the spectra showed a dramatic change with an increase in area of 20% and a decrease in λ_{max} of 20 nm. The area increased slightly by day 91 and λ_{max} increased by 6nm. By day 126, the area of the spectra decreased significantly (by 11%) and λ_{max} increased by a further 7nm whereafter the spectra remained relatively constant by day 159.

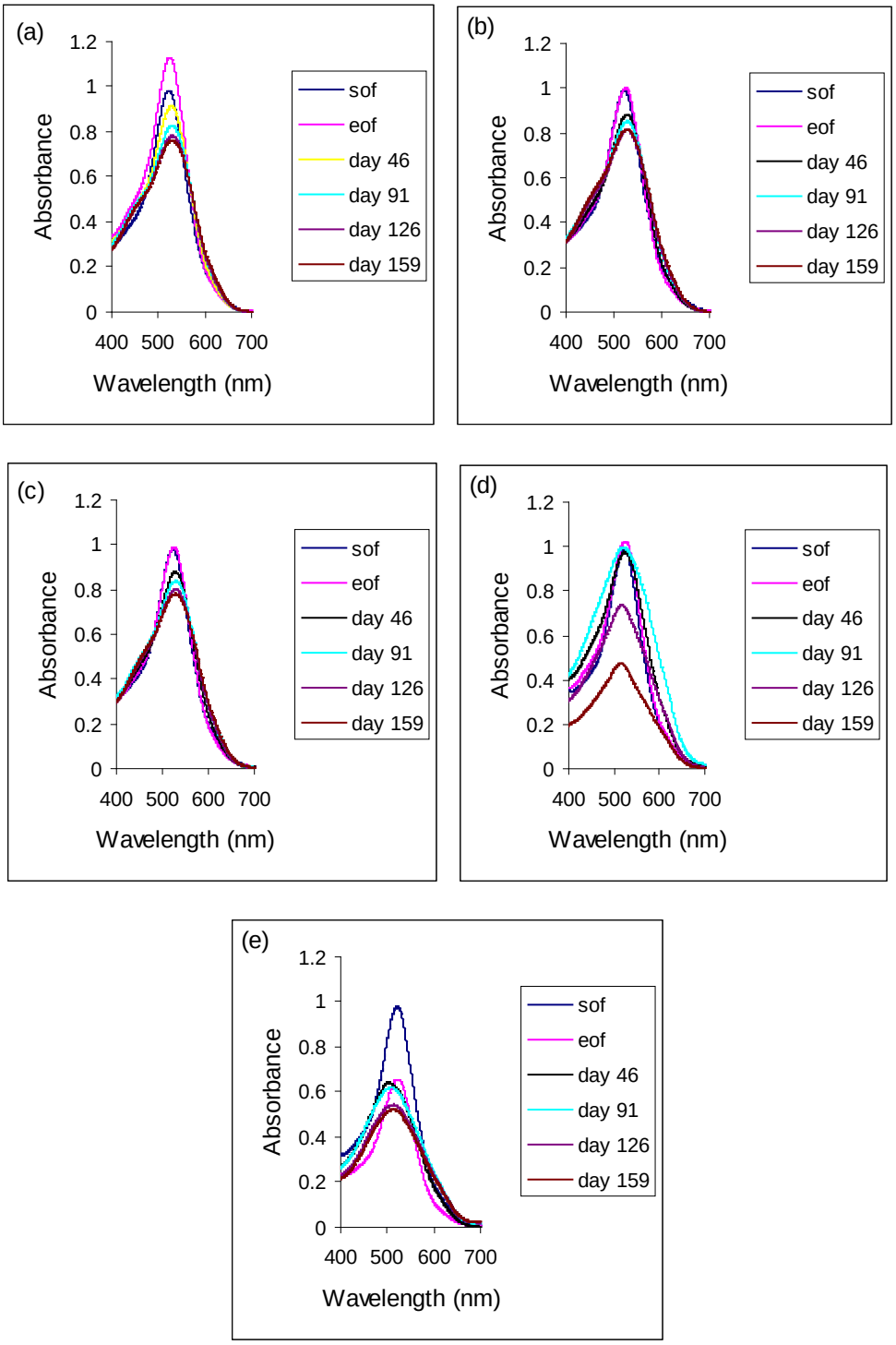

Figure 7.5. Spectral evolution of the wines formed from the fermentations involving (a) catechin, (b) proanthocyanidin B3, (c) proanthocyanidin B4, (d) proanthocyanidins B1 & B2 and (e) no flavan-3-ols. sof = start of fermentation, eof = end of fermentation, day No. refers to the number of days from the start of fermentation.

At the end of fermentation, the colour density was slightly higher in the wines containing catechin and proanthocyanidins B1 & B2 (11% and 6% respectively), whilst it remained similar for the wines containing proanthocyanidin B3 and proanthocyanidin B4 (Figure 7.17). The wine containing no flavan-3-ols had a 30% decrease in colour density at the end of fermentation, from 6.5 au to 4.6 au which remained at that level until day 159 where it decreased to 3.8 au. The wine containing catechin had a gradual decrease in colour density from 7.6 au at the end of fermentation to 5.3 au at day 159. The colour density for the wine containing proanthocyanidins B1 & B2 gradually increased from 7.0 au at the end of fermentation to reach a maximum at day 91 (7.6) whereafter it dramatically decreased to 3.8 au at day 159. This decrease in colour density corresponded with the formation of pigmented precipitate. The wines containing proanthocyanidin B3 and proanthocyanidin B4 had a gradual decrease in colour density during maturation, from 6.7 au, at the end of fermentation, to 6.0 au and 5.7 au, at day 159, respectively.

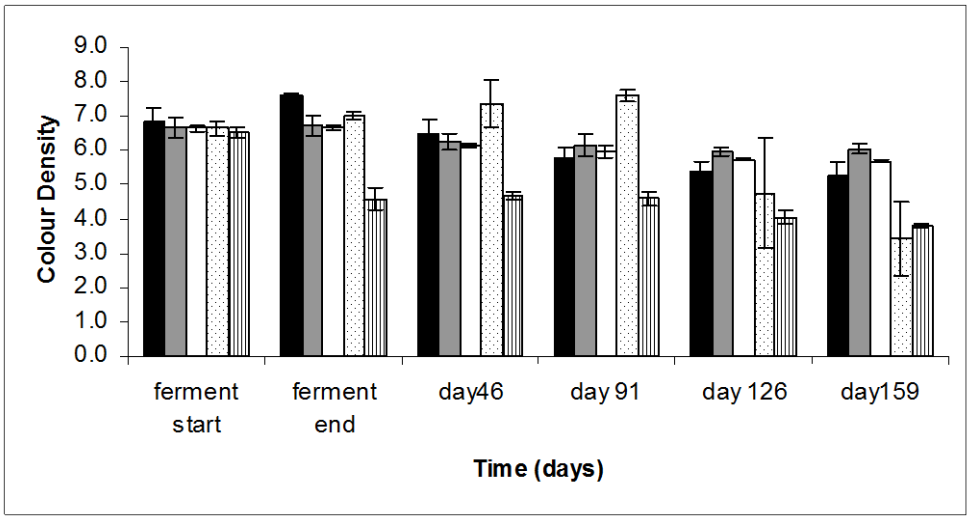

Figure 7.17. Colour density evolution for wines formed from the fermentations involving the flavan-3-ols (■) catechin, (■) proanthocyanidin B3, (□) proanthocyanidin B4, (⊡) proanthocyanidins B1 & B2 and (▥) no flavan-3-ols.

As with the wines produced by different yeasts, the Glories' colour densities of the wines (Figure 7.18) followed a similar trend to the colour densities although the magnitude of the changes differed slightly. The Glories' colour density increased by 9% at the end of fermentation for the wines containing catechin, then the densities decreased at a steadily by day 126 (decrease of 17%) whereafter they remained constant. The densities of the wines containing proanthocyanidin B3 underwent a slight decrease (by 5%) by the end of

fermentation whereafter the densities remained relatively stable. There was little change in densities at the end of fermentation for the wines containing proanthocyanidin B4. Thereafter the densities gradually decreased by 10% by 126 days whereafter they remained constant. The wines containing proanthocyanidins B1 & B2 had increased densities at the end of fermentation (by 6%) which continued to increase by a further 20% by day 91. Thereafter the densities dramatically decreased by 38% by day 126 and continued to decrease by a further 29% by day 159. The densities decreased significantly for wines containing no flava-3-ols at the end of fermentation (by 31%). By day 91 the densities had increased by 11% whereafter there was a constant decrease of 17% by day 159.

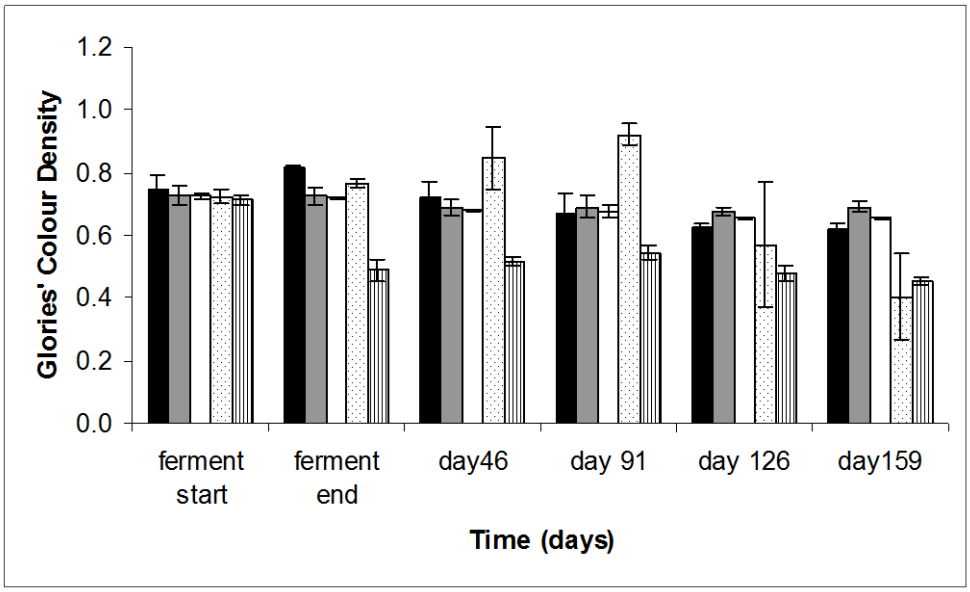

Figure 7.18. Glories' colour density evolution for wines formed from the fermentations involving the flavan-3-ols (■) catechin, (■) proanthocyanidin B3, (□) proanthocyanidin B4, (⬚) proanthocyanidins B1 & B2 and (▥) no flavan-3-ols.

At the start of fermentation there were slight differences in hue values of the wines with wines containing proanthocyanidin B3 and proanthocyanidins B1 & B2 having higher hues than the other wines. At the end of fermentation there was little change in hue values for all wines (Figure 7.19). For wines containing flavan-3-ols the hue values gradually increased by 28% to 31% reaching a maximum at 91 days whereafter they remained relatively constant (except for the wines containing proanthocyanidins B1 & B2 which underwent a slight decrease of 6%). The hue value for the wine containing no flavan-3-ols increased by 46% by day 46, increased slightly (4%) by day 91 whereafter they decreased

by 6% by day 159. By day 159 the hue values were of approximately the same value for all of the wines.

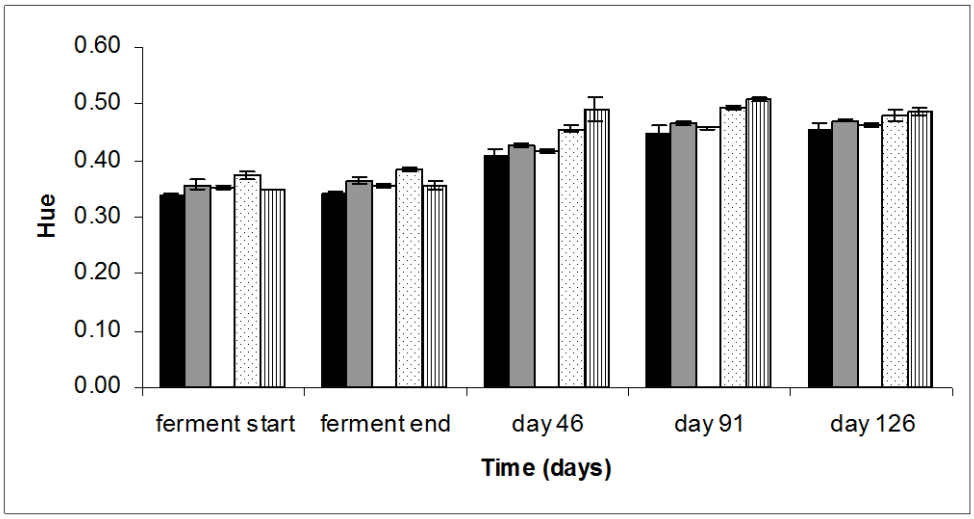

Figure 7.19. Hue evolution for wines formed from the fermentations involving the flavan-3-ols (■) catechin, (■) proanthocyanidin B3, (□) proanthocyanidin B4, (⬚) proanthocyanidins B1 & B2 and (▥) no flavan-3-ols.

7.3 Discussion

Vivar-Quintana et al. (1999) reported the formation of 8,8-methylmethine-flavan-3-ol-anthocyanin pigments in experimental red wines. In this study, in all the wines containing flavan-3-ols, the major pigments formed with MV3G are the 8,8-methylmethine-flavan-3-ol-MV3G compounds, irrespective of the yeast involved, the length of fermentation and the type of flavan-3-ol involved. The higher levels of 8,8-methylmethine-flavan-3-ol-MV3G compounds in this study (c.f. Vivar-Quintana et al. (1999)) can be attributed to the absence of sulfur dioxide (which would bind to any acetaldehyde produced).

The formation of 8,8-methylmethine-flavan-3-ol-MV3G compounds in the wines is indicative of significant levels of acetaldehyde production. This would suggest that the yeasts studied are producing acetaldehyde, as the compounds were formed during and immediately after fermentation. Furthermore, the amounts of 8,8-methylmethine-flavan-3-ol-MV3G compounds are of concentrations greater than that which would be produced solely by ethanol oxidation as proposed by Wildenradt and Singleton (1974).

Different yeast strains have different levels of formation of carbonyl compounds (Romano et al., 1994). The yeast variety has a significant influence on the formation of 8,8-methylmethine-catechin-MV3G compounds. The different levels of MC1 and MC2 produced in the different wines suggest that there are different levels of acetaldehyde in the wines. Although the EC1118 and BDX had the same length of fermentations and similar concentrations of MC1 and MC2 at the end of fermentation (39 mg/L and 45 mg/L respectively) the concentrations of MC1 and MC2 increased in the EC1118 wines whilst they remained relatively constant in the BDX wines. This suggests that there were higher concentrations of acetaldehyde in the EC1118 wines, hence the increase in the concentrations of MC1 and MC2, than the BDX wines. Acetaldehyde would still be present in the BDX wines as the concentrations of MC1 and MC2 remained constant rather than decreasing due to degradation as discussed in Chapter 5.

The significant levels of acetaldehyde production in the Syrah wines could be due to the yeast strain as discussed previously. Alternatively it could be due to the length of fermentation. The Syrah wines had a considerably longer duration of fermentation (5 days) as compared to the other yeast strains (2 days) studied. If the Syrah yeast produced acetaldehyde at the same rate as either the EC1118 or BDX yeasts considerably more acetaldehyde would be produced due to the lengthened fermentation. The increased acetaldehyde levels were observed through the higher concentrations of MC1 and MC2 at the end of fermentation (60 mg/L). The concentrations of MC1 and MC2 continued to increase until day 45. The dramatic decrease in the levels of MC1 and MC2 thereafter could be due to further polymerisation either involving or not involving acetaldehyde. By this stage there is practically no MV3G to take part in the formation of MC1 and MC2. If there was acetaldehyde still present in the wines it would expected to react with MC1 and MC2, which would react with other compounds (flavan-3-ols, MC1, MC2 etc), thereby causing their dramatic decreases.

The type of flavan-3-ol had little influence on the formation of 8,8-methylmethine-flavan-3-ol-MV3G compounds as shown by the similar rates of formation (0.008 day^{-1} to 0.011 day^{-1}) after the end of fermentation. This indicates that either the MV3G or the flavan-3-ol is the limiting factor and not the levels of acetaldehyde. Although the type of flavan-3-ol had little influence on the formation of 8,8-methylmethine-flavan-3-ol-MV3G compounds, there was a significantly higher rate of degradation of the 8,8-methylmethine-proanthocyanidin (B1/B2)-MV3G compounds. This could be due to higher rates of acetaldehyde production or the greater reactivity of the compounds formed with the proanthocyanidin B1 & B2 mixture.

The levels of MV3G at 159 days were considerably higher (16mg/L to 79 mg/L) in the all the wines except those made with the Syrah yeast (~0mg/L), those made with EC1118 yeast containing proanthocyanidins B1 & B2 (2mg/L) and containing no flavan-3-ols (2mg/L). In the wines containing no flavan-3-ols, MV3G has no protection from reactions with acetaldehyde and other compounds. In the wines containing flavan-3-ols, the rate of degradation of MV3G reflected the rate of degradation of 8,8-methylmethine-flavan-3-ol-MV3G compounds. The presence of flavan-3-ols allows the formation of 8,8-

methylmethine-flavan-3-ol-MV3G compounds which via gradual degradation allows a pool of MV3G that can be utilised to form colour and temporally stable pigments.

Vinyl-linked MV3G and flavan-3-ols compounds were formed in significant amounts in the wines containing flavan-3-ols. In the wines containing catechin, the levels of the vinyl-linked pigments were greater than one thousand fold compared to the degradation studies of MC1 and MC2 under anaerobic conditions (Chapter 5). There are two possible explanations for this, either the wine matrix is promoting the formation of the vinyl-linked compounds from the degradation of the 8,8-methylmethine-flavan-3-ol-MV3G pigments or that the compounds are formed via an alternative pathway. The wine matrix has a stabilising influence on the degradation of MV3G (Asenstorfer, 2001) so therefore it is possible that the matrix is influencing the degradation of the 8,8-methylmethine-flavan-3-ol-MV3G pigments to form the vinyl-linked compounds as postulated by Francia-Aricha et al. (1997) and discussed in Chapter 1.

In the wines from the Syrah yeast, containing MV3G and catechin, and the EC1118 yeast, containing MV3G and no flavan-3-ols, the pyranoanthocyanins underwent dramatic decreases in concentration. The pyranoanthocyanins involved vinyl-linked MV3G and catechin in the Syrah wine and vitisins A and B in the EC1118 wines. In both cases, the concentrations of the pyranoanthocyanins were considerable at 20 days after the start of fermentation and the decrease occurred when there was little or no MV3G in the wines involved. The vinyl-linked MV3G and catechin could undergo further condensation with other compounds present (MV3G, flavan-3-ols, other pyranoanthocyanins etc.). The condensation could take place, via either direct condensation or via acetaldehyde, through the catechin moiety. An alternative, which also applies to the vitisin compounds, is for the pyranoanthocyanins to form 8,8-methylmethine-flavan-3-ol-pyranoanthocyanin compounds in a similar manner to MV3G (Atanasova et al., 2002).

The concentration of other pigments reached a maxima 30 to 50 days after 8,8-methylmethine-flavan-3-ol-MV3G compounds reached their peak. Apart from compounds forming at a slower rate (e.g. directly condensed MV3G and flavan-3-ol compounds) the degradation of 8,8-methylmethine-flavan-3-ol-MV3G compounds would make a significant contribution pigment development as discussed in Chapter 5. Although there

were significant levels of other pigments in the wines containing no flavan-3-ols and proanthocyanidins B1 & B2, these are not colour stable, with respect to wine pH, as shown by the lower colour densities in these wines.

The influence of 8,8-methylmethine-flavan-3-ol-anthocyanin compounds on wine colour density has been inferred by Ribereau-Gayon et al., (1983). This study has shown that the 8,8-methylmethine-flavan-3-ol-MV3G compounds make a significant contribution to the colour of red wine as shown by the spectra (Figure 7.7 and Figure 7.16) of the wines studied and by the evolution of the colour densities of the wines. The colour densities of the wines, after the end of fermentation, follow the concentrations of 8,8-methylmethine-flavan-3-ol-MV3G compounds. 8,8-Methylmethine-flavan-3-ol-MV3G compounds do not however, significantly affect the hue of red wine as the hues of the wines studied did not reflect the concentrations of 8,8-methylmethine-flavan-3-ol-MV3G compounds present in the wines.

The yeast used in primary fermentation and the flavan-3-ols present, significantly influenced the colour of the wines studied. This is through the formation of different pigment compositions of the wines. The yeasts afforded different levels of MV3G, MC1 and MC2. The levels of MV3G, MC1 and MC2 influenced the densities of the wines whilst the levels of MV3G and other pigments influenced the hues. The presence of flavan-3-ols has a significant influence on the colour densities of the wine through the formation of 8,8-methylmethine-flavan-3-ol-MV3G compounds. As with the ferments involving different yeasts, the levels of MV3G and 8,8-methylmethine-flavan-3-ol-MV3G compounds influence the differences in the densities for the wines containing different/no flavan-3-ols, the levels of MV3G and other pigments influenced the hues. Although the wines containing different flavan-3-ols varied in colour densities, their hues were similar at the end of the study.

Chapter 8 - Summary

Studies with young red model wines found that 8,8-methylmethine-flavan-3-ol-MV3G pigments are formed during and after fermentation. These pigments make a significant contribution to wine colour through their colour stability at wine pH. Although 8,8-methylmethine-flavan-3-ol-MV3G are colour stable, they are temporally unstable and lead to the formation of other pigments such as pyranthocyanins.

An important factor in the study of colour stability of red wines is the isolation of the pigments that are formed during fermentation and maturation. Furthermore, it is necessary to isolate significant quantities of the grape anthocyanins. Size-exclusion chromatography followed by ion-exchange chromatography allows the isolation of 8,8-methylmethine-(epi)catechin)-MV3G pigments (83% to 90% purity) and also grape anthocyanins (82% to 96% purity). An advantage of this technique is that it allows the recycling of the mobile phases. Alternative ion sources to that of hydrochloric acid need to be investigated so as to reduce the level of hydration of the grape anthocyanins. The use of size-exclusion chromatography allowed the isolation of the "hump" observed in HPLC chromatograms characteristic of grapes and wines. Although the "hump" was isolated, it was not possible to achieve further isolation of individual components.

The positioning (8-8) of the bridge, via one & two-dimensional NMR, of 8,8-methylmethine-(epi)catechin-MV3G compounds is in agreement with previous studies of similar compounds (Escribano-Bailon et al., 1996;Shoji et al., 2002). Through molecular modelling, it is proposed that the (epi)catechin moiety folds over/under the MV3G moiety, this has been previously proposed for an 8,8-methylmethine-catechin-flavylium diastereomer (Escribano-Bailon et al., 1996). The location of the (epi)catechin moiety with respect to the MV3G moiety for MC1, MC2, ME1 and ME2 influences their HPLC elution profiles, their ionisation/hydration constants and their colour and temporal stabilities. For example, the HPLC elution profiles for MC1, MC2, ME1 and ME2 are in agreement with the structures proposed in this study. That is, although MC1 and ME1 are larger (in calculated volume) than MC2 and ME2, they are considerably more polar and therefore elute earlier.

Although the location of the (epi)catechin moiety could be deduced with respect the glucoside moiety, the location of the glucoside moiety with respect to the malvidin aglycone is unknown. Therefore, apart from the proposed structures of MC1, MC2, ME1 and ME2, alternative structures have been proposed that have similar sizes and polarities as the proposed structures. Due to this, the definitive stereochemistries of MC1, MC2, ME1 and ME2 have not been determined in this study. X-ray crystallography can be used to determine the definitive structure from which the stereochemistries of the compounds can be determined. Although the structures of anthocyanidins have been determined via X-ray crystallography (Ueno and Saito, 1977a; Ueno and Saito, 1977b), the structures of anthocyanins have not been determined. This is possibly due to the amorphous nature of their glucoside moieties. It is possible that the larger structures of the 8,8-methylmethine-(epi)catechin-MV3G compounds would allow their analysis through X-ray crystallography. However, if this is not the case then there are alternative methods to determine the stereochemistries of these compounds via X-ray crystallography. One method to study the stereochemistry via X-ray crystallography is to use the corresponding flavylium salt, which should be easier to crystallise. It should be noted, however, that the corresponding compounds would be expected to have higher instabilities than the corresponding MV3G compounds (due to the increased instability of the flavylium salt). Another method may be to acetylate the alcohol groups of either/both of the MV3G and (epi)catechin moieties. It should be noted, however, that the reaction conditions required to undertake this would be conducive to the degradation of the 8,8-methylmethine-(epi)catechin-MV3G compounds.

This study has shown, in agreement with other studies (Escribano-Bailón et al., 2001; Duenas et al., 2006), that MC1, MC2, ME1 and ME2 have greater resistance to colour loss due to change in pH or sulfur dioxide bleaching. The proposed structures provide steric hindrance at the 4-position of the MV3G moiety limits hydration, thereby allowing greater resistance to colour loss due to change in pH. The resistance to bleaching by sulfur dioxide, as with change in pH, can be explained by steric hindrance at the 4-position of the MV3G moiety. However, in both cases, the 4-position of the MV3G moiety is not fully protected from nucleophilic attack. It is postulated that further protection is afforded through steric hindrance, via inertia to structure change through the (epi)catechin moiety or via self-association/dimerisation of the compounds.

Although MC1 and MC2 have greater colour stabilities, to change in pH or sulfur dioxide bleaching, than the parent MV3G, they have lower temporal stabilities. The postulated cause of degradation is due to cleavage of the ethyl-bridge between (epi)catechin and MV3G moieties, comparable with acid catalysed interflavan bond cleavage of condensed tannins (Haslam, 1980). A reactive form of MV3G results from the postulated route of degradation. This can react with a hydrogen ion (to form MV3G), with an ethyl-(epi)catechin moiety (to reform the original 8,8-methylmethine-(epi)catechin-MV3G compound or its diastereomer) or with other components in the wine matrix (to form new pigments). Thus, the 8,8-methylmethine-flavan-3-ol-anthocyanin compounds are a possible source of anthocyanins to form new pigments. To have a greater understanding of the new pigments formed, the 8,8-methylmethine-flavan-3-ol-anthocyanin compounds need to be degraded in the presence of other wine components and also in greater concentrations so that the new pigments can be isolated, characterised and their colour and temporal stabilities further studied.

HVPE and UV-visible spectroscopy has been used in this study to determine the ionisation/hydration constants of MC1, MC2, ME1 and ME2. HVPE data is dependant upon the ionisation state of the compound studied (through their relative mobility). UV-visible spectroscopic data is dependant upon the change in spectra through ionisation or the decrease in spectra through hydration. The ionisation/hydration constants determined via the two methods used correlated, therefore the constants determined can be regarded as ionisation constants. This is in contrast with Duenas et al., (2006) who determined that MC1 underwent hydration whilst MC2 did not. In this study both MC1 and MC2 have similar decreases in the visible-spectra area, which would indicate that both compounds undergo the same level of hydration.

The presence of isosbestic points is a further indicator to the lack of hydration occurring for MC1, MC2, ME1 and ME2. If significant hydrations were occurring, isosbestic points would not be present, due to the decreases in the visible spectra (as in the case of MV3G). It is possible that copigmentation is negating the effects of hydration. However, to preserve the isosbestic points, this would require the effect of copigmentation to completely negate the loss of colour due to hydration. The proposed structures of MC1,

MC2, ME1 and ME2 explain the lack of hydration. The folding over/under of the (epi)catechin moiety provides steric hindrance to nucleophilic attack at the 4-position of the MV3G. Further steric hindrance to hydration is via inertia to the change in structure through the (epi)catechin moiety on the A-ring of MV3G. To determine whether hydration is occurring for MC1, MC2, ME1 and ME2, tests can be undertaken using a flow through cell. Alternative methods such as HPLC and NMR can also be used. It may be possible to separate the quinonoidal base from the hydrated forms via HPLC (depending upon the size and polarities of the forms studied) by carrying out the chromatography at a pH of approximately 5 and studying the chromatograms at approximately 280nm. Studying the NMR spectra with respect to pH, as undertaken by (Cheminat and Brouillard, 1986) with MV3G, can further elucidate the structural transformations of MC1, MC2, ME1 and ME2.

The first ionisation constants (pKa_1) for MC1, MC2, ME1 and ME2 (2.43-2.47) were determined to be significantly higher than the parent MV3G (1.76) (Asenstorfer et al., 2003). As the pKa_1 values for MC1, MC2, ME1 and ME2 are similar it can be surmised that substitution at the 8-position of MV3G is influencing the initial deprotonation. The pKa_2 values determined for MC1, MC2, ME1 and ME2 are significantly lower than of the parent MV3G (5.36) (Asenstorfer et al., 2003). The second ionisation constants (pKa_2) determined for MC2 and ME2 (3.73 & 3.57 respectively) are significantly lower than the values determined for MC1 and ME1 (4.11 & 4.09 respectively) indicates that the position of the (epi)catechin moiety influences the deprotonation. The third ionisation constant (pKa_3) was determined by both HVPE and UV-visible spectroscopy for MC1 (6.46) whilst it was determined via UV-visible spectroscopy for MC2, ME1 and ME2. Again, the pKa_3 values determined for MC1, MC2, ME1 and ME2 (6.27 – 6.46) are significantly lower than of the parent MV3G (Asenstorfer et al., 2003) indicating that the substitution of MV3G is again being influenced by the substitution. It should be noted however, that the third ionisation constant was determined via both methods only for MC1 but not for MC2, ME1 and ME2. The ionisation constants determined were ascribed to the MV3G moiety as the pH ranges studied did not include the pH range where the deprotonation of (epi)catechin occurs. To verify the ionisation constants determined through UV-visible spectroscopy for these compounds, HVPE analysis should be undertaken that includes a higher pH range.

The effect of an 8,8-methylmethine substitution on the 8-position of MV3G on its ionisation/hydration constants can be investigated further by substituting (epi)catechin with either its catechol-less form (i.e. chroman-3,5,7-triol, A, Figure 8.1) or an alkyl derivative of pyrogallol (B, Figure 8.1). A di-substituted form of pyrogallol (R_1 = R_2 = alkyl, B, Figure 8.1) would be preferential to a mono-substituted form (R_1 = alkyl, R_2 = H, B, Figure 8.1) as this would prevent polymerisation. The proposed substituents would not protect the 4-position of MV3G and therefore the resultant 8,8-methylmethine compounds would be expected to have larger susceptibilities to hydration, and also have different ionisation constants, compared to those of MC1, MC2, ME1 and ME2.

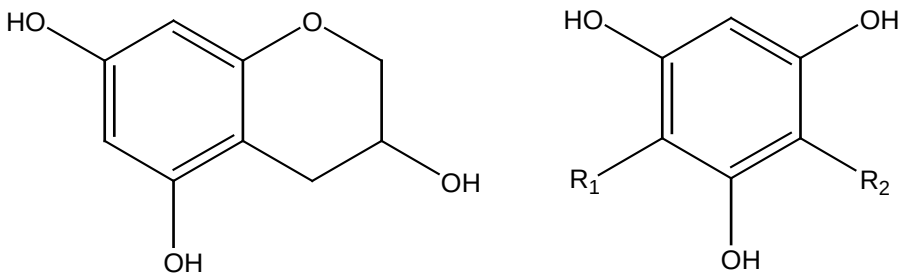

A **B**

Figure 8.1. Proposed 8,8-methylmethine pigment substituents. **A** - chroman-3,5,7-triol, **B** - pyrogallol derivative

During wine fermentation and maturation grape anthocyanins react with other compounds to form colour stable pigments. In this study, in the absence of sulfur dioxide, the major pigments formed are 8,8-methylmethine-flavan-3-ol-MV3G compounds (36mg/L to 92 mg/L MC2 eq) when both MV3G and flavan-3-ols are present. The presence of sulfur dioxide would be expected to decrease the levels of the 8,8-methylmethine-flavan-3-ol-MV3G compounds, as it would bind to the acetaldehyde produced (Bridle et al., 1996). Although the levels of 8,8-methylmethine-flavan-3-ol-anthocyanin compounds would be lower in wines with sulfur dioxide present, they would still make a contribution to the wine colour as they are still coloured at wine pH and have a resistance to bisulfite bleaching.

The formation of 8,8-methylmethine-flavan-3-ol-MV3G pigments in wines during and after fermentation indicates that significant levels of acetaldehyde are being produced during fermentation. The levels of acetaldehyde in the wines were not monitored in this study. Further investigations need to be undertaken to study the relationships between

acetaldehyde levels, yeasts used, the presence/absence of sulfur dioxide, fermentation conditions on 8,8-methylmethine-flavan-3-ol-anthocyanin pigment formation, the formation of other pigments and their effect on red wine colour.

In the presence of flavan-3-ols, MV3G was protected from degradation by the formation of 8,8-methylmethine-flavan-3-ol-MV3G compounds. The gradual degradation of 8,8-methylmethine-flavan-3-ol-MV3G compounds afforded a pool of MV3G that could be utilised to form colour stable pigments. This is reflected in colour stabilities of the wines where there was a gradual degradation of 8,8-methylmethine-flavan-3-ol-MV3G compounds.

The levels of vinyl-linked MV3G and (epi)catechin compounds in the model wines (1-7mg/L) were higher, by a considerable factor, than that observed in the degradation of MC1 and MC2 under anaerobic conditions (<1μg/L). This would suggest that either the wine matrix is favouring the formation of the vinyl-linked compounds, or that there are alternative pathways. One alternative pathway could involve glycolaldehyde, formed from glyoxal during malolactic fermentation (Flamini et al., 2002). This could explain why the first observation of vinyl-linked MV3G and (epi)catechin compounds occurs 2-3 weeks after the end of primary fermentation. The glycolaldehyde initially reacts with catechin in a similar manner to acetaldehyde (Figure 8.2). The glycolacetaldehyde- adduct is dehydrated either via the primary alcohol (scheme A Figure 8.2) or via the tertiary alcohol (scheme B Figure 8.2). In this postulation, scheme B would be preferred as it involves the dehydration of a tertiary alcohol that is easier than the dehydration of a primary alcohol. In both cases the vinyl-catechin compound reacts with MV3G in a similar manner, as postulated by (Francia-Aricha et al., 1997), to form the isomers of vinyl-linked MV3G and flavan-3-ol compounds (Figure 8.2). To ensure the formation of the vinyl-linked MV3G and flavan-3-ol compound resulting from scheme A, acetic acid (or a derivative) would be required.

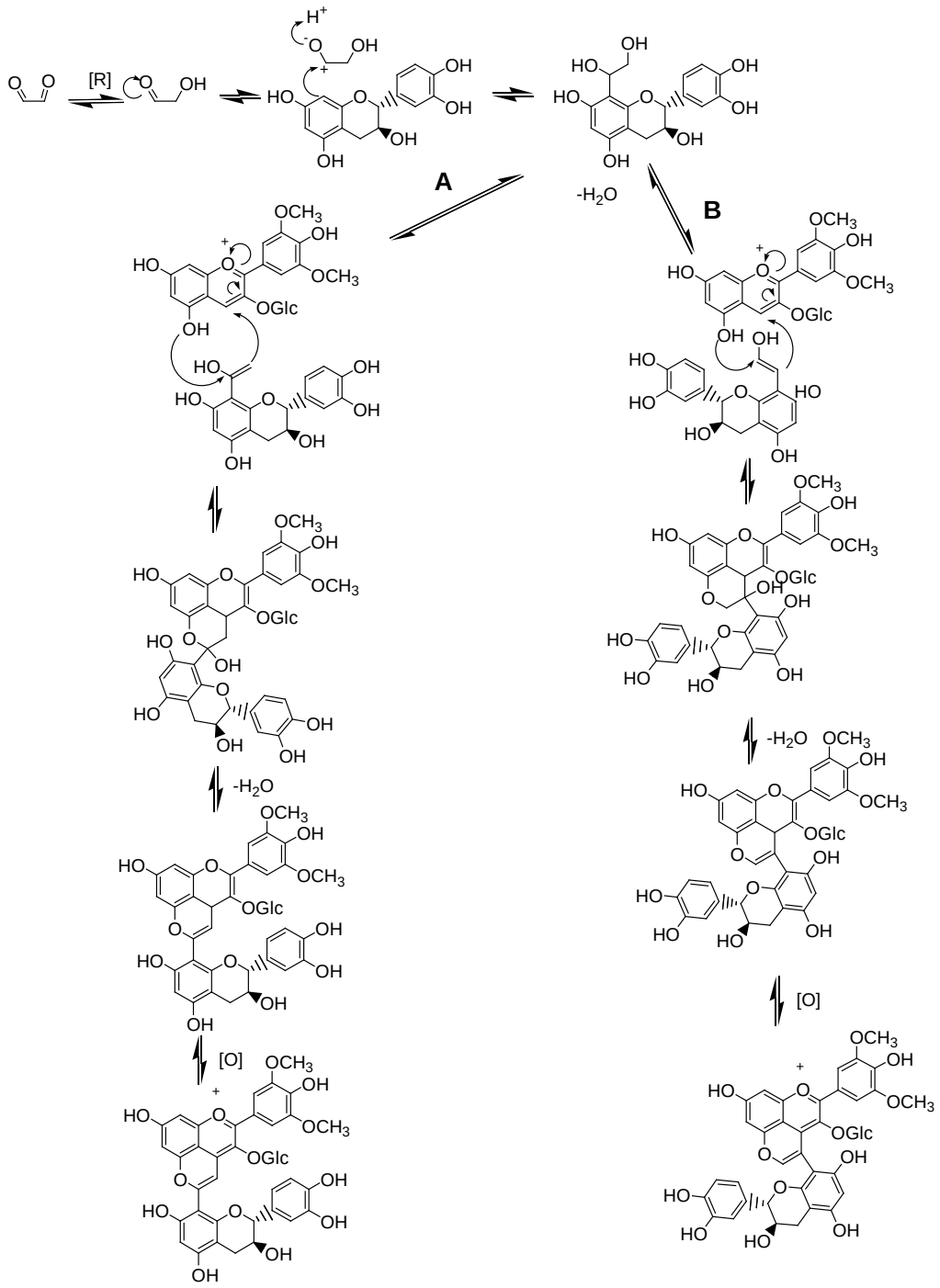

Figure 8.2. Proposed route for the formation involving glycolaldehyde of vinyl-linked MV3G and catechin compounds.

The postulated structures for MC1, MC2, ME1 and ME2 help explain their properties such as their ionisation constants, lack of hydration, colour stabilities (with respect to change in pH and sulfur dioxide) and temporal stabilities. Although these pigments are colour stable, with regards to change in pH and to bisulfite bleaching, they are temporally unstable. When both MV3G and (epi)catechin are present, 8,8-methylmethine-flavan-3-ol-MV3G pigments are the major pigments formed after fermentation (in the absence of sulfur dioxide). These pigments would be expected to stabilise colour during the early stages of maturation and are a possible source for further colour and temporal stable pigments. The knowledge of the formation of these colour and temporal stable pigments will assist in the production of colour stable red wines.

References

Amerine, M. A.; Ough, C. S. Studies with controlled fermentation. VIII. Factors affecting aldehyde accumulation. *Am. J. Enol. Vitic.* **1964**, *15*, 23-33.

Arnold, R. A.; Noble, A. C.; Singleton, V. L. Bitterness and astringency of phenolic fractions in wine. *J. Agric. Food Chem.* **1980**, *28*, 675-678.

Asenstorfer, R. E. Isolation, structures and properties of anthocyanins and wine pigments, PhD, University of Adelaide, 2001.

Asenstorfer, R. E.; Hayasaka, Y.; Jones, J. P. Isolation and structures of oligomeric wine pigments by bisulfite-mediated ion-exchange chromatography. *J. Agric. Food Chem.* **2001**, *49*, 5957-5963.

Asenstorfer, R. E.; Iland, P. G.; Tate, M. E.; Jones, J. P. Charge equilibria and pKa of malvidin-3-glucoside by electrophoresis. *Anal. Biochem.* **2003**, *318*, 291-299.

Atanasova, V.; Fulcrand, H.; Le Guerneve, C.; Cheynier, V.; Moutounet, M. Structure of a new dimeric acetaldehyde malvidin 3-glucoside condensation product. *Tetrahedron Lett.* **2002**, *43*, 6151-6153.

Bakker, J.; Picinelli, A.; Bridle, P. Model wine solutions: Colour and composition changes during ageing. *Vitis* **1993**, *32*, 111-118.

Bakker, J.; Timberlake, C. F. Isolation, identification and characterization of new color-stable anthocyanins occurring in some red wines. *J. Agric. Food Chem.* **1997**, *45*, 35-43.

Balas, L.; Vercauteren, J. Extensive high-resolution reverse 2D NMR analysis for the structural elucidation of proanthocyanidin oligomers. *Mag. Res. Chem.* 1 **94**, *32*, 386-393.

Baranowski, E. S.; Nagel, C. W. Kinetics of malvidin-3-glucoside condensation n wine model systems. *J. Food. Sci.* **1983**, *48*, 419-421.

Benabdeljalil, C.; Cheynier, V.; Fulcrand, H.; Hakiki, A.; Mosaddak, M.; Moutc net, M. Mise en evidence de nouveaux pigments formes par reaction des anthocya es avec des metabolites de levure. *Sc. des Aliments* **2000**, *20*, 203-220.

Berke, B.; Cheze, C.; Deffieux, G.; Vercauteren, J. Sulfur dioxide decoloriz tion or resistance of anthocyanins: NMR structural elucidation of bisulfite-ad cts. In *Plant Polyphenols 2: Chemistry, Biology, Pharmacology, Ecology*; G. G. C oss; R. W. Hemingway and T. Yoshida, Eds.; Kluwer Academic: New York, 1999; pp 779-790.

Berke, B.; Cheze, C.; Vercauteren, J.; Deffieux, G. Bisulfite addition to anthocyanins: revisited structures of colourless adducts. *Tetrahedron Lett.* **1998**, *39*, 5771-5774.

Bridle, P.; Bakker, J.; Garcia-Viguera, C.; Picinelli, A. Polymerisation reactions in red wines and the effect of Sulphur dioxide. In *Agri-Food Quality: An Interdisciplinary Approach*; G. R. Fenwick; C. Hedley; R. L. Richards and S. Khokhar, Eds.; Royal Society of Chemistry: Cambridge, 1996; pp 258-260.

Brouillard, R.; Delaporte, B. Chemistry of anthocyanin pigments. 2. Kinetic and thermodynamic study of proton transfer, hydration and tautomeric reactions of malvidin-3-glucoside. *J. Am. Chem. Soc.* **1977**, *99*, 8461-8468.

Brouillard, R.; Iacobucci, G. A.; Sweeny, J. G. Chemistry of anthocyanin pigments 9. UV-visible spectrophotometric determination of the acidity constants of apigeninidin and three related 3-deoxyflavylium salts. *J. Am. Chem. Soc.* **1982**, *104*, 7585-7590.

Brouillard, R.; Lang, J. The hemiacetal-*cis*-chalcone equilibrium of malvin, a natural anthocyanin. *Can. J. Chem.* **1990**, *68*, 755-761.

Cai, Y.; Lilley, T. H.; Haslam, E. Polyphenol-anthocyanin copigmentation. *J. Chem. Soc., Chem. Commun.* **1990**, 380-383.

Cheminat, A.; Brouillard, R. NMR spectrometry of anthocyanins. *Bulletin de Liaison du Groupe Polyphenols* **1986**, *13*, 142-144.

Cheynier, V.; Doco, T.; Fulcrand, H.; Guyot, S.; Le Roux, E.; Souquet, J. M.; Rigaud, J.; Moutounet, M. ESI-MS analysis of polyphenolic oligomers and polymers. *Analusis* **1997**, *25*, M33-M37.

Cheynier, V.; Rigaud, J.; Ricardo da Silva, J. M. Structure of proanthocyanidin oligomers isolated from grape seeds in relation to some of their chemical properties. In *Plant Polyphenols*; R. W. Hemingway and P. E. Laks, Eds.; Plenum Press: New York, 1992; pp 281-294.

Dallas, C.; Laureano, O. Effects of pH, sulphur dioxide, alcohol content, temperature and storage time on colour composition of a young portuguese red table wine. *J. Sci. Food Agric.* **1994**, *65*, 477-485.

Dallas, C.; Ricardo-da-Silva, J. M.; Laureano, O. Interactions of oligomeric proanthocyanidins in model wine solutions containing malvidin-3-glucoside and acetaldehyde. *J. Sci. Food Agric.* **1996a**, *70*, 493-500.

Dallas, C.; Ricardo-da-Silva, J. M.; Laureano, O. Products formed in model wine solutions involving anthocyanins, proanthocyanidin B_2, and acetaldehyde. *J. Agric. Food Chem.* **1996b**, *44*, 2402-2407.

Degenhardt, A.; Hofmann, S.; Knapp, H.; Winterhalter, P. Preparative isolation of anthocyanins by high-speed countercurrent chromatography and application of the color activity concept to red wine. *J. Agric. Food Chem.* **2000a**, *48*, 5812-5818.

Degenhardt, A.; Knapp, H.; Winterhalter, P. Rapid isolation of malvidin-3-glucoside by high-speed countercurrent chromatography (HSCCC). *Vitis* **2000b**, *39*, 43-44.

Duenas, M.; Salas, E.; Cheynier, V.; Dangles, O.; Fulcrand, H. UV-visible spectroscopic investigation of the 8,8-methylmethine catechin-malvidin 3-glucoside pigments in aqueous solution: Structural transformations and molecular complexation with chlorogenic acid. *J. Agric. Food Chem.* **2006**, *54*, 189-196.

Ebeler, S. E.; Spaulding, R. S. Characterization and measurement of aldehydes in wine. In *Chemistry of wine flavor*; A. L. Waterhouse and S. E. Ebeler, Eds.; American Chemical society: Washington, 1998; pp 166-179.

Escribano-Bailón, T.; Álverez-García, M.; Rivas-Gonzalo, J. C.; Heredia, F. J.; Santos-Buelga, C. Color and stability of pigments derived from the acetaldehyde-mediated condensation between malvidin-3-O-glucoside and (+)-catechin. *J. Agric. Food Chem.* **2001**, *49*, 1213-1217.

Escribano-Bailon, T.; Dangles, O.; Brouillard, R. Coupling reactions between flavylium ions and catechin. *Phytochemistry* **1996**, *41*, 1583-1592.

Es-Safi, N.-E.; Fulcrand, H.; Cheynier, V.; Moutounet, M. Competition between (+)-catechin and (-)-epicatechin in acetaldehyde-induced polymerization of flavanols. *J. Agric. Food Chem.* **1999a**, *47*, 2088-2095.

Es-Safi, N.-E.; Fulcrand, H.; Cheynier, V.; Moutounet, M. Studies on the acetaldehyde-induced condensation of (-)-epicatechin and malvidin 3-*O*-glucoside in a model solution system. *J. Agric. Food Chem.* **1999b**, *47*, 2096-2102.

Flamini, R.; De Luca, G.; Di Stefano, R. Changes in carbonyl compounds in Chardonnay and Cabernet Sauvignon wines as a consequence of malolactic fermentation. *Vitis* **2002**, *41*, 107-112.

Francia-Aricha, E. M.; Guerra, M. T.; Rivas-Gonzalo, J. C.; Santos-Buelga, C. New anthocyanin pigments formed after condensation with flavanols. *J. Agric. Food Chem.* **1997**, *45*, 2262-2266.

Fulcrand, H.; Doco, T.; Es-Safi, N.-E.; Cheynier, V.; Moutounet, M. Study of the acetaldehyde induced polymerisation of flavan-3-ols by liquid chromatography - ion spray mass spectrometry. *J. Chromat. A* **1996**, *752*, 85-91.

Garcia-Viguera, C.; Bridle, P.; Bakker, J. The effect of pH on the formation of coloured compounds in model wine solutions containing anthocyanins, catechin and acetaldehyde. *Vitis* **1994**, *33*, 37-40.

Glories, Y. La couleur des vins rouges. 2. Mesure, origine et interpretation. Connaiss. Vigne Vin 1984, 18, 253-271.

Haslam, E. In Vino Veritas: oligomeric proanthocyanidins and the ageing of red wines. *Phytochemistry* **1980**, *19*, 2577-2582.

Hayasaka, Y.; Asenstorfer, R. E. Screening for potential pigments derived from anthocyanins in red wine using nanoelectrospray tandem mass spectrosopy. *J. Agric. Food Chem.* **2002**, *50*, 756-761.

Heredia, F. J.; Francia-Aricha, E. M.; Rivas-Gonzalo, J. C.; Vicario, I. M.; Santos-Buelga, C. Chromatic characterization of anthocyanins from red grapes - I. pH effect. *Food Chem.* **1998**, *63*, 491-498.

Iland, P.; Ewart, A.; Sitters, J.; Markides, A.; Bruer, N. *Techniques for Chemical Analysis and Quality Monitoring During Winemaking*; P. Iland Wine Promotions: Campbelltown, 2000.

Johnston, T. V.; Morris, J. R. Separation of anthocyanin pigments in wine by low pressure column chromatography. *J. Food Sci.* **1996**, *61*, 109-111.

Jones, G. P.; Asenstorfer, R. E. Development of anthocyanin-derived pigments in young red wine. In *Proceedings ASVO Seminar: Phenolics and Extraction*;; Wine Titles: Adelaide, 1997; pp 33-37.

Jurd, L. Anthocyanins and related compounds. III. Oxidation of substituted flavylium salts to 2-phenylbenzofurans. *J. Org. Chem.* **1964**, *29*, 2602-2605.

Jurd, L. Anthocyanidins and related compounds. X. Peroxide oxidation products of 3-alkylflavylium salts. *Tetrahedron* **1966**, *22*, 2913-2921.

Jurd, L. Anthocyanins and related compounds. XI. Catechin-flavylium salt condensation reactions. *Tetrahedron* **1967**, *23*, 1057-1064.

Kantz, K.; Singleton, V. L. Isolation and determination of polymeric polyphenols using sephadex LH-20 and anylsis of grape tissue extracts. *Am. J. Enol. Vitic.* **1990**, *41*, 223-228.

Kraemer-Schafhalter, A.; Fuchs, H.; Pfannhauser, W. Solid-phase extraction (SPE) - a comparison of 16 materials for the purification of anthocyanins from Aronia melanocarpa var Nero. *J. Sci. Food Agric.* **1998**, *78*, 435-440.

Liao, H.; Cai, Y.; Haslam, E. Polyphenol interactions. Anthocyanins: co-pigmentation and colour changes in red wines. *J. Sci. Food. Agric.* **1992**, *59*, 299-305.

Litchev, V. Influence of oxidation processes on the development of the taste and flavor of wine distillates. *Am. J. Enol. Vitic.* **1989**, *40*, 31-35.

Mazza, G.; Brouillard, R. Color stability and structural transformations of cyanidin and 3,5-diglucoside and four 3-deoxyanthocyanins in aqueous solutions. *J. Agric. Food Chem.* **1987**, *35*, 422-426.

Millan, M. C.; Moreno, J.; Medina, M.; Ortega, J. M. Influence of the physiological state of the inoculum on fermentation of musts from Pedro Ximenez grapes by Saccharomyces cerevisiae. *Microbios* **1991**, *65*, 87-96.

Mistry, T. V.; Cai, Y.; Lilley, T. H.; Haslam, E. Polyphenol interactions. Part 5. Anthocyanin co-pigmentation. *J. Chem. Soc., Perkin Trans. II* **1991**, 1287-1296.

Monagas, M.; Nunez, V.; Bartolome, B.; Gomez-Cordoves, C. Anthocyanin-derived pigments in Graciano, Tempranillo, and Cabernet Sauvignon wines produced in Spain. *Am. J. Enol. Vitic.* **2003**, *54*, 163-169.

Montreau, F.-R.; Lattes, A.; Margulis, H. Sur la dégradation par oxydation des anthocyanosides du raisin et du vin. *C. R. Acad. Sci., Serie D* **1970**, *270*, 1178-1181.

Ough, C. S.; Amerine, M. A. *Methods for Analysis of Musts and Wines*; Wiley & Sons: New York, 1988.

Perrin, D. D.; Dempsey, B.; Serjeant, E. P. *pK_a Prediction for Organic Acids and Bases*; Chapman and Hall: London, 1981.

Piergiovanni, L.; Volonterio, G. Tecniche cromatografiche nello studio della frazione antocianica delle uve. *Riv. Vitic. Enol.* **1980**, *33*, 289-308.

Prieur, C.; Rigaud, J.; Cheynier, V.; Moutounet, M. Oligomeric and polymeric proanthocyanidins from grape seeds. *Phytochemistry* **1994**, *36*, 781-784.

Prior, R. L.; Lazarus, S. A.; Cao, G.; Muccitelli, H.; Hammerstone, M. Identification of proanthocyanidins and anthocyanins in blueberries and cranberries (*Vaccinium Spp.*) using high-performance liquid chromatography/mass spectrometry. *J. Agric. Food Chem.* **2001**, *49*, 1270-1276.

Ribereau-Gayon, P. The chemistry of red wine colour. In *Chemistry of Winemaking*; D. A. Webb, Ed.; American Chemical Society: Washington, 1974; pp 50-87.

Ribereau-Gayon, P.; Pontallier, P.; Glories, Y. Some interpretations of colour changes in young red wines during their conservation. *J. Sci. Food Agric.* **1983**, *34*, 505-516.

Rivas-Gonzalo, J.; Bravo-Haro, S.; Santos-Buelga, C. Detection of compounds formed through the reaction of malvidin-3-monoglucoside and catechin in the presence of acetaldehyde. *J. Agric. Food Chem.* **1995**, *43*, 1444-1449.

Roggero, J. P.; Coen, S.; Archer, P.; Rocheville-Divorne, C. Etude par C.L.H.P. de la reaction glucoside de malvidine-acetaldehyde-compose phenolique. *Connaiss. Vigne Vin* **1987**, *21*, 163-168.

Romano, P.; Suzzi, G.; Turbanti, L.; Polsinelli, M. Acetaldehyde productions in *Saccharomyces cerevisiae* wine yeasts. *FEMS Microbiol Lett* **1994**, *118*, 213-218.

Saucier, C.; Pianet, I.; Laguerre, M.; Glories, Y. NMR and molecular modelling: application to wine ageing. *J. Chim. Phys.* **1998**, *95*, 357-365.

Shoji, T.; Goda, Y.; Toyoda, M.; Yanagida, A.; Kanda, T. Characterization and structures of anthocyanin pigments generated in rose cider during vinification. *Phytochemistry* **2002**, *59*, 183-189.

Singleton, V. L.; Berg, H. W.; Guymon, J. F. Anthocyanin color level in port-type wines as affected by the use of wine spirits containing aldehydes. *Am. J. Enol. Vitic.* **1964**, *15*, 75-81.

Singleton, V. L.; Noble, A. C. Wine flavor and phenolic substances. In *Phenolic, Sulfur and Nitrogen Compounds in Food Flavours*; I. Katz, Ed.; American Chemical Society: Washington, 1976; pp 47-70.

Slabbert, N. P. Ionisation of some flavanols and dihydroflavonols. *Tetrahedron* **1977**, *33*, 821-824.

Somers, T. C. The polymeric nature of wine pigments. *Phytochemistry* **1971**, *10*, 2175.

Spagna, G.; Pifferi, P. G. Purification and separation of oenocyanin anthocyanins on sulphoxyethylcellulose. *Food Chem.* **1992**, *44*, 185-188.

Sudraud, P. Interprétation des courbes d'absorption des vin rouges. *Ann. Tech. Agric.* **1958**, *7*, 203-208.

Sweeny, J. G.; Iacobucci, G. A. Effect of substitution on the stability of 3-deoxyanthocyanidins in aqueous solutions. *J. Agric. Food Chem.* **1983**, *31*, 531-533.

Tate, M. E. Determination of ionization constants by paper electrophoresis. *Biochem. J.* **1981**, *195*, 419-426.

Timberlake, C. F.; Bridle, P. Flavylium salts, anthocyanidins and anthocyanins. I. Structural transformation in acid solutions. *J. Sci. Food Agric.* **1967**, *18*, 473-478.

Timberlake, C. F.; Bridle, P. Flavylium salts resistant to sulphur dioxide. *Chem. Ind.* **1968**, 1489.

Timberlake, C. F.; Bridle, P. Interactions between anthocyanins, phenolic compounds, and acetaldehyde and their significance in red wines. *Am. J. Enol. Vitic.* **1976**, *27*, 97-105.

Ueno, K.; Saito, N. 4',6,7-Trihydroxyflavylium chloride monohydrate; a synthetic anthocyanidin. *Acta Cryst.* **1977a**, *B33*, 111-113.

Ueno, K.; Saito, N. Cyanidin bromide monohydrate (3,5,7,3',4'-pentahydroxyflavylium bromide monohydrate). *Acta Cryst.* **1977b**, *B33*, 114-116.

Vivar-Quintana, A. M.; Santos-Buelga, C.; Francia-Aricha, E.; Rivas-Gonzalo, J. C. Formation of anthocyanidin derived pigments in experimental wines. *Food Sci. Tech. Int.* **1999**, *5*, 347-352.

Weeks, C. Production of sulfur dioxide-binding compounds and of sulfur dioxide by two *Saccharomyces* yeasts. *Am. J. Enol. Vitic.* **1969**, *20*, 32-39.

Wildenradt, H. L.; Singleton, V. L. The production of aldehydes as a result of oxidation of polyphenolic compounds and its relation to wine aging. *Am. J. Enol. Vitic.* **1974**, *25*, 119-126.

Willstatter, R.; Zollinger, E. H. Uber die farbstoffe der weintraube und der heidelbeere, II. *Ju. Lieb. Ann. Chem.* **1916**, *412*, 195-216.

Wulf, L. W.; Nagel, C. W. High-pressure liquid chromatographic separation of anthocyanins of *Vitis vinifera*. *Am. J. Enol. Vitic.* **1978**, *29*, 42-49.

Appendix 1

Estimation of Ionisation Constants Using High Voltage Paper Electrophoresis (HVPE)

Calculations

The calculations used for the estimation of ionisation constants were derived by Tate (1981) and are outlined below.

The loss of a proton by a polyprotic acid $(H_nB)^m$ of charge m, where n is the maximum number of dissociable protons and m is an integer, can be depicted by the following equation:

$$(H_nB)^x \rightleftharpoons (H_{n-1}B)^{x-1} + H^+ \qquad \text{Equation 9.1}$$

The Brønsted macroscopic ionisation constant ${}^BK_a$ for the first ionisation of the polyprotic acid can be depicted by:

$${}^BK_a = \frac{[(H_{n-1}B)^{x-1}][H^+]}{[(H_nB)^x]} \qquad \text{Equation 9.2}$$

where the concentrations of the species are expressed in square brackets ([]).

The mobility of the first ionisation product $H_{n-1}B$ relative to a standard is m_1 and the relative mobility of the fully protonated acid H_nB is m_0 (Tate, 1981). At pH values where the ionisation of H_nB is incomplete, the relative net mobility m_n is determined by the sum of the relative mobilites of the acid, m_0, and of the ionisation product, m_1 (Tate, 1981). For a single ionisation the relative electrophoretic mobility can be represented by:

$$m_r = m_0 \cdot \frac{[(H_nB)^x]}{[(H_nB)^x] + [(H_{n-1}B)^{x-1}]} + m_1 \cdot \frac{[(H_{n-1}B)^{x-1}]}{[(H_nB)^x] + [(H_{n-1}B)^{x-1}]} \qquad \text{Equation 9.3}$$

By substituting Equation 9.2 into Equation 9.3 and rearranging, the Brønsted macroscopic ionisation constant ${}^{B}K_a$ may be derived by one of the following linear equations:

$$\frac{1}{[H^+]} = \frac{1}{{}^{B}K_a}.\frac{(m_r - m_0)}{(m_1 - m_r)} \qquad \text{Equation 9.4}$$

$$m_r = m_0 + {}^{B}K_a.\frac{(m_1 - m_r)}{[H^+]} \qquad \text{Equation 9.5}$$

$$m_r = m_1 + \frac{1}{{}^{B}K_a}.[H^+].(m_0 - m_r) \qquad \text{Equation 9.6}$$

where $[H^+]$ is equal to the antilogarithm of the negative value of the measured pH (i.e. $[H^+] = 10^{-pH}$ (Tate, 1981)).

It should be noted that Equation is not valid when $m_r = m_1$ as

$${}^{B}K_a.\frac{(m_1 - m_r)}{[H^+]} = 0 \qquad \text{Equation 9.7}$$

and therefore $m_r = m_0$. It is necessary to have a statistical difference between m_1 and m_r to obtain a valid estimate of ${}^{B}K_a$. Equation 9.5 is not valid when $m_r = m_0$ for similar reasons. Estimates of pKa can be biased by linear transformations so it is preferable to fit the predicted mobility (m_p) curve directly to the data (Tate, 1981):

$$m_p = \frac{m_0 + m_1.10^{pH-pK_1} + m_2.10^{2pH-pK_1-pK_2} + ...}{1 + 10^{pH-pK_1} + 10^{2pH-pK_1-pK_2} + ...} \qquad \text{Equation 9.8}$$

The predicted mobility (m_p) can be predicted at each pH by Equation 9.8. The number of terms in the numerator and the divisor is dependent upon the number of ionisations, e.g. for a single ionisation only the first two terms are required. It should be noted that Equation 9.8 is constrained by the number of variables, therefore due to experimental effects, e.g. buffer ion concentration, a slight deviation of the experimental data from the theoretical curve may occur.

Due to discontinuities between the buffers used it is not always possible to obtain a continuous mobility profile across all the buffers used. It is therefore preferred to consider each buffer separately when estimating macroscopic pKa calculations.

Estimation of Hydration and Ionisation Constants using UV-visible Spectrophotometry

Calculations

The calculations used for the estimation of ionisation constants were derived by Asenstorfer (2001) and are outlined below.

The equilibrium of the flavylium ion (AH^+) with the hemiketal/pseudobase (A^{OH}) in the presence of water can be depicted by the following equation:

$$AH^+ + H_2O \rightleftharpoons A^{OH} + H^+ \qquad \text{Equation 9.9}$$

For MV3G the hemiketal is in equilibrium with the *cis*- and *trans*-chalcones. A rapid base-catalysed tautomerisation occurs between the hemiketal and the *cis*-chalcone (Brouillard and Lang, 1990). The isomerisation of the *cis*-chalcone to the *trans*-chalcone is a slow reaction (Brouillard and Delaporte, 1977) so the contribution of the *trans*-chalcone to the pK_H is negligible. Therefore the equilibrium constant for the hemiketal/pseudobase formation can be estimated by:

$$K_H = \frac{([A^{OH}]+[C_{cis}]).[H^+]}{[AH^+]} \qquad \text{Equation 9.10}$$

Equation 9.10 is analogous to the pKa of a Brønsted acid as shown previously in Equation 9.2. The hydration constant pK_H is the hydrogen ion concentration where the flavylium plus the hemiketal and the cis-chalcone species are present in equal amounts.

At a sufficiently high pH, the quinonoidal anion may be formed by the dehydration and ionisation of the hemiketal.

$$A^{OH} \rightleftharpoons A^- + H_2O + H^+ \qquad \text{Equation 9.11}$$

which can be depicted in the following equation:

$$K_{H2} = \frac{[A^-].[H^+]}{([A^{OH}]+[C_{cis}])} \qquad \text{Equation 9.12}$$

Again, this is analogous to the pKa of a Brønsted acid. The hydration constant pK_{H2} is the hydrogen ion concentration where the hemiketal plus the *cis*-chalcone and the quinonoidal anion species are present in equal amounts.

In a two component system, assuming that Beer's Law is obeyed, the observed absorbance Abs_r is the sum of the absorbance of the two species Abs_0 and Abs_1 (Equation 9.13).

$$Abs_r = Abs_0 + Abs_1 \qquad \text{Equation 9.13}$$

The absorbance of either species is related to the molar concentration, C, the optical pathlength of the cell, ℓ, and the molar absorbance coefficient ε and can be expressed as:

$$Abs = \varepsilon.\ell.C \qquad \text{Equation 9.14}$$

The concentration of an ionised species is dependent upon the fraction ionised, F_0 and therefore its contribution to the observed absorbance can be expressed as:

$$Abs_0 = \varepsilon_0.\ell.F_0.C \qquad \text{Equation 9.15}$$

If the same cell pathlength is used the observed absorbance is:

$$Abs_r = (\varepsilon_0.F_0 + \varepsilon_1.F_1).C \qquad \text{Equation 9.16}$$

However,

$$\varepsilon_0 = \frac{Abs_0}{C_0.\ell} \qquad \text{Equation 9.17}$$

which can be substituted into Equation 9.15 and after rearranging:

$$F_0 = \frac{C_0}{C} \qquad \text{Equation 9.18}$$

where C is the total concentration and C_0 is the concentration of the ionised species. Therefore Equation 9.18 can be written as:

$$F_0 = \frac{[AH^+]}{[AH^+] + ([A^{OH}] + [C_{cis}])} \qquad \text{Equation 9.19}$$

Similarly, the fractio present in the molecular form can be expressed as:

$$F_1 = \frac{([A^{OH}] + [C_{cis}])}{([A^{OH}] + [C_{cis}]) + [AH^+]} \qquad \text{Equation 9.20}$$

The observed absorbance, Abs_r, is equal to the sum of the absorbances of the fractional concentrations F_0 and F_1 of each of the species

$$Abs_r = Abs_0.F_0 + Abs_1F_1 \qquad \text{Equation 9.21}$$

which can be expanded into:

$$Abs_r = Abs_0 . \frac{[AH^+]}{[AH^+] + ([A^{OH}] + [C_{cis}])} + Abs_1 . \frac{([A^{OH}] + [C_{cis}])}{([A^{OH}] + [C_{cis}]) + [AH^+]}$$ Equation 9.22

By substituting $(H_nB)^x$ for the flavylium species, $(H_{n-1}B)^{x-1}$ for the hemiketal and the *cis*-chalcone species, Equation 9.22 can be rewritten as:

$$Abs_r = Abs_0 . \frac{[(H_nB)^x]}{[(H_nB)^x] + [(H_{n-1}B)^{x-1}]} + Abs_1 . \frac{[(H_{n-1}B)^{x-1}]}{[(H_nB)^x] + [(H_{n-1}B)^{x-1}]}$$ Equation 9.23

The Brønsted ionisation can be derived by the following linear equations after substituting Equation 9.2 into Equation 9.23:

$$\frac{1}{[H^+]} = \frac{1}{{}^B K_a} . \frac{(Abs_r - Abs_0)}{(Abs_1 - Abs_r)}$$ Equation 9.24

$$Abs_r = Abs_0 + {}^B K_a . \frac{(Abs_1 - Abs_r)}{[H^+]}$$ Equation 9.25

$$Abs_r = Abs_1 + \frac{1}{{}^B K_a} . [H^+] . (Abs_0 - Abs_r)$$ Equation 9.26

Furthermore, Equation 9.26 can be rewritten as:

$$pK_a = pH + \frac{(Abs_1 - Abs_r)}{(Abs_r - Abs_0)}$$ Equation 9.27

From Equation 9.27, the predicted absorbance Abs_p, at any particular wavelength, can be determined, for a two component system, from the following equation:

$$Abs_p = \frac{Abs_0 + Abs_1 . 10^{pH - pK_1}}{1 + 10^{pH - pK_1}}$$ Equation 9.28

Equation 9.28 is analogous to Equation 9.8, so for a multiple component system it is possible to extend this equation:

Equation 9.29

$$Abs_p = \frac{Abs_0 + Abs_1 . 10^{pH - pK_1} + Abs_2 . 10^{2pH - pK_1 - pK_2} + ...}{1 + 10^{pH - pK_1} + 10^{2pH - pK_1 - pK_2} + ...}$$

The calculation of macroscopic pK values can be determined by applying Equation 9.29 to UV-visible spectroscopic data. As noted previously for Equation 9.8, Equation 9.29 is constrained by the number of variables. Therefore due to experimental effects a slight deviation of the experimental data from the theoretical curve may occur.

Appendix 2

Grams/32 Program

The following basic program was written to calculate the absorbance at a particular wavelength and to obtain the wavelengths and absorbances of the peaks:

```
dim fname(100) : fname=0
dim rname(100) : rname=0
dim peaka(100) : peaka=0
dim peakb(100) : peakb=0
n=0
menufile $fname,"select traces to process: *.spc",2
STRNAME 3, $rname=$fname
'load spectra
100 loadspc $fname
'open file "uvdata.txt"
      open #1, "c:\dave\pkh\uvdata.txt"
'define the wavelengths x1,x2,x3..xn
      x1=wavelength 1
      x2=wavelength 2
      x3=wavelength 3
'calculate the absorbance (y) at x
'where #s=amplitude (absorbance) at x
      y1=#s(x1)
      y2=#s(x2)
      y3=#s(x3)
'goto end of file
      seek #1, -0
'append data to file
      print #1; $rname, x1,y1,x2,y2,x3,y3
      close #1
'get number of peaks
      peaktable 9,, n
'open file "peakdata.txt"
```

```
        open #3, "c:\dave\pkh\peakdata.txt"
        seek #3, -0
        print #3; "pH", $rname
'get peak data
for i=0 to n-1
        peaktable 10,i,a
        peaktable 11,i,b
        string $peaka=a
        string $peakb=b
        seek #3, -0
        print #3; $peaka, $peakb
        peaka=0
        peakb=0
next
'reset values
        fname=0
        rname=0
'open next spectra
        menufile $fname="",3
        onerror 200
        STRNAME 3, $rname=$fname
goto 100
200
fname=0
rname=0
end
```